

**INVOLVEMENT OF *NM23-M2* IN DOPAMINERGIC
NEURONAL DIFFERENTIATION AND CELL CYCLE
ARREST**

LOH CHIN CHIEH

NATIONAL UNIVERSITY OF SINGAPORE

2006

**INVOLVEMENT OF NM23-M2 IN DOPAMINERGIC
NEURONAL DIFFERENTIATION AND CELL CYCLE
ARREST**

LOH CHIN CHIEH
(B. Appl. Sci. (2nd Upper Hons.), NUS)

**A THESIS SUBMITTED
FOR THE DEGREE OF MASTER OF SCIENCE
DEPARTMENT OF BIOLOGICAL SCIENCES
NATIONAL UNIVERSITY OF SINGAPORE**

2006

Acknowledgements

This present thesis work has been arduous yet enriching and rewarding experience for me. I would like to acknowledge all those who have been a part of this experience without whom I could not have completed the undertaken task.

Firstly I would like to thank my research advisor, Associate Professor Lim Tit Meng, Vice Dean of Science Faculty, NUS and principal investigator of Developmental Biology Laboratory (DBL) in Department of Biological Sciences, to whom I am greatly indebted for professional guidance and encouragement throughout my graduate studies. I am very fortunate to have him as a considerate advisor and deeply appreciative of him for giving me this opportunity to be involved in his ongoing research.

I would also like to thank Mr. Yan Tie, our laboratory manager for his excellent technical support and valuable advices, hence making it possible for me to carry out my bench-work with ease.

I will also cherish the memorable time that I spent working in this laboratory. Special thanks to my mentor, Ms. Christina Teh Hui Leng for giving me continual guidance and help; to my fellow colleagues, Mr. Kevin Lam Koi Yau, Mr. Rikki Tay Kian Ghee, for lending a listening ear to my thoughts; and to all colleagues working in the DBL for their sincere help and technical support in one way or another.

Last but not least, I would like to thank my loved ones, my parents and my sister for their love and understanding. Special heartfelt thanks to my future wife, Ms. Lee Hui Cheng for showering me with love and continual support especially during this period.

Contents

Acknowledgements	i
Contents	ii
Summary	vii
List of figures	ix
List of tables	xi
List of abbreviations	xii
Chapter 1: Introduction	1
1.1 Prevalence of Parkinson's Disease in Singapore	2
1.2 Parkinson's Disease	2
1.3 Dopaminergic neurons	3
1.4 Therapies used in treatment of Parkinson's disease	4
1.4.1 Neuroprotection by neurotrophic factor interventions	6
1.4.2 Gene transfer therapy	6
1.4.3 Xenogeneic transplantation therapy	8
1.4.4 Cell replacement therapy	8
1.4.5 Deep brain stimulation therapy	9
1.5 Neural stem cell and MN9D hybrid cell line	10
1.6 Differentiation of neural stem cells (NSC)	12
1.6.1 Intracellular factors that cause differentiation of NSC into dopaminergic neurons	12
1.6.2 Extracellular factors that cause differentiation of NSC into dopaminergic neurons	15
1.7 Significance of genes involved in dopaminergic neuron differentiation	16
1.8 Literature reviews on factors that cause neurite outgrowth and	17

	differentiation in MN9D	
1.9	The <i>nm23</i> gene family	18
1.9.1	Biochemical functions of <i>nm23</i> /NDPK proteins	19
1.9.2	Cellular studies support a role for <i>nm23</i> /NDPK in signal transduction	22
1.9.3	<i>Nm23</i> /NDPK homologues in fruit fly development and differentiation	23
1.9.4	<i>Nm23</i> /NDPK in hematopoietic differentiation	24
1.9.5	<i>Nm23</i> /NDPK in mammalian neuronal cell development and differentiation	25
1.9.6	Role of <i>nm23</i> /NDPK in neuroblastoma differentiation	27
1.10	Objective of this study	28
	Chapter 2: Materials and methods	30
2.1	Routine cell culture of MN9D and SH-SY5Y cell lines	31
2.2	Cloning of full length <i>nm23</i> -M2 gene	32
2.2.1	Total RNA isolation	32
2.2.2	Reverse Transcriptase-PCR (RT-PCR) of full length <i>nm23</i> -M2 gene	34
2.2.3	Gel extraction and DNA purification of <i>nm23</i> -M2	34
2.2.4	Cloning of full length <i>nm23</i> -M2 coding sequence into pGEM-T Easy TM plasmid vector	35
2.2.5	Transformation of recombinant plasmids into bacterial competent cells	36
2.2.5.1	Preparation of bacterial competent cells	36
2.2.5.2	Transformation	36

2.2.6	Colony PCR screening for positive clones	37
2.2.7	Plasmid DNA isolation from positive clones	38
2.2.8	Cloning of full length <i>nm23</i> -M2 coding sequence into mammalian pcDNA3.1-GFP and pcDNA 3.1-MYC plasmid vector	39
2.2.9	Cycle sequencing	40
2.2.10	Ethanol/sodium acetate precipitation for DNA purification	41
2.2.11	Capillary electrophoresis sequencing on ABI PRISM 3100 Genetic Analyzer	41
2.2.12	DNA gel electrophoresis	42
2.3	Construction of cDNAs for Real-time PCR	42
2.4	Real-time PCR	43
2.5	Transfection of plasmid construct to mammalian cells	44
2.6	Protein work	44
2.6.1	Isolation of total cell lysate	44
2.6.2	Bio-Rad Bradford protein quantification assay	45
2.6.3	Protein separation using sodium dodecyl sulphate- polyacrylamide electrophoresis (SDS-PAGE)	45
2.6.4	Western immunoblot analysis	46
2.7	Subcellular fractionation	48
2.8	Fluorescence microscopy and neurite assay	48
2.9	Flow cytometry	49
2.10	siRNA interference	50

Chapter 3: Results	56
3.1 Cloning and characterization of full-length <i>nm23</i> -M2 cDNA	57
3.1.1 Cloning of full-length pcDNA3.1(-)_ fl <i>nm23</i> -M2_GFP and pcDNA3.1(-)_fl <i>nm23</i> -M2_MYC	57
3.1.2 Routine tissue culture	61
3.1.3 Temporal expression of <i>nm23</i> -M2 during MN9D cell differentiation	64
3.1.4 Spatial expression of <i>nm23</i> -M2 in MN9D and SH-SY5Y cells	66
3.1.5 Subcellular localization of <i>nm23</i> -M2	68
3.2 Overexpression studies of <i>nm23</i> -M2 in MN9D cells	70
3.2.1 Morphological appearance of MN9D overexpressing pcDNA3.1(-)_fl <i>nm23</i> -M2_GFP	70
3.2.2 MN9D cells showed cell growth arrest when treated with <i>n</i> -butyric acid and transfected with <i>nm23</i> -M2	72
3.2.3 SNAP-25 protein expression was up-regulated in MN9D cells overexpressing pcDNA3.1(-)_fl <i>nm23</i> -M2_GFP	74
3.2.4 Cyclin D1 mRNA and protein expression was down-regulated in MN9D cells overexpressing pcDNA3.1(-)_fl <i>nm23</i> -M2_GFP	76
3.3 SiRNA interference studies of <i>nm23</i> -M2 in MN9D cells	78
3.3.1 Knockdown expression of <i>nm23</i> -M2 mRNA upon siRNA interference	78
3.3.2 Morphological appearance of MN9D cells after transient siRNA knockdown of <i>nm23</i> -M2	79
3.3.3 Cell cycle analysis of <i>n</i> -butyric acid-treated MN9D cells when <i>nm23</i> -M2 siRNA was added	81
3.3.4 SNAP-25 protein level of <i>n</i> -butyric acid-treated MN9D cells	82

did not increase when <i>nm23</i> -M2 siRNA was added	
3.3.5 Cyclin D1 protein level of <i>n</i> -butyric acid-treated MN9D cells	83
did not decrease when <i>nm23</i> -M2 siRNA was added	
Chapter 4: Discussion	84
4.1 Choice of cell line model	85
4.2 Temporal and spatial expression of <i>nm23</i> -M2 gene	85
4.3 The role of <i>nm23</i> -M2 in dopaminergic MN9D differentiation	87
4.4 The role of <i>nm23</i> -M2 in inducing cell cycle arrest	89
4.5 Further studies to elucidate the differentiation pathway	92
4.6 Future experiments	94
4.7 Conclusion	95
References	97

Summary

Nm23 genes which encode nucleoside diphosphate kinases (NDPKs) are ubiquitous metabolic enzymes, responsible for the synthesis of nonadenine nucleoside triphosphates from the corresponding diphosphates, with ATP as phosphoryl donor. In the brain, *nm23*/NDPK have been implicated to modulate neuronal cell proliferation, differentiation, and neurite outgrowth. The *nm23*-M2 gene is the focus of this thesis because this gene was found to be up-regulated during *n*-butyric acid induced MN9D differentiation through subtractive library screening and micro-array analysis. Reviews of relevant literature also supported its involvement in cell development and differentiation. Moreover, overexpression of *nm23* genes induces neuritogenesis and stimulates the differentiation pathways in many cell lineages.

In order to determine what role, if any, *nm23*-M2 gene might play in dopaminergic neuronal differentiation, this study made use of a catecholamine producing hybrid dopaminergic cell line, MN9D as an *in vitro* cell model system for overexpression and siRNA interference experimentation. The temporal expression was studied during *n*-butyric acid induced MN9D differentiation by measuring the endogenous level of *nm23*-M2 mRNA by semi-quantitative real-time PCR. GFP reporter system was also used to analyze the spatial expression pattern of *nm23*-M2-GFP protein in MN9D and SH-SY5Y cell lines using fluorescent microscopy techniques. It was demonstrated for the first time that overexpression of *nm23*-M2 itself in MN9D cell line resulted in significant increase in the number of cells bearing neurites and an alteration of the cell cycle, increased G₁-phase. Analysis of immunoblots revealed that this morphological differentiation was accompanied by an increased expression of a neuronal maturation marker, synaptosomal protein SNAP-25 and decreased expression of a G₁ stage cell cycle marker, cyclin D1. The *n*-butyric acid-induced neurite outgrowth in MN9D cells was also abolished by

nm23-M2 siRNA treatment although the level of SNAP-25 and cyclin D1 remained unaltered by siRNA interference. Therefore, it is plausible that *nm23-M2* gene 1) regulates neurite outgrowth in dopaminergic MN9D cells acting via the modulation of SNAP-25 gene expression, and 2) represses transcription of positive regulators, cyclin D1 of cell cycle, to initiate cell cycle arrest.

These data support the hypothesis that *nm23-M2* plays a role in dopaminergic neuronal differentiation through initiating neurite outgrowth and inducing growth arrest. The findings and proposed future work may eventually contribute to the understanding of pathways or mechanisms on the induction of dopaminergic neuron differentiation that could facilitate the development of gene delivery or cell replacement therapeutics for brain neurodegenerative disorders.

List of figures

Figure 2.1	Plasmid map and sequence reference points of pGEM-T Easy cloning vector	52
Figure 2.2	Plasmid map and sequence reference points of pcDNA3.1(+/-) cloning vector	53
Figure 3.1	Total RNA isolation	59
Figure 3.2	NM_008705 <i>nm23</i> -M2 mRNA	59
Figure 3.3	RT-PCR amplification of full-length <i>nm23</i> -M2 cDNA	59
Figure 3.4	Restriction enzyme digestion of pGEM-T Easy_mNm23-M2 recombinant plasmid	60
Figure 3.5	Restriction enzyme digestion of pcDNA3.1(-)_mNm23-M2 recombinant plasmid	60
Figure 3.6	MN9D time-course differentiation	63
Figure 3.7	Model of a single amplification plot used in real-time PCR	64
Figure 3.8	A graph showing multiple amplification plots during the real-time PCR run	65
Figure 3.9	A graphical representation showing changes in endogenous mRNA level of <i>nm23</i> -M2 post-induction of MN9D cells with 1mM <i>n</i> -butyric acid	65
Figure 3.10	Spatial expression of <i>nm23</i> -M2 in MN9D and SH-SY5Y cells	67
Figure 3.11	Western immunoblot analysis of GFP in transfected MN9D cells	68
Figure 3.12	Western immunoblot analysis of Oct-1 and C-Myc	69
Figure 3.13	Morphology of transfected MN9D cells	71
Figure 3.14	A graph showing the morphological changes of MN9D cells after 2 days post-transfection of <i>nm23</i> -M2	72

Figure 3.15	A table showing the percentage of MN9D cells at different stages of the cell cycle in different conditions	73
Figure 3.16	A graph showing the percentage of MN9D cells after 2 days post-transfection of GFP null plasmid and <i>nm23-M2</i> plasmid	73
Figure 3.17	Western immunoblots showing overexpression results after 48hr of transfection using mouse anti-SNAP-25 monoclonal antibody	75
Figure 3.18	Western immunoblots using mouse anti-cyclin D1 monoclonal antibody and RT-PCR of cyclin D1 showing overexpression results after 48hr of transfection	77
Figure 3.19	RT-PCR of <i>nm23-M2</i> after siRNA interference	78
Figure 3.20	A graph showing the morphological changes of MN9D cells after 24hr post-transfection of control siRNA and <i>nm23-M2</i> siRNA	80
Figure 3.21	A graph showing the percentage of MN9D cells after 48hr post-transfection of control and <i>nm23-M2</i> siRNA	81
Figure 3.22	Western immunoblots showing siRNA interference results after 24hr of transfection using mouse anti-SNAP-25 monoclonal antibody	82
Figure 3.23	Western immunoblots showing siRNA interference results after 24hr of transfection using mouse anti-Cyclin D1 monoclonal antibody	83
Figure 4.1	A schematic representation of cell cycle progression showing cyclins function as regulators of CDK kinases	90
Figure 4.2	A schematic representation showing positive and negative regulators in the cell cycle progression	91

List of tables

Table 2.1	Preparation of SDS-PAGE gel with the listed required components	54
Table 2.2	Primary and secondary antibodies application for western blotting in this thesis	55

List of abbreviations

6-OHDA	6-hydroxydopamine
A_{260}	Absorbance at 260 nm
AMP, ADP, ATP	Adenosine 5'-mono-, di-, or triphosphate
APS	Ammonium persulphate
<i>awd</i>	Abnormal wing discs
BDNF	Brain-derived neurotrophic factor
bFGF	basic fibroblast growth factor
bp	Base pair
BSA	Bovine serum albumin
CKI	CDK inhibitors
CDKs	Cyclin-dependent kinases
cDNA	Complementary DNA
CO ₂	Carbon dioxide
CTP	Cytidine 5' triphosphate
DA	Dopamine
DBS	Deep brain stimulation
DDS	Dopamine dysregulation syndrome
DMEM	Dubecco's Modified Eagle's Medium
DNA	Deoxyribonucleic acid
dNTP	Deoxynucleoside 5' triphosphate
DTT	Dithiothreitol
EDTA	Ethylenediaminetetraacetate
EGF	Epidermal growth factor

ETBR	Ethidium Bromide
EtOH	Ethanol
FACS	Fluorescence Activated Cell Sorting
Fgf8	Fibroblast growth factor 8
<i>g</i> (eg. 5,000 x <i>g</i>)	Gravity
GDNF	Glial cell line-derived neurotrophic factor
GFP	Green fluorescent protein
GTP	Guanosine 5' triphosphate
HPRT	Hypoxanthine-Guanine Phosphoribosyl Transferase
Hr	Hour
HRP	Horse radish peroxidase
IPTG	Isopropyl-β-D-thiogalactopyranoside
JNK	c-Jun N-terminal kinase
<i>k-pn</i>	<i>Killer of prune</i>
kB	Kilobase
kD	Kilodalton
LB	Luria-Bertani
LBs	Lewy bodies
L-Dopa	Levodopa
M	Molar
MAPK	Mitogen-activated protein kinase
MgCl ₂	Magnesium chloride
mg	Milligram
Min	Minute
ml	Milliliter

mM	Millimolar
MPP+	<i>N</i> -methyl-4-phenylpyridinium ion
MPTP	<i>N</i> -methyl-4-phenyl-1,2,3,6-tetrahydropyridine
mRNA	Messenger RNA
NaCl	Sodium chloride
NADH	Nicotinamide adenine dinucleotide
NaOAc	Sodium acetate
ng	Nanogram
nm	Nanometer
NDPK	Nucleotide diphosphate kinase
NGF	Nerve growth factor
NHE	Nuclease hypersensitive element
NSC	Neural stem cell
NTF	Neurotrophic factor
NTN	Neurturin
OD	Optical density
PAGE	Polyacrylamide electrophoresis
PBS	Phosphate-buffered saline
PC12	Pheochromocytoma cell line
PCR	Polymerase chain reaction
PD	Parkinson's disease
Rb	Retinoblastoma
RMT	Rostal mesencephalic tegmentum
RNA	Ribonucleic acid
RNase	Ribonuclease

ROS	Reactive oxygen species
rRNA	Ribosomal RNA
RT	Reverse transcriptase
RT-PCR	Reverse transcription-PCR
SDS	Sodium dodecyl sulfate
SHH	Sonic hedgehog
siRNA	Small interference RNA
SNAP-25	Synaptosomal-associated protein of 25 kDa
SNpc	Substantia nigra pars compacta
STN	Subthalamic nucleus
TAE	Tris acetate
TBS	Tris buffer saline
TEMED	N, N, N, N-tetramethylethylenediamine
TGF- β	Transforming growth factor- β
TH	Tyrosine hydroxylase
TPA	12-O-tetradecanoylphorbol-13-acetate
Tris	Tris(hydroxymethyl)-aminomethane
Tris-HCl	Tris-hydrochloride
USA	United States of America
UTP	Uridine 5' triphosphate
VM	Ventral mesencephalon
VTa	Ventral tegmental area
μ g	Microgram
μ l	Microliter
UV	Ultraviolet

μm	Micrometer
%	Percent
$^{\circ}\text{C}$	Degree Celsius

Chapter 1:

Introduction

Chapter 1: Introduction

1.1 Prevalence of Parkinson's Disease in Singapore

Parkinson Disease (PD) is the 2nd most common neurodegenerative disorder after Alzheimer's disease. Estimate of prevalence rates worldwide range from 10 to 450 per 100,000 population (Zhang and Roman, 1993). Both genetic and environmental agents have been implicated in PD (Tan et al. 2000; Allam et al. 2005). A recent study in Singapore (Tan et al. 2004) showed that PD occurs as commonly as in the West. 3 out of every thousand individuals, aged 50 years and above, will have this disease. Prevalence of PD was also investigated between Singapore Chinese, Malays and Indians and the environmental factors may be more important than racially determined genetic factors in the development of PD. As Singapore's population continues to age, the number of people with PD is expected to rise. Due to the increasing proportion of elderly individuals, PD represents a growing burden on the health care system.

1.2 Parkinson's Disease

In 1817, British physician and geologist James Parkinson gave the first clear description of what is now known as PD in "An Essay on the Shaking Palsy". By observing people on the streets on London, he noticed that some had tremors, or shaking palsy, that worsened over time. In this early stage of medical science, physical tests and examinations of this disease were unheard of. Dr. James Parkinson could not know the full range of symptoms that would eventually be referred as PD. Through years of dedicated research, scientists searched further for the causes and symptoms of PD. It is now known that PD is a

neurodegenerative disorder in which the most predominant neuropathological feature is characterized by a progressive loss of the midbrain mesencephalic dopaminergic neurons located in the substantia nigra pars compacta (SNpc) and ventral tegmental area (VTA) that provides innervation to the striatum (nigrostriatal system) and the cortex and limbic areas (mesocortical and mesolimbic system), respectively. Clinically, most PD patients show signs of the cardinal symptoms of bradykinesia, resting tremor, rigidity, and postural instability (Bergman and Deuschl, 2002; Fahn, 2003). A number of patients also suffer from autonomic, cognitive, and psychiatric disturbances. The pathological hallmarks of PD are round eosinophilic intracytoplasmic proteinaceous inclusions termed Lewy bodies (LBs) and dystrophic neuritis (Lewy neuritis) present in surviving neurons (Forno, 1996).

1.3 Dopaminergic neurons

Dopaminergic neurons are an anatomically and functionally heterogeneous group of cells, localized in the diencephalons, mesencephalon and the olfactory bulb (Björklund & Lindvall, 1984). The most prominent dopaminergic cell group resides in the ventral part of mesencephalon, which contains approximately 90% of the total number of brain dopaminergic cells. The mesencephalic dopaminergic system has been subdivided into the nigrostriatal, mesolimbic and mesocortical system. The mesolimbic and mesocortical dopaminergic systems, which arise from dopaminergic cells present in the ventral tegmental area (VTA). The cells of the VTA in mesolimbic dopaminergic system project most prominently into the nucleus accumbens, olfactory tubercle but also innervate the septum, amygdale and hippocampus, whereas the cells in the medial VTA of the mesocortical

dopaminergic system project to the prefrontal, cingulate and perirhinal cortex. Probably the best known is the nigrostriatal system which originates in the zona compacta of the substantia nigra and extends its fibers into the caudate-putamen (dorsal striatum). The identity of early proliferating dopaminergic progenitor cells and development of the nigrostriatal dopaminergic neurons in the ventral mesencephalon floor are specified by the existence of two secreted signaling proteins, sonic hedgehog (Shh) (Hynes et al. 1995) and fibroblast growth factor 8 (Fgf8) (Ye et al. 1998), derived from the floor plate of the ventral midline and the mid/hindbrain border, respectively. These neurons are the source of striatal dopamine (DA), a major neurotransmitter that is responsible for motor functions. The specific loss of dopaminergic neurons in the SNpc is a trait of PD and results in severe motor disturbances and abnormalities, while alterations in dopaminergic transmission from the VTA has been implicated in schizophrenia and drug addiction. Due to the importance of these DA neurons in human pathology, survival and induction of dopaminergic neurons has always been the subject of intense study.

1.4 Therapies used in treatment of Parkinson's disease

While there are multiple causes of this neurodegenerative disease including environmental, genetic and age-associated factors, the treatments may be targeted at similar underlying mechanisms via neuroprotective and reparative intervention. Many data show that the selectively susceptible DA neurons in the substantia nigra of the patients that have developed Parkinson's disease can be altered by protective and reparative therapies. Traditional oral drug administration of levodopa (L-Dopa), the precursor of DA, initially was shown to improve life

expectancy and relieves parkinsonian motor signs during the first six years of therapy (Dunnett and Bjorklund, 1999; Tan, 2001; Weiner 1982), but its protective effectiveness was subsequently shown to decline and long term use is associated with severe fluctuations in drug response (Agid et al. 1990; Curtis et al. 1984). Pramipexole, an antiparkinsonian agent which is neuroprotective against 1-methyl-4-phenyl-1,2,3,6-tetrahydropyridine (MPTP)-induced damage to the DA system in mice (Kitamura et al. 1997). This dopamine agonist has become an efficient and safe drug for the treatment of Parkinson's disease recently (Bennett and Piercey, 1999). However, particular caution has to be exercised in younger Parkinson's disease patients with a shorter disease duration regarding the occurrence of sudden onset of sleep (Moller and Oertel, 2005). Initial symptoms in PD such as oxidative stress, protein abnormalities, and cellular inclusions could be treated by antioxidants (Prasad et al. 1999; Shults, 2005) and trophic factors (Grondin and Gash, 1998). If the delay of degeneration is not sufficient, then immature dopamine neurons can be placed in the parkinsonian brain by transplantation. Such neurons can be derived from stem cell sources or even stimulated to repair from endogenous stem cells. Many new strategies are being pursued in the development of new therapies for PD. These range from the use of neurotrophic factors (Takayama et al. 1995), gene therapy or genetic manipulation to increase the volume of dopamine production by increasing the number of human tyrosine hydroxylase (TH) transcripts by employing viral vectors (Choi-Lundberg et al. 1997), or transplantation of xenogeneic materials (Deacon et al. 1997), or transplantation of human fetal tissue (Olanow et al. 1996) to deep brain stimulation (Diamond and Jankovic, 2005; Olanow et al. 2000). The search for candidate molecules that promote the regeneration and survival capacities of DA

neurons is a major area of investigation and hope. A better characterization of the developmental pathways that govern the specification, differentiation, and survival of these neurons will be essential in devising therapies aimed to rescue or replace midbrain DA neurons in Parkinson's patients.

1.4.1 Neuroprotection by neurotrophic factor interventions

The replacement or supplementation of a DA neurotrophic factor (NTF) may protect or slow down the neuronal degeneration of PD. Several NTFs have shown trophic activity in the DA system, including brain-derived neurotrophic factor (BDNF) (Hyman et al. 1991), neurotrophin NT-3, NT-4/5 (Hyman et al. 1994b, Hynes et al. 1994), basic fibroblast growth factor (bFGF) (Knusel et al. 1990; Mayer et al. 1993; Takayama et al. 1995), transforming growth factor- β (TGF- β) (Poulson et al. 1994), and glial cell line-derived neurotrophic factor (GDNF) (Lin et al. 1993). Of relevance to the neurodegenerative processes of PD, pretreatment of DA neurons with BDNF protects against the neurotoxic effects of *N*-methyl-4-phenylpyridinium ion (MPP⁺) and 6-hydroxydopamine (6-OHDA) *in vitro*, perhaps by increasing levels of antioxidant enzyme glutathione reductase (Spina et al. 1992). NT-4/5 (Hynes et al. 1994), bFGF (Park and Mytilineou, 1992), GDNF (Hou et al. 1996), and TGF- β (Krieglstein and Unsicker, 1994) also protect against the toxic effects of MPP⁺ *in vitro*.

1.4.2 Gene transfer therapy

Future treatment modality for PD may also rely on using gene delivery or gene therapy. Recent development in aging PD models using lentiviral transfer of GDNF has also created hope and interest in the development of PD treatment

(Kordower et al. 1993). Much advancement in viral-based vectors for gene delivery to cells of the brain has been achieved (Bowers et al. 1997; Mandel et al. 1998; Verma and Somia, 1997). However, future improvements must still be made in respect to the safety and efficiency of gene transfer to neurons. Some desired features of the viral vectors for gene transfer to the brains are (i) a large transgene capacity needed within a vector to include gene(s) of interest and its appropriate regulators, (ii) a high transduction efficiency needed to transfer a gene of interest to a population of neural cells, (iii) a good stability in transgene expression, (iv) that an appropriate dose of transgene product can be critical (Bowers *et al.* 1997), (v) the cell specificity of gene transfer within the central nervous system dependent on the cell-specific promoters (Klein et al. 1998; Song et al. 1997), expression of viral vector-specific receptors (Montgomery et al. 1996), or route of axonal transport of the vector in the brain, and finally (vi) the lack of both toxicity and inflammatory immune response is essential for clinical application of viral vector-mediated gene transfer (During et al. 1994; Fraefel et al. 2000). Fjord-Larsen et al. 2005 recently has demonstrated Neurturin (NTN) has neuroprotective effects on DA neurons. However, unlike GDNF, NTN has not previously been applied in PD models using an *in vivo* gene therapy approach. The difficulties with lentiviral gene delivery of wild type NTN motivate the authors to evaluate different NTN constructs in order to optimize gene therapy with NTN. Currently, the enhanced secretion of active mature NTN using the IgSP-NTN construct was reproduced *in vivo* in lentiviral-transduced rat striatal cells and, unlike wt NTN, enabled efficient neuroprotection of lesioned nigral DA neurons, similar to GDNF (Fjord-Larsen et al. 2005).

1.4.3 Xenogeneic transplantation therapy

An astonishing homogeneity in neurons and glial basic cellular structure and function suggested that even discordant mammalian species (rodents to non-human primates) could effectively replace local synaptic function after cell loss in the adult brain (Isacson et al. 1989; Hantraye et al. 1992). Such across-species cell transfer or xenotransplantation allows a more standardized acquisition of larger amount of fetal tissue as compared to human fetal tissue during abortions. Past transplantation studies have shown survival, function, and afferent/efferent connections of xenogeneic cells when transplanted into animal hosts (Galpern et al. 1995; Isacson et al. 1995). The immunological reaction of complement activation rejection and T-cell mediated responses leading to the rejection of the xenografts can be in many ways be inhibited by immune suppression. In fetal neural cell xenotransplantation into rodent host brains (in the absence of preformed anti-species specific antibodies), cyclosporine and other immune suppressive regimes (prednisolone and azathioprine), which are regularly used in humans for allogeneic kidney and heart transplantation, are usually sufficient to prevent massive rejection (Pedersen et al. 1995).

1.4.4 Cell replacement therapy

One of the most promising therapies in treatment of PD is cell replacement therapy. It involves the transplantation of dopamine-secreting cells originated from human fetal ventral mesencephalon (VM) directly into the striatum. It seeks to replace the loss in synaptic signaling cause by the neuronal degeneration. Although this approach has been used successfully as a therapy for PD, one of the main concerns with this procedure is the significant amount of fetal tissue required

per transplantation. It has been previously established that, on average, it is necessary to obtain VM tissue from 9-12 fetuses in order to complete a bilateral implantation in one PD patient (Olanow et al. 1996). Another major problem is that the majority of the cells die during the tissue preparation (Fawcett et al. 1995) and first week following the graft (Barker et al. 1996; Brundin et al. 2000). Another problem is the use of the fetal tissue that raises ethical concerns and moral issues. One solution to avoid the requirement of large number of fetuses is the use of neural stem cell tissue since these cells can be expanded in large number in culture for several months. These stem cells were isolated and purified from the walls of ventricles - cavities that are filled with cerebrospinal fluid within the brain. In this region, only about one in three hundred cells is a stem cell (Cassidy and Frisen, 2001).

1.4.5 Deep brain stimulation therapy

Deep brain stimulation (DBS) has emerged rapidly as an effective therapy for all the cardinal features of Parkinson's disease (Breit et al. 2004). DBS includes an implanted brain electrode and a pacemaker-like implanted pulse generator. Subthalamic nucleus (STN) DBS by means of permanently implanted brain electrodes in appropriate patients resulted in motor improvement is accompanied by a significantly improved quality of life and a reduced necessity for medication (Israel and Hassin-Baer, 2005). Patients suffering from disabling motor fluctuations and dyskinesia associated with severe dopamine dysregulation syndrome (DDS), which is characterized by severe dopamine addiction and behavioral disorders such as manic psychosis, hypersexuality, pathological gambling, and mood swings, STN DBS greatly reduced the behavioral disorders

as well as completely abolished the addiction to dopaminergic treatment (Witjas et al. 2005). Furthermore, DBS patients may experience a significant long-term reduction in the cost of their pharmacologic treatment (Charles et al. 2004). However, mechanical failure of the DBS system is a potential complication (Alex Mohit et al. 2004) and signs of decreased efficacy can be seen after 12 months (Ghika et al. 1998).

1.5 Neural stem cell and MN9D hybrid cell line

A neural stem cell (NSC) is defined as a single cell with the ability to (i) proliferate neuronal tissue, (ii) exhibit self-maintenance or renewal over the lifetime of the organism, (iii) give rise to a large number of clonally related progeny through asymmetric cell division, (iv) retain its multilineage potential over time, and (v) produce new cells in response to injury and disease (Zigova and Sanberg, 1998). The availability of a stable immortalized clonal cell lines expressing phenotypic characteristics of a particular subset of neurons from a specific area of the brain would greatly aid in the study of the neural stem cell differentiation into mesencephalic dopaminergic neurons. Cells generated by the fusion of N18TG2 cells with neurons expressing specific phenotypes of interest permits cloning and unlimited expansion of these monoclonal cell populations (Heller et al. 2000).

Among this cell line is a clonal catecholamine producing hybrid cell line designated as MN9D. It was derived from cells of mesencephalon and contains substantial quantities of dopamine (105 ng/mg of protein), tyrosine hydroxylase (TH) protein and TH mRNA. Briefly, the MN9D hybrid cells were prepared by polyethylene glycol-mediated fusion of cells from the embryonic rostral

mesencephalic tegmentum (RMT) with neuroblastoma cells (N18TG2), followed by isolation of monoclonal cells expressing a dopaminergic phenotype (Choi et al. 1992).

The MN9D cell line shows neuronal properties including catecholamine-specific histofluorescence, neurite formation with strong immunoreactivity to neurofilament proteins, and large voltage-sensitive sodium currents with the generation of action potentials. In contrast to the pheochromocytoma cell line (PC12), the dopamine content of the MN9D hybrid cell line is depleted by low concentration of dopamine cell-specific neurotoxin *N*-methyl-4-phenylpyridinium ion (MPP⁺), the active metabolite of the neurotoxin *N*-methyl-4-phenyl-1,2,3,6-tetrahydropyridine (MPTP) (Choi et al. 1991). Choi et al. (1992) also showed that the availability of MN9D cell line makes it possible to study the molecular mechanisms underlying trophic interactions between the central neurons. When MN9D cells were coaggregated with primary embryonic cells of optic tectum, a brain region that does not receive a dopaminergic innervation, there was a significant reduction in their dopamine content, tyrosine hydroxylase immunoreactivity, and tyrosine hydroxylase mRNA. Therefore, this shows that the MN9D hybrid cells are able to respond to an inhibitory factor(s) from the cell derived from brain areas that are not targets for dopaminergic neurons, whereas catecholamine-producing PC12 cells did not respond in a similar manner, suggesting that only the response of MN9D cells is a function of their mesencephalic origin (Choi et al. 1992). MN9D hybrid cell line was also reported to be morphological differentiated by exposure to *n*-butyrate (Choi et al. 1991; Wainwright et al. 1995).

1.6 Differentiation of neural stem cells (NSC)

The knowledge of how DA neurons can be formed would allow a reasonable process to be established for industrially producing a large number of such cells. These cells could be used for effective cell transplantation or cell therapy in which needed cells could be implanted under local anesthesia to brain regions that have lost more than 60-80% of the normal human set (500,000-1,000,000 DA cells in the human brain, substantia nigra region) (Isacson et al. 2001). The ability of neural stem cells to provide us with improved health and longevity is reliant on our ability to identify the extrinsic and intrinsic factors that direct the differentiation of neural stem cells to a desired lineage or phenotype. Induction of neural stem cells to make DA is a promising first step for cell replacement therapy in Parkinson's patients. However, a number of critical biological and safety issues have to be resolved before clinical utility of embryonic stem-derived DA neurons become viable.

1.6.1 Intracellular factors that cause differentiation of NSC into dopaminergic neurons

In order to study the creation of dopamine neurons from NSC to their highly specialized form in the adult brain, we need to start at the genetic level. The identification of genes controlling developmental mechanisms of ventral mesencephalic dopaminergic neurons can provide new insights in the etiology of Parkinson's disease. A number of genes related to the development or control of dopaminergic identity and specialization, such as *Nurr1* and sonic hedgehog protein, act in concert with transcription factors and downstream genetic activation of specific transmitter enzymes, for instance, TH and dopa-

decarboxylase, in dopaminergic neurons (Bjorklund et al. 2000; Deacon et al. 1998; Hynes and Rosenthal, 2000).

Nurr1 is an orphan nuclear receptor that belongs to the nuclear receptor superfamily of transcription factors that is expressed predominantly in the central nervous system, including developing and mature dopaminergic neurons. Nuclear receptors play fundamental roles in adult physiology and during development where they are essential for cell fate specification and differentiation of various cell types both within and outside of the nervous system (Kastner et al. 1995). During development, *Nurr1* is expressed at high levels in the VM region where DA neurons are being generated (Zetterström et al. 1996), and *Nurr1* is essential for the induction of phenotypic markers of ventral mid-brain dopaminergic neurons whose generation is specified by the floor plate-derived morphogenic signal sonic hedgehog. Studies have also shown that in absence of *Nurr1*, neuroepithelial cells undergo normal ventralization, differentiate into neurons, and adopt a specific mesencephalic phenotype that is identified by the homeodomain, *Pitx3* (Smidt et al. 1997). However, these dopamine precursor cells are arrested in a developmental state described by a lack of dopamine markers and die as development progresses to the neonatal stage (Saucedo-Cardenas et al. 1998). Therefore, *Nurr1* is also needed for both survival and final differentiation of VM late dopaminergic precursor neurons into a complete dopaminergic phenotype.

A previous study by Castro et al. (2001) has shown that *Nurr1* can induce cell cycle arrest and a highly differentiated morphology in MN9D cells. However, the mechanism whereby *Nurr1* promotes differentiation has remained unknown. They have also reported that retinoids could also promote the differentiation of MN9D cells independently of *Nurr1*. Retinoids (vitamin A derivatives) are known

to be potent inducers of cell differentiation in a variety of tissues *in vivo* as well as in many different cell lines cultured *in vitro*. They have demonstrated that both *Nurr1* and retinoids promotes cell cycle arrest at the G₁ phase and induce a mature and highly differentiated phenotype characterized by extension of long neurites (Castro et al. 2001).

Pitx3, a bicoid-related homeobox gene from the *Pitx*-subfamily, is a unique transcription factor marking the mesencephalic dopaminergic neurons at the exclusion of other dopaminergic neurons, are also reported to be involved in developmental determination of this neuronal lineage. *Pitx3* expression completely overlapped with TH-positive cells, demonstrating that *Pitx3* is expressed in dopaminergic neurons of mesencephalic system. Results suggested that *Pitx3* and *Nurr1* form a regulatory cascade for development of the mesencephalic dopaminergic neuron system in which *Nurr1* may act as an upstream activator (Smidt et al. 1997).

Smidt et al. (2000) also reported that they have identified another transcription factor expressed in mesencephalic dopaminergic neurons, the LIM homeobox gene, *Lmx1b*, and demonstrated that, together with *Pitx3*, this gene constitutes a molecular cascade independent of *Nurr1* and TH. This independent pathway seems to be essential for proper development of the system and may be linked to aspects of the mesencephalic dopaminergic system other than neurotransmitter identity. The data also suggested that at least two molecular cascades operate during the specification of the mesencephalic dopaminergic system, one involving *Lmx1b* and *Pitx3* pathway that may confer mesencephalic dopaminergic neurons unique intrinsic properties that might be useful in directing

commitment of dopaminergic cells *in vitro*, and the other involving *Nurr1*, essential for specifying neurotransmitter phenotype.

Arenas (2002) had reviewed that targeted deletions of *Pax2* (Favor et al. 1996) and *Pax5* (Urbanek et al. 1994), *Pax 2/5* (Schwarz et al. 1997), *wnt1* (McMahon and Bradley, 1990), *engrailed-1* (Wurst et al. 1994), *engrailed-2* (Hanks et al. 1995) and *FGF8* (Meyers et al. 1998), have all resulted in patterning defects in the midbrain-hindbrain region, arguing for a role of these genes in the establishment of midbrain and hindbrain identities.

1.6.2 Extracellular factors that cause differentiation of NSC into dopaminergic neurons

Ling et al. (1998) and Potter et al. (1999) reported that pluripotent lineage-restricted precursors derived from rat mesencephalic tissue could be expanded *in vitro* and differentiated into dopaminergic neurons using a combination of cytokines, growth factors, membrane fragments, and striatal culture conditioned media. These cells possessed numerous markers for DA neurons and were shown not only to survive transplantation into 6-OHDA-lesioned rats, but also produce significant functional recovery (Carvey et al. 2000).

Neurotrophic factor such as GDNF was reported to induce morphological differentiation of MN9D hybrid cell line (Heller et al. 1996; Lin et al. 1993). In another report (Rolletschek et al. 2001), neurotrophic factors, such as basic fibroblast growth factor (bFGF) and epidermal growth factor (EGF), in combination with survival-promoting factors, such as interleukin-1 β , GDNF, neurturin, TGF- β_3 and dibutyryl-cyclic AMP, significantly enhanced *Nurr1* and TH mRNA level. They also concluded that these survival-promoting factors

enhance differentiation, survival and maintenance of dopaminergic neurons derived from embryonic stem cells *in vitro*.

1.7 Significance of genes involved in dopaminergic neuron differentiation

The elucidation of the genes and mechanisms that regulate the development of the dopaminergic neurons is an important goal. In addition to being of immense intellectual interest, the study of such genes may provide valuable information related to the causes and treatment of neurological and neurodegenerative disorder such as Parkinson's disease. Over the past years, it has become clear that specific genes control dopaminergic neuron differentiation. Genes that are involved in the induction and regulation of such neural differentiation are just beginning to be discovered. However, given the enormous heterogeneity of genes involved and the complexity in dopaminergic neuron differentiation, it is not surprisingly that only a few of the required regulatory genes have been characterized, such as *Nurr1*, *Pitx3*, *Lmx1b*, etc. Thus, systematic searches for such genes and their differentiation pathways would be of significance.

We have previously combined the technologies of suppressive subtractive hybridization and custom cDNA micro-array to develop a high throughput screening procedure to identify genes differentially expressed in association with dopaminergic neuron differentiation (manuscript in preparation). This subtraction-coupled custom micro-array approach has successfully yielded a long list of candidate genes that were up-regulated during dopaminergic neuron differentiation. In this study, one of the genes in the list, namely *nm23-M2* was

being selected for further investigation in the elucidation of its role in dopaminergic neuron differentiation.

1.8 Literature reviews on factors that cause neurite outgrowth and differentiation in MN9D

At present, there are only 9 papers documented on investigating neurite outgrowth and differentiation of dopaminergic cell line using MN9D as an *in vitro* model. The originator of MN9D cell line, Heller et al. 1996, first reported on the application of an extrinsic neurotrophic factor, GDNF to induce morphological differentiation of MN9D cell line.

A number of putative genes were reported to induce MN9D neurite outgrowth such as Bcl-2 (Oh et al. 1996) and Calbindin-D28K (Choi et al. 2001). Overexpression of Bcl-2 in MD9D cells led to robust neurite formation without cessation of cell division and the neurite extension was enhanced via activation of c-Jun N-terminal kinase (JNK) (Eom et al. 2004, 2005). As mentioned earlier, both *Nurr1* and retinoids promotes cell cycle arrest at the G₁ phase and induce a mature and highly differentiated phenotype characterized by extension of long neurites (Castro et al. 2001).

Neurotransmitter receptors are known to have direct roles in the modulation of neuronal morphogenesis. Brief stimulation of D2, D3, D4 receptor-expressing MN9D cells also elicited increased neurite outgrowth when treated with quinpirole, an agonist of D2-like receptors (Swarzenski et al. 1994). This stimulation which could also be mimicked by the Gi/G(o) protein activator mastoparandopamine in D3 receptor. This implied that D3 receptor stimulation

has an immediate, G-protein-mediated role in neuronal morphogenesis (Swarzenski et al. 1996).

Many studies have suggest that dysfunction of mitochondrial proton-translocating NADH-ubiquinone oxidoreductase (complex I) is associated with Parkinson's disease (Wallace et al. 1992, Lestienne et al. 1990, Schapira et al. 1990, Swerdlow et al. 1996). The single-subunit NADH dehydrogenase of *Saccharomyces cerevisiae* (Ndi1P) can be used as a replacement for complex I in mammalian cells. Using a recombinant adeno-associated virus vector carrying the NDI1 gene, the Ndi1 enzyme was expressed in MN9D (Seo et al. 2002). NDI1-transduced cells were still capable of morphological maturation as examined by induction of neurite outgrowth. Hence, it is plausible that the NDI1 gene is useful in gene therapy in the treatment of neurodegenerative conditions caused by complex I inhibition.

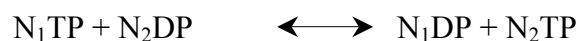
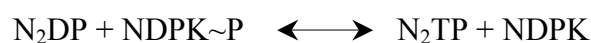
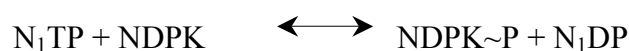
1.9 The *nm23* gene family

The *nm23* gene family includes four murine and eight human genes (Amrein et al. 2005). In mouse, *nm23*-M1, -M2, -M3, and -M4 encode for NDPKs A, B, C, and D, respectively. The first, referred to as *nm23*-M1, was isolated by subtractive cloning on the basis of its reduced expression in highly metastasis murine K-135 melanoma cell lines, as compared with their nonmetastasis counterparts, and has therefore been proposed as a metastasis suppressor gene (Steeg et al. 1988). Urano et al. 1992 first isolated the second mouse *nm23* gene, *nm23*-M2 from the normal mouse liver mRNA with primers designed for the human *nm23*-H2 gene, and *nm23*-M2 is also intimately related with the suppression of metastasis in the murine body (Baba et al. 1995). Seven human

nm23 genes have been documented, namely *nm23*-H1 (Rosengard et al. 1989), *nm23*-H2 (Stahl et al. 1991), DR-*nm23* (Venturelli et al. 1995), *nm23*-H4 (Milon et al. 1997), *nm23*-H5 (Munier et al. 1998), *nm23*-H6 (Tsuiki et al. 1999) and *nm23*-H7 (Seifert et al. 2005). Mehus and Lambeth identified the *nm23*-H8 gene in 1999 and its nucleotide sequences have been submitted to the GenBank database with the accession number AF202051 but have not yet been published (Amrein et al. 2005). *Nm23*-H1 gene has been proposed as a suppressor of metastatic ability in some tumor cells (Bevilacqua et al. 1989 and Fujimoto et al. 1998). *Nm23*-H2 was identified as c-myc transcription factor named purine-binding factor (PuF) (Postel et al. 1993). Several genes with highly homologous sequences have been characterized and shown to code for nucleoside diphosphosphate kinase (NDPK, EC 2.7.4.6) in a wide variety of organisms, including the prokaryote (*Myxococcus xanthus*) (Munoz-Dorado et al. 1990), lower eukaryotes (*Dictyostelium discoidium*) (Lacombe et al. 1990), and higher eukaryotes such as *Drosophila* (Biggs et al. 1990), *Xenopus* (Ouatas et al. 1997), and rat (Kimura et al. 1990; Shimada et al. 1993).

1.9.1 Biochemical functions of *nm23*/NDPK proteins

The *nm23* gene which encodes NDPK are classic ubiquitous metabolic enzyme that catalyzes the reversible transfer of γ -phosphate from nucleoside triphosphates to nucleoside diphosphates through autophosphorylation (Parks and Agarwal, 1973):



where NDP and NTP are nucleoside (or 2'-deoxynucleotide) diphosphate and triphosphate, respectively. The reaction involves the transient phosphorylation of a conserved histidine, namely histidine 118 in the human NDPK enzymes (Gilles et al. 1991). For example, it provides nucleoside triphosphates for nucleic acid synthesis, CTP for lipid synthesis, UTP for polysaccharide synthesis, and GTP for protein elongation. Therefore, it is an important enzyme for maintaining stable GTP levels through nucleotide homeostasis in various metabolic pathways such as protein and DNA synthesis and GTP-mediated signal transduction pathways. The X-ray structure of several NDPKs has been solved, showing that in eukaryotes, NDPKs are hexamers composed of two identical trimers (Dumas et al. 1992; Chiadmi et al. 1993; Williams et al 1993). Eukaryotic NDPKs have been reported to be catalytically active only as homo- or hetero-hexamers. In humans, the hexamers consist of two highly homologous subunits *nm23-H1*/NDPK A and *nm23-H2*/NDPK B, having an 88% amino acid sequence identity (Gilles et al. 1991). In mouse, although the four recombinant NDP kinases can be reconstituted into hetero-hexamers *in vitro* (Lascu et al. 2000), no information is presently available either on the physiological effects of the relative concentration of each subunits in the complex formation, or on a possible involvement of these isoforms *in vivo* in the hexameric conformation of the protein.

Nm23/NDPK have also been reported to exhibit a histidine protein kinase activity (Wagner et al. 1995; Freije et al. 1997) and a histidine-dependent protein phosphotransferase activity (Engel et al. 1995; Freije et al. 1997; Wagner et al. 1997) that has been indicated as functionally involved in the metastasis suppressive effect of *nm23*-H1 (Freije et al. 1997). Specifically, the transfer of phosphate from recombinant *nm23*-H1 to aspartates or glutamates on other proteins correlates with the suppression of cell motility (Wagner et al. 1997).

Transactivating factor PuF which interacts with a nuclease hypersensitive element (NHE) locates upstreams from the *c-myc* gene. *C-myc* gene is a key regulator of cellular proliferation, embryonic differentiation and apoptosis. *Nm23*-H2 recognizes the CT element/PuF site in the *c-myc* promoter through which it activates *in vitro* transcription (Postel et al. 1993) independently of NDPK catalytic activity (Postel and Ferrone, 1994). Moreover, it has been shown that *nm23*-H2 exhibits a poor binding activity to double-stranded oligonucleotides while preferentially binds single-stranded polypyrimidine-rich sequences (Hildebrandt et al. 1995; Agou et al. 1999) and it has been suggested that it regulates gene expression by altering promoter DNA structure (Postel, 1988). Furthermore, the murine *nm23*-M2 transactivates the *c-myc* gene and controls the cell cycle, S-phase, indirectly via a cellular cofactor in the murine cell line (Lee et al. 1997) and *nm23*-M2 activates endogenous *c-myc* expression both at transcriptional and translational levels (Arnaud-Dabernat et al. 2004).

1.9.2 Cellular studies support a role for *nm23*/NDPK in signal transduction

Increasing evidence indicates that the *nm23* genes, initially documented as suppressors of metastasis progression, are involved in normal development and differentiation. Several reports suggest that, in addition to their basic enzymatic activity and probably independently of their catalytic site, NDPK isoforms are involved in other cellular functions, such as cell growth and differentiation, embryonic development, tumor progression, metastasis, and apoptosis (Otero 2000; Hartsough and Steeg 2000; Kimura et al. 2000; Lacombe et al. 2000; Postel et al. 2000). There are many reports that document the involvement of *nm23*/NDPK in the responsiveness of cells to extracellular stimuli. Melanoma and breast carcinoma cells over-expressing *nm23*-H1 display a reduced response to the cytokine TGF- β 1 (Leone et al. 1991, 1993) and their motility in response to serum, PDGF, and IGF-1 is markedly inhibited (Kantor et al. 1993; MacDonald et al. 1996; Russell et al. 1998). However, there are also inconsistent observations on the effect of *nm23*/NDPK on NGF signaling in PC12 cells: in one case, overexpression of *nm23*-H1 promoted NGF-induced differentiation (Gervasi et al. 1996), while in another, it caused cells to differentiate in the absence of NGF (Ishijima et al. 1999). Evidently, *nm23*/NDPK modulate cellular signal transduction networks. However, the results do not follow an obviously apparent pattern, to date, there is still no unifying hypothesis for the role of *nm23*/NDPK in signal transduction.

1.9.3 *Nm23*/NDPK homologues in fruit fly development and differentiation

The existence of multiple *nm23*/NDPK proteins raises the question whether they carry out redundant NDPK activity or, instead, perform specialized functions, not necessarily related to nucleoside phosphorylation, and probably depending on different cellular contexts. The involvement of the *nm23* genes in normal development and differentiation is supported by several observations. The NDPK exhibit an approximate 75% homology with the *Drosophila melanogaster nm23* homologue, abnormal wing discs (*awd*) protein (Rosengard et al. 1989) which also displays NDPK activity and is required for proper differentiation of tissues of epithelial origins. Null mutations or reduced expression of the gene allows normal embryonic development until metamorphosis but cause widespread abnormalities at the onset of tissue differentiation. The altered larvae development is characterized by abnormal tissue morphology, aberrant differentiation, and eventual necrosis of the imaginal discs, brain and proventriculus (Dearolf et al. 1988). Normal development and differentiation are restored by transfecting the mutant *awd* germline with the wild-type *awd* gene (Timmons et al. 1993). The *killer of prune* (*k-pn*) mutation of the *awd* gene that changes proline 97 to serine in the *awd* protein has no effects by itself but is lethal in the genetic context of the *prune* (*pn*) eye color mutation (Biggs et al. 1988). Interestingly, it has been shown that the *k-pn* mutation, without coordinate expression of *pn*, suppresses the *tum-1* hematopoietic oncogene of *Drosophila* (Zinyk et al. 1993). The mechanisms underlying the developmental abnormalities due to *awd* mutations and the lethal interaction between *pn* and *k-pn* are still unclear (Timmons and Shearn, 1997).

1.9.4 *Nm23*/NDPK in hematopoietic differentiation

The relation of *Nm23* genes expression to hematopoietic differentiation has also been investigated in several studies (Yamashiro et al. 1994). It has been reported that intracellular *nm23*-H1 expression levels decrease during *in vitro* induced differentiation of megakaryoblastic MEG-01 and promyelotic HL-60 leukemia cell lines (Zhu et al. 2001). On the contrary, during differentiation of human K562 erythroleukemia cells, *nm23*-H1 expression levels increase. Furthermore, *nm23*-H1 cDNA-transfected K562 cells are better induced to synthesize hemoglobin (Yamashiro et al. 1994). The authors concluded that *nm23*-H1 might contribute to the maintenance of the immature phenotype in some leukemia cells, whereas it might play a role in the differentiation of erythroleukemia cells. The presence of NDPK in human plasma and down-regulation of *nm23* expression (H1, H2 and H3) was also observed during maturation of CD34⁺ progenitor cells (Willems et al 1998; Venturelli et al. 1995), and *nm23*-H1 and *nm23*-H2 were strongly up-regulated after activation of peripheral blood lymphocytes (Keim et al. 1992). The partial amino acid sequence determined from cyanogens bromide fragments of the differentiation inhibiting factor (I-factor), purified from the conditioned medium of the differentiation-resistant mouse myeloid leukemia M1 cell line, has shown identity with *nm23*-M2 (Okabe-kado et al. 1995a), and the differentiation inhibitory activity of the *nm23*/NDPK protein is independent of its enzyme activity and requires the presence of N-terminal peptides (Okabe-kado et al. 1995a, 1995b). The expression of *nm23*-H1 and *nm23*-H2 in the majority of cells of hematopoietic origin suggests that, during hematopoiesis, the *nm23* genes regulate different stages of

the differentiation process, depending on the specific cellular lineage (Okabe-kado et al. 2002).

1.9.5 *Nm23*/NDPK in mammalian neuronal cell development and differentiation

The positive role of *nm23*/NDPK during development and differentiation of cells and tissues has been frequently described in the literature. The high level of NDPK expression at the mRNA and protein levels was demonstrated in postmitotic rat tissues, such as heart and brain (Kimura et al. 1990; Shimada et al. 1993). *In situ* hybridization and reverse transcriptase-polymerase chain reaction analysis demonstrated high levels of *nm23*-M1, -M2, and -M3 mRNA expression in peripheral nervous tissue and showed the differential expression of *nm23* genes in adult mouse root ganglia (Barraud et al. 2002). Considering that the specific activity of NDPK in brain was higher (0.15 U/mg protein) than in other tissues (Mourad et al. 1966) and its expression was accumulating preferentially in the nervous system during the early embryonic development (Lakso et al. 1992), NDPK could play a pivotal role in brain functions to modulate neuronal cell proliferation, differentiation, and neurite outgrowth.

The pattern of *nm23* expression in tissue development has been studied by different approaches during embryogenesis and organogenesis. Previous immunohistochemical studies aiming to provide a detailed analysis of *nm23* expression patterns during mouse embryonic development have often been hindered by the use of antibodies unable to discriminate between the isoforms (Lakso et al. 1992). Subsequently, a few studies involving the use of specific mRNA probes have revealed the nervous expression of mRNA encoding the

NDPK A isoform in *Xenopus* (Ouatas et al. 1998), rat (Shimada et al. 1993) and mouse (Gervasi et al. 1998; Dabernat et al. 1999; Masse et al. 2002). In all organisms studied, the NDPK B isoform is expressed in most tissues. In a recent paper (Amrein et al. 2005), differential expression of mRNAs encoding NDPK A, B, C and D isoforms at different stages of mouse development were analyzed by in situ hybridization on whole-mount embryos and cryostat sections. Their expression in adult and embryonic central and peripheral nervous system suggests that *nm23* gene products participate in neuronal functions.

The association of NDP kinase with microtubule protein has been observed in mammalian cell system (Nickerson and Wells, 1984; Lombardi et al., 1995). An increase in the expression of *nm23*-M1 protein and a pattern of coimmunoprecipitation of *nm23*-M1 protein (NDP kinase alpha) and β -tubulin has been detected under differentiation conditions, and that the number of *nm23*-M1/ β -tubulin complexes increased during the differentiation process of murine myogenic cells. All these suggested a participation of *nm23* in microtubule assembly during differentiation (Lombardi et al. 1995). In brain, *nm23*/NDPK has been reported to be co-localized with microtubules and suggested to influence neurite outgrowth by altering microtubule dynamics (Huitorel et al. 1984).

The overexpression of *nm23*/NDPK could rapidly induce neurite outgrowth with the increased expression of neurofilament and microtubule proteins (Gervasi et al. 1996; Ishijima et al. 1999), brain *nm23*/NDKP has an ability to drive neuritogenesis by influencing the expression of cytoskeleton proteins and its deterioration could result in the defect of neuronal processes such as neurite outgrowth and axonal sprouting. The protective effect of NDPKs against oxidative stress induced cell death in BAF3 cells was also documented in

Arnaud-Dabernat et al. 2004. This also coincides with the report in *Arabidopsis thaliana*, the orthologous NDPK2 gene was shown to induce plant tolerance against several environmental stresses such as cold, salt and H₂O₂ by decreasing the level of reactive oxygen species (ROS) (Moon et al. 2003). Interestingly, the role of *nm23*/NDPK in neurodegenerative diseases was investigated in Kim et al. 2002 and *Nm23-H1*/NDPK-A protein level was shown to be significantly decreased in brain regions (frontal, occipital, and parietal cortices) of both Alzheimer's disease and Down syndrome. They proposed that oxidative modification of NDPK could lead to the decreased activity of NDPK and subsequently, influence several neuronal functions in neurodegenerative diseases as multifunctional enzyme through several mechanisms.

1.9.6 Role of *nm23*/NDPK in neuroblastoma differentiation

DR-*nm23* (*nm23-H3*) was well studied during neuroblastoma cells differentiation in many papers (Amendola et al. 1997, 2001; Martinez et al. 1997). DR-*nm23* expression increased after retinoic acid induction of differentiation in human cell lines SK-N-SH and LAN-5. Overexpression of DR-*nm23* promotes differentiation of human neuroblastoma cells towards neuronal and schwannocytic phenotype. The cells exhibited marked decrease in proliferation, increased differentiation related proteins such as vimentin and collagen type IV, modulation of integrin expression, and underwent growth arrest, which were relevant to differentiation. Overexpression of DR-*nm23* in the murine neuroblastoma cell line N1E-115 also showed neurite outgrowth and a striking enhancement of beta1 integrin expression, while mutations in the catalytic domain and in the serine 61 phosphorylation site, possibly required for protein-protein interactions, impair the

ability of DR-nm23 to induce neural differentiation (Negroni et al. 2000). Overexpression of wild type *nm23*-H1 proteins in IMR-32 human neuroblastoma cells also stimulated spontaneous neurite outgrowth and enhanced differentiation in response to serum starvation and retinoic acid (Backer et al. 2000).

1.10 Objective of this study

In order to determine what role, if any, *nm23*-M2 gene might play in dopaminergic neuronal differentiation, this study makes use of a catecholamine producing hybrid dopaminergic cell line, MN9D as an *in vitro* cell model system. *Nm23*-M2 gene was selected based on the previous findings that this gene was found to be up-regulated during *n*-butyric acid induced MN9D differentiation and that various relevant literature reviews also supported the notion of *nm23*/NDPK being involved in development and differentiation, moreover, overexpression of *nm23* genes induces neuritogenesis and stimulates the differentiation pathways in many cell lineage. The findings of this present study may serve as a fundamental knowledge of how *nm23*-M2 gene may be involved in dopaminergic neuron differentiation and ultimately aid in the development of gene therapy in treating neurodegenerative disorders such as PD.

The cloning, temporal and spatial pattern of gene expression, cellular localization of *nm23*-M2 will be explored in details. Both hypothesizes of: 1) overexpression of *nm23*-M2 gene will cause MN9D cells to differentiate, inducing neuritogenesis and cell cycle arrest, and 2) siRNA interference of *nm23*-M2 gene will abolish neurite outgrowth of MN9D cells in differentiation conditions, were tested in this study. The role of *nm23*-M2 in dopaminergic neuronal differentiation would thus be elucidated by overexpression and siRNA interference studies.

Laboratory techniques such as molecular cloning, cell culture and transfection, real-time PCR, western blot analysis and flow cytometry analysis were employed in this study. Cell cycle analysis was performed to look at events of cell cycle arrest, which is a characteristic of terminal differentiation. The alteration in protein levels of a maturation marker, synaptosomal associated protein, SNAP-25, and a key cell cycle regulatory gene, cyclin D1, was monitored after each overexpression and RNA interference studies to investigate dopaminergic cell maturation and differentiation.

Chapter 2:

Materials and methods

Chapter 2: Materials and methods

2.1 Routine cell culture of MN9D and SH-SY5Y cell lines

The MN9D cell is a mouse dopaminergic neuronal cell line derived from the fusion of rostral mesencephalic neurons from embryonic C57BL/6J mice with N18TG2 neuroblastoma cells (Choi et al. 1991). MN9D was deemed suitable in this study because it is dopaminergic and neuronal in nature – a fundamental feature for cell lines used as PD models. In addition, it is of mesencephalic origin – a feature absent in other cell models used currently. SH-SY5Y is a human neuroblastoma cell line established from a highly malignant tumour. The cells have retained a capacity to differentiate *in vitro* in response to low concentrations of the phorbol ester 12-O-tetradecanoylphorbol-13-acetate (TPA) in the presence of serum or defined growth factors. Differentiated cells are characterized by neurite formation and upregulation of neuronal marker genes. The MN9D cells were from Dr J. Chen of the University of Pittsburgh, used with permission from Dr A. Heller of the University of Chicago and SH-SY5Y cells were obtained with courtesy from Dr. K. L. Lim (National Neuroscience Institute, Singapore).

Both MN9D and SH-SY5Y cells were routinely cultured in Primaria-coated petri dishes (BD Bioscience, USA) or 100mm x 20mm polystyrene-treated Corning plate (Corning, USA) in Dulbecco's MEM (DMEM) (NUMI, Singapore) containing 10% fetal bovine serum (Hyclone, USA) and 1% v/v penicillin-streptomycin (Sigma, USA). Some MN9D hybrid cells were differentiated by addition of 1mM *n*-butyric acid (Sigma, USA) to DMEM culture medium. All cell lines were maintained in a CO₂ incubator (Binder, Germany) at 37°C, 5% carbon dioxide / 95% room air. The cell medium was changed every alternate day. When the cells were about 80-90% confluence, the medium was removed and the cells

were washed with 1X phosphate buffer saline (PBS) (NUMI, Singapore). The cells were then dislodged from the bottom of the petri dish with 1X Trypsin-EDTA (Sigma, USA). Fresh DMEM culture medium was added to inactivate Trypsin-EDTA followed by dilution and distribution of the cells equally into new culture plates to grow.

2.2 Cloning of full length *nm23-M2* gene

2.2.1 Total RNA isolation

Cells were grown to about 80-90% confluence prior to total RNA isolation. Approximately 10^7 cells were used for each RNA isolation batch. Total RNA was isolated using RNeasy Mini Kit (Qiagen, USA). The RNeasy mini protocol for isolation of total RNA from animal cells can be obtained in RNeasy Mini Handbook, Third Edition (June 2001, page 31-35). The cells were disrupted by addition of 600 μ l of Buffer RLT and homogenized by passing the lysate at least 5 times through a 20-gauge needle fitted to an RNase-free syringe. A volume of 600 μ l 70% ethanol was mixed well with the homogenized lysate by pipetting. The sample was then applied onto an RNeasy mini column placed in a 2ml collection tube. The column was then centrifuged for 15 sec at more than 8000 x g. The flow-through was then discarded. A volume of 700 μ l Buffer RW1 was added to the RNeasy column and centrifuged for 15 sec at more than 8,000 x g to wash the column. The flow-through was again discarded. The column was then transferred into a new 2ml collection tube, in addition, 500 μ l of Buffer RPE was applied to the column and centrifuged for 15 sec at more than 8,000 x g. The flow-through was then discarded. Another 500 μ l of Buffer RPE was added to the column and centrifuged for 2 min at more than 8,000 x g. The flow-through was

again discarded and the column was transferred into a new 1.5ml collection tube. A volume of 30 μ l RNase-free water was passed through the RNeasy silica-gel membrane to elute the total RNA. The column was centrifuged for 1 min at more than 8,000 x g. This process was repeated with another 10 μ l of RNase-free water to obtain a higher total RNA concentration. The eluted total RNA was then ethanol-precipitated by adding 180 μ l of absolute ethanol and 6 μ l of 3M sodium acetate. The samples were placed in -80°C freezer for at least 1 hour and centrifuged at 14,000 x g, 4°C for 30 min. The supernatant was then discarded by pipetting. The pellet was washed with 200 μ l of 70% ethanol and centrifuged for 5 min at 4°C, 14,000 x g. The supernatant was then discarded and the pellet was air-dried. The pellet was re-dissolved in 10 μ l of RNase-free water and stored in -80°C freezer for later use. The integrity of the total RNA can be determined by running a 1% agarose gel electrophoresis to see if there is any degradation of total RNA. The total RNA concentrations were then measured by using mass spectrophotometer. The total RNA was diluted with RNase-free water, placed into a 100 μ l quartz microcuvette and the absorbency at 260nm and 280nm wavelengths were recorded. The following formula was used to calculate the concentration of the total RNA:

$$[\text{RNA}] = (0.04\mu\text{g}/\mu\text{l}) (A_{260}) (\text{Dilution factor})$$

The purity of the total RNA can be estimated by the ratio of the absorbency at 260 nm wavelength over the absorbency at 280nm wavelength.

The total RNA yield can be calculated by multiplying the concentration by the volume of the total RNA sample in milliliters.

2.2.2 Reverse Transcriptase-PCR (RT-PCR) of full length *nm23-M2* gene

First-strand cDNAs were synthesized from the total RNA isolated and polymerase chain reaction (PCR) amplification of full length mouse *nm23-M2* cDNA was carried out using Access RT-PCR System (Promega, USA). The PCR amplification was carried out with 1 set of specific primers (NdpkB-Forward: 5'-ATG GCC AAC CTC GAG CGT-3' and NdpkB-Reverse: 5'-CTA CTC GTA CAC CCA GTC-3') to generate full length *nm23-M2* cDNA insert.

2.2.3 Gel extraction and DNA purification of *nm23-M2*

The PCR product of full length *nm23-M2* cDNA was subjected to DNA agarose electrophoresis to check on the molecular size of the cDNA insert. The full length *nm23-M2* DNA fragment from the agarose gel was excised with a clean scalpel and was purified using QIAquick Gel Extraction Kit (Qiagen, USA). The gel slice was weighed and 3 volumes of Buffer QG was added to 1 volume of gel (100mg ~ 100µl). The gel slice was incubated at 50°C for 10 min while vortexing the tube every 2-3 min to help in dissolving the gel. Isopropanol of 1 volume was added and the sample was applied to the QIAquick column, and centrifuged for 1 min. The flow-through was discarded while 500µl of Buffer QG was then added and centrifuged for 1 min. The flow-through was discarded while 750µl of Buffer PE was added to wash the column. The sample was centrifuged for 1 min and the flow-through was then discarded. The column was then centrifuged again for an additional of 1 min to remove the residual ethanol. The column was placed into a clean 1.5ml microcentrifuge tube and 40µl of sterile water was used to elute the purified DNA.

2.2.4 Cloning of full length *nm23-M2* coding sequence into pGEM-T EasyTM plasmid vector

The amplified full length *nm23-M2* cDNA were subsequently sub-cloned into the vector by using pGEM-T Easy vector system I kit (Promega, USA) and the recombinant plasmid was termed as pGEM-T Easy_mNm23-M2. DNA ligation reaction was carried out typically in 10ul of volume, containing 5µl of 2X ligation buffer, 0.5µl of vector DNA, 3µl of insert DNA generated by *Taq* DNA polymerase and 1µl of T4 DNA ligase and topped up with PCR water to a final volume of 10µl. The ligation mixture was incubated at 4°C for about 16 hr before transformation. The pGEM-T Easy vector map is shown in figure 2.1.

Alternatively, thermostable DNA polymerases with proofreading activity, such as *Pfu* DNA polymerase and *Tfl* DNA polymerase generate blunt-ended fragments during PCR amplification. Nevertheless, these PCR fragments can be modified using the A-tailing procedure before ligating them into the pGEM-T easy vectors. Using this TA cloning method, only one insert will be ligated into the vector as compared to multiple insertions that can occur with blunt-ended cloning. In addition, there is no need to de-phosphorylate the vector with TA cloning. Briefly, 1-7µl of purified PCR fragment was mixed with 1µl *Taq* DNA polymerase 10X reaction buffer with MgCl₂, 5 units of *Taq* DNA polymerase and dATP was added to a final concentration of 0.2mM. The reaction mixture was topped with deionized water to a final reaction volume of 10µl and then incubated at 70°C for 15-30 min. The modified PCR fragment can then be ligated directly into pGEM-T easy vector using standard protocol as above.

2.2.5 Transformation of recombinant plasmids into bacterial competent cells

2.2.5.1 Preparation of bacterial competent cells

For the preparation of bacteria competent cells, 100ml of LB broth was incubated with a 5ml of *Escherichia coli* (*E. coli*) strain DH5 α (Invitrogen, USA) at 37 $^{\circ}$ C with 2,700 x *g* shaking overnight. In the following morning, 1ml of the culture was spiked into 200ml of fresh LB medium and subjected to shaking at 2,700 x *g* at 37 $^{\circ}$ C until OD₅₉₀ reached around 0.4. The culture was chilled on ice for 15 min and transferred to pre-chilled sterile 50ml Falcon 2070 tubes. Cells were pelleted by centrifugation at 3,000 x *g* at 4 $^{\circ}$ C for 5 min. The LB medium was decanted off and the tubes left standing upside-down on a pad of C-Fold towels for 1 min. The cell pellet was re-suspended in 0.1M CaCl₂ and put in ice for 45 min. The cells were then pelleted by centrifugation 3,000 x *g* at 4 $^{\circ}$ C for 8 min. The supernatant was discarded and the cell pellets were re-suspended in 2ml of ice-cold 0.1M CaCl₂ for each 50ml of original culture. At this point, the cells were either use directly for transformation or aliquoted into 1.5ml microcentrifuge tubes After 20 min incubation on ice, the competent cells were stored at -80 $^{\circ}$ C freezer for several months.

2.2.5.2 Transformation

A volume of 5 μ l of ligation reaction was mixed with 100 μ l of *E. coli* DH5 α competent cells as prepared in section 2.2.4.1. The mixture was incubated on ice for 20 min and then heated at 37 $^{\circ}$ C for 5 min. The tube was cooled immediately on ice for 2 min and mixed with 400 μ l of LB (Luria-Bertani) broth (OXOID, UK) without antibiotics. After incubating it at 37 $^{\circ}$ C for 1 hr with

shaking at 2700 x g, the transformation mixture were centrifuged at 1600 x g for 1 min and one-tenth of the mixture was aliquoted and was spread onto fresh LB agar plates by inoculating loops for colony selection. The LB plates were supplemented with X-gal (Bio-Rad, USA) and IPTG (Bio-Rad, USA) in the presence of 20µg/ml ampicillin (Sigma, USA). After an overnight incubation at 37⁰C, colonies of transformed cells were selected according to their antibiotic resistance and *lac*⁻ phenotype. White bacterial colonies were chosen, from each of which bacteria cells were picked up via a sterile toothpick and were subjected to colony screening for positive clones. Individual selected bacteria cells were also streaked onto a master LB agar plate and stored at 4⁰C for later use. The bacteria cells on individual toothpick were also inoculated onto LB medium supplemented with 20µg/ml ampicillin with incubation overnight at 37⁰C for DNA plasmid isolation.

2.2.6 Colony PCR screening for positive clones

Using colony PCR screening method, the following PCR reaction mixture was prepared:

Reagents	Volume (µl)
10 mM dNTPs	0.4
10X PCR reaction buffer	2.0
MgCl ₂ (25 mM)	1.2
T7 primer (20 pmol/µl)	0.2
SP6 primer (20 pmol/µl)	0.2
<i>Taq</i> polymerase	0.2
Deionized water	15.8
Total volume	20.0

White bacterial colonies in the culture plates were picked and individually mixed with the PCR reaction mixture. The following conditions were set for the

PCR reaction in a Peltier-Effect Cycling PTC-1000 Programmable Thermal Controller (MJ Research, USA):

Stage 1: Initial denaturation: 94°C for 2 minutes in 1 cycle.

Stage 2: Step 1, denaturation: 94°C for 30 seconds.

Step 2, Annealing: 55°C for 30 seconds.

Step 3, Elongation: 72°C for 1 minute.

Stage 2 was carried out for 40 cycles.

Stage 3: Final elongation: 72°C for 7 minutes.

Colonies which contained the inserts were identified by agarose gel electrophoresis and were prepared for sequencing as described in section 2.2.6 – 2.2.8. The positive clones were identified as those that contained the full length sequence of *nm23-M2* cDNA.

2.2.7 Plasmid DNA isolation from positive clones

Small-scale isolation of plasmid DNA from positive clones was carried out using Qiagen Mini-prep Kit (Qiagen, Germany). It involved alkaline lyses followed by binding of plasmid DNA to a silica-based resin. DNA was eluted in low salt buffer or water. Up to 10µg of high copy number plasmid DNA can be isolated from 3ml of overnight bacteria culture in LB medium.

Firstly, the bacteria in LB liquid medium with appropriate antibiotics were harvested by centrifugation for 5 min at 10,000 x *g* using the 5417C centrifuge (Eppendorf, Germany). The bacterial pellet was then re-suspended in 250µl of Cell Re-suspension Solution P1 (10mg/ml RNase A; 10mM EDTA; 25mM Tris-HCl, pH 7.5). 250µl of Cell Lysis Solution P2 (0.2M NaOH; 1% SDS) was added to the bacterial suspension and mixed by gently inverting the tubes for 4-6 times.

The mixture was neutralized by adding 350µl of Neutralization Buffer N3 (1.32M KOAc, pH 4.8). After being centrifuged in a micro-centrifuge tube at 10,000 x g for 10 min, the supernatant was applied into the QIAprep spin column with a purification resin and a fresh 2ml collection tube. The resin/DNA mix was washed with 750µl of Column Wash Buffer PE by centrifugation for 1 min and the flow-through was discarded. Residual wash buffer was completely drained by spinning down into the collection tube at 10,000 x g for another 1 minute. The mini-column was then transferred to a new microcentrifuge tube and eluted with 40µl of PCR water. After 1 min incubation at room temperature, plasmid DNA was eluted from the column by centrifugation at 10,000 x g for 1 min.

2.2.8 Cloning of full length *nm23*-M2 coding sequence into mammalian pcDNA3.1-GFP and pcDNA 3.1-MYC plasmid vector

The eukaryotic expression vector pcDNA3.1 (plasmid map shown in figure 2.2) tagged with *c-Myc* or GFP were obtained with courtesy from Dr. Arenas E. (Karolinska Institute, Sweden). Expression plasmid encoding a GFP epitope-tagged version of the mouse *nm23*-M2 protein termed as pcDNA3.1(-)_fl *nm23*-M2_GFP was constructed as follows: PCR amplification of the full length *Nm23*-M2 gene was carried out using pGEM-TEasy_mNm23-M2 plasmid described above as a template with the following set of specific primers (NdpkB(*Xba*I+KS)-Forward: 5'-GGG CCC TCT AGA ACC ATG GCC AAC CTC GAG CGT A-3' and NdpkB(Stop+*Eco*RI)-Reverse: 5'-GTG GTG GAA TTC CTC GTA CAC CCA GTC ATG-3'. The amplified DNA product was then digested with the restriction enzymes *Xba*I and *Eco*RI and ligated into the

pcDNA3.1(-)_GFP vector. For expression plasmid encoding a *c-Myc* epitope-tagged version of the mouse *nm23*-M2 protein termed as pcDNA3.1(-)_fl *nm23*-M2_MYC, the amplified DNA product was also digested with the restriction enzymes *XbaI* and *EcoRI* and ligated into the pcDNA3.1(-)_MYC vector.

2.2.9 Cycle sequencing

ABI PRISM® BigDye™ Terminator v3.0 Ready Reaction Cycle Sequencing Kit

(Applied Biosystems, USA) was used for the sequencing reactions and the following reaction mixtures were prepared:

Reagents	Volume (μl)
Terminator Ready Reaction Mix	8.0
T7 Primer (2 pmol/μl)	1.6
DNA Template	8.0
Deionized water	2.4
Total volume	20.0

The following conditions were set for the PCR reaction in a Peltier-Effect Cycling PTC-1000 Programmable Thermal Controller (MJ Research, USA):

Stage 1: Rapid thermal ramp to 96°C,
 Stage 2: Step 1: 96°C for 10 sec,
 Step 2: Rapid thermal ramp to 50°C,
 Step 3: 50°C for 5 sec,
 Step 4: Rapid thermal ramp to 60°C,
 Step 5: 60°C for 4 min,
 Repeat the following for 25 cycles.

Stage 3: Rapid thermal ramp to 4°C and hold until ready to purify.

2.2.10 Ethanol/sodium acetate precipitation for DNA purification

In order to precipitate in microcentrifuge tubes, the following mixture were prepared and combined to each sample:

- 3.0µl of 3M sodium acetate (NaOAc), pH 4.6
- 62.5µl of non-denatured 95% ethanol (EtOH)
- 14.5µl of deionized water

This 80µl of ethanol/sodium acetate solution was added to 20µl of reaction mixture and vortexed briefly. The tubes were then incubated at room temperature for 15 min to precipitate the extension products. The tubes were spun in a microcentrifuge for 20 min at maximum speed. Followed by, aspirating and discarding of the supernatants with a separate pipette tip for each sample. 70% ethanol of 500µl was added to the tubes and mixed briefly. The tubes were then centrifuged again for 5 min at maximum speed. The supernatants were then discarded carefully and the samples were air-dried for 10-15 min.

2.2.11 Capillary electrophoresis sequencing on ABI PRISM 3100

Genetic Analyzer

Each sample pellet was re-suspended in 10µl of deionized high-dye formamide and vortexed thoroughly. The samples were denatured by heating at 95°C for 2 min followed by chilling on ice for another 2 min. The samples were then loaded into the *ABI PRISM® 3100 Genetic Analyzer* (Applied Biosystems, USA) for automated sequencing.

2.2.12 DNA gel electrophoresis

PCR products were analyzed by gel electrophoresis. The DNA samples were first mixed with 1X loading dye (6X Blue/Orange Loading Dye, Promega, USA). They were then loaded into the wells of 1.0% agarose (Promega, USA) gel in 1X TAE buffer (0.04M Tris-acetate, 0.01M EDTA, pH 8.0) with 0.4µg/ml ethidium bromide (Boehringer Mannheim, GmbH, Germany). A 100bp or 1kb DNA ladder (Promega, USA) was loaded into the wells for verifying the molecular size of the DNA fragments. Electrophoresis was normally carried out at a constant voltage of 90-100 volts in 1×TAE buffer, until the bromophenol blue front had migrated two-third of the length of the gel. The DNA samples were visualized in ultra-violet light at 254nm using BioDoc-It System UV transilluminator (Ultra-Violet Products, UVP, USA) and documented onto thermal paper by digital thermal printer (Mitsubishi, 115V, UVP, USA).

2.3 Construction of cDNAs for Real-time PCR

RNA was isolated using the RNeasy Mini kit (Qiagen, USA) as described in section 2.2.1. To remove any contamination of genomic DNA, 1µl of DNase (1 unit/µl) was added to 1µg of RNA and topped up with deionized water to a final volume of 10.5µl. The mixture was then incubated at 37°C for 40 min. Next, 1µl of 0.02M EDTA was added followed by an incubation at 65°C for 10 min. Random priming was carried out by adding 0.5µl of random primers and incubating at 65°C for 10 min and then placed on ice. For reverse transcription, the random-primed RNA was split into 2 tubes – RT+ and RT- (6µl each) and 6µl of deionized water, 4µl of 5 X first strand buffer, 2µl of 0.1M DTT and 1µl dNTPs were added into each tube. The tubes were then incubated at 25°C for 10

min followed by 42°C for 2 min after which 1µl of reverse transcriptase was added to the RT+ tube. The tubes were then incubated at 42°C for 50 min, 70°C for 10 min and stored at -20°C.

2.4 Real-time PCR

The five cDNA standards used were undiluted cDNAs synthesized from total RNA of untreated MN9D cells. Standard and test cDNA templates were added with SYBR green master mix, specific sets of primers (*nm23-M2* mRNA: NdpkB(28)-Forward: 5'-CCT CGAGCG TAC CTT CAT TGC-3' and NdpkB(154)-Reverse: 5'-TTC AGA GGC CCG AAG GAA C-3'; HPRT mRNA: *mHPRT*-Forward: 5'-GAA TCT GCA AAT ACG AGG AGT CCT-3' and *mHPRT*-Reverse: 5'-CCT TAC TAG GCA GAT GGC CAC A-3'), and sterile water to top up to total volume of 50µl. The PCR mixtures were aliquoted to MicroAmp optical 96-well reaction plate (Applied Biosystems, USA). The 96-well reaction plate were placed in the ABI Prism 7000 sequence detection system (Applied Biosystems, USA) and PCR reaction was started with 50°C for 2 min, followed by 95°C for 10 min and then continued with 40 cycles of 95°C for 15 sec and 60°C for 1 min. A melting curve was obtained for each PCR product after each run to confirm that the signal corresponded to a unique amplicon of the predicted size. The specificity of the PCR product was verified by DNA sequencing. Expression levels were obtained by subtracting the value for each sample in the absence of reverse transcriptase from the corresponding value in the presence of reverse transcriptase and then normalizing to the housekeeping gene encoding Hypoxanthine-Guanine Phosphoribosyl Transferase (*mHPRT*), obtained for every sample in parallel assays in two to four independent experiments. The

real-time PCR results were then analyzed using ABI Prism 7000 Sequence Detection System Software version 1.0 (Applied Biosystems, USA).

2.5 Transfection of plasmid construct to mammalian cells

For transient transfection in over-expression experiments, 2×10^5 cells were plated in 6-well plate (Corning, USA) and grown to 90-95% confluent at the time of transfection. The plasmid DNA to be transfected into the cells and lipofectamine 2000 was diluted in DMEM without serum individually. Both were mixed gently and incubated for 20 min at room temperature. The complexes were then added to each well containing the cells and medium. The cells were incubated at 37°C for 48 hr prior to testing for transgene expression. After 48 hours, the cells were collected and processed for the respective experiments. Transcriptional levels of *nm23-M2*, Cyclin D1 and β -Actin were investigated by RT-PCR using specific primers (*nm23-M2* mRNA: NdpkB(28)-Forward: 5'-CCT CGAGCG TAC CTT CAT TGC-3' and NdpkB(154)-Reverse: 5'-TTC AGA GGC CCG AAG GAA C-3', *cycD1*(191)-Forward: 5'-ACA CCA ATC TCC TCA ACG A-3' and *cycD1*(815)-Reverse: 5'-TAG CAG GAG AGG AAG TTG T-3', β -Actin(214)-Forward: 5'-TGG GAA TGG GTC AGA AGG AC-3' and β -Actin(689)-Reverse: 5'-TGT GGT GGT GAA GCT GTA GCC-3').

2.6 Protein work

2.6.1 Isolation of total cell lysate

MN9D cells subjected to various control and experimental conditions were washed twice with PBS to remove the residual culture medium and followed by lysing the cells with a volume of 50-200 μ l of lysis buffer (100mM HEPES,

150mM NaCl, 5mM MgCl₂, 1mM EDTA and 1% Triton X-100). Total cell lysates were collected and incubated overnight at -20°C. Cell debris was removed by centrifugation at 12,000 x *g* for 5 min at 4°C and the supernatant was stored at -20°C for later use.

2.6.2 Bio-Rad Bradford protein quantification assay

Protein concentration was determined by Bio-Rad Bradford assay kit (Bio-Rad, USA). Standard protein solutions were prepared by using bovine serum albumin (BSA) diluted to concentration of 5 mg/ml, 10 mg/ml, 15 mg/ml, 20 mg/ml and 25 mg/ml, respectively, to obtain the standard curve for determination of the protein concentration of the unknown samples. A volume of 25µl of Bradford assay solution was added to 100µl of each of the protein samples of known dilution factor as well as the standards. The mixtures were incubated at room temperature for 5 min before the optical density was determined at 595nm. The concentration was measured by SpectraMax 250 spectrophotometer and analysed by SOFTmax Pro Life Sciences Edition software (Molecular Devices). The protein concentrations of the samples were determined by using its optical density value to plot against the standard curve.

2.6.3 Protein separation using sodium dodecyl sulphate-polyacrylamide electrophoresis (SDS-PAGE)

The protein samples were normalized to a standard concentration of 20-40mg/ml by diluting with sterile water and the required amount were mixed with the 4X loading buffer {100mM Dithiothreitol (DTT, Bio-Rad, USA), 160mM

Tris pH 6.8, 4% SDS, 20% glycerol and 0.1% bromophenol blue}. The mixtures were boiled at 95°C for 5 min to denature the proteins. The pre-calculated amounts of each protein sample were then loaded into the wells of a 12-15% SDS-PAGE gel and subjected to a constant voltage of 80V (stacking gel part) or 120V (resolving gel part) for 1.5-3.0 hr in 1X running buffer (192mM glycine, 25mM Tris and 0.1% SDS). The SDS-PAGE gels were casted using the Bio-Rad protein mini-gel apparatus (Bio-Rad, USA). 10 ml of 12% w/v resolving gel and 4 ml of 4% stacking gel were prepared as in Table 2.1. APS (ammonium persulphate) and TEMED (N, N, N, N-tetramethylethylene-diamine) were added after the gel mixture was degassed. The resolving gel was poured into the space between the two plates to a height such that it was about 5mm from the bottom of the comb. The gel was layered with isopropanol to allow the polymerization of polyacrylamide. After the resolving gel was set, the isopropanol was decanted and the excess was absorbed by a slide of filter paper. The stacking gel was poured above the resolving gel and the comb was inserted. The gel was allowed to polymerize for about 30 min.

After electrophoresis, the gel was stained in 50ml of staining solution (10% acetic acid, 45% isopropanol, 0.1% Coomassie brilliant blue) for 30 min for visualization of the protein bands. The gel was then destained in destaining solution (10% (v/v) methanol; 10% (v/v) acetic acid) for several hours to overnight by gently shaking.

2.6.4 Western immunoblot analysis

Protein separation was performed using SDS-PAGE in 12-15% gels as described above. The proteins were then transferred to nitrocellulose membranes

(Bio-Rad, USA) using an electro-blotting apparatus (Bio-Rad, USA) at a constant voltage of 85V for 1.5 hr in the western transferring buffer (7.202g of glycine, 12 ml of 1M Tris-HCl (pH 7.4), 20% methanol). After the proteins were transferred, the membranes were stained with Ponceau S dye (Sigma, USA) to visualize the protein bands. After rinsing the membranes with Tris buffer saline (TBS) (27ml of 5M NaCl, 12ml of 1M Tris-HCl pH 7.4) to remove the red stain, the blots were blocked overnight in a blocking buffer {TBS + 0.1% Tween-20 (TBS-T) + 5% BSA (Albumin fraction V from bovine serum, Merck, Germany) or non-fat dry milk}. After blocking out non-specific binding, the blots were then incubated with a primary antibody in TBS-T + 2% BSA or non-fat dry milk at 4⁰C overnight with gently shaking. All the blots were washed five times at 5 min each with TBS-T and then incubated with the secondary antibodies {anti-rabbit-HRP (1:1000) or anti-mouse-HRP (1:1000)} against the primary antibodies for 1-2 hr at room temperature. The unbound antibodies were removed by five washes with TBS-T for 5 min each at room temperature. The blots were finally developed with the enhanced chemiluminescent (ECL) kit (Pierce Biotechnology, USA) and the signals were detected on Pierce films (Pierce biotechnology, USA). Respective primary antibodies used were: Cyclin D1 (DCS6) mouse monoclonal antibody (Cell Signaling, USA), Mouse monoclonal Anti- β -Tubulin Clone 2-28-33 antibody (Sigma, USA), c-Myc (C-8) mouse monoclonal antibody: sc-41, GFP (FL) rabbit polyclonal HRP conjugate antibody: sc-8334 HRP, Oct-1 (C-21) rabbit polyclonal IgG antibody: sc-232, SNAP-25 (SP12): sc-20038 antibody (Santa Cruz Biotechnology, USA), respective secondary antibodies used were: goat anti-rabbit IgG HRP: sc-2004, goat anti-mouse IgG HRP: sc-2005 (Santa

Cruz Biotechnology, USA). The different blotting conditions and antibody applications are indicated on Table 2.2.

2.7 Subcellular fractionation

Subcellular fractionation of the MN9D cells was carried out using BioVision Nuclear / Cytosol Fractionation Kit (BioVision, USA) as recommended by the manufacturer. This Nuclear / Cytosol Extraction Kit provides a complete system that enables the separation of nuclear extract from the cytoplasmic fraction of mammalian cells. The MN9D cells were collected by centrifugation at 600 x *g* for 5 min at 4°C and the supernatant was discarded. A volume of 0.2ml Cytosol Extraction Buffer (CEB)-A mix containing DTT and Protease Inhibitors were added to the cell pellet and were vortexed vigorously to re-suspend the cell pellet. The tube was incubated on ice for 10 min. A volume of 11µl of ice-cold Cytosol Extraction Buffer (CEB)-B was added to the tube, vortexed for 5 sec and incubated on ice for 1 min. The tube was then vortexed for 5 sec and centrifuged for 5 min at maximal speed. The supernatant (cytoplasmic extract) fraction was then transferred to a clean pre-chilled tube. The pellet was re-suspended in 100µl of ice-cold Nuclear Extraction Buffer (NEB) Mix. The tube was vortexed for 15 sec and returned to ice while continuing vortexing for 15 sec every 10 min, for a total of 40 min. Next, the tube was centrifuged at full speed for 10 min. The supernatant (Nuclear extract) was immediately transferred to a clean pre-chilled tube and placed on ice. All extracts were stored at -80°C until use.

2.8 Fluorescence microscopy and neurite assay

Cells were plated at a density of 10^5 - 10^6 on 6-well plate (Corning, USA). Individual wells transfected with the null plasmid and pcDNA3.1(-)_fl *nm23*-

M2_GFP plasmid. The cells were stained with Hoechst dye for 5 min to stain the nucleus and fixed in 0.5% paraformaldehyde in 1X PBS, pH 7.4 for 30 min at room temperature after 2 days post-transfection. The cells were then examined with Zeiss Axiovert 25CFL inverted microscope and photographs of cells were captured using DP controller, Olympus (Olympus, USA). The proportion of neurite-bearing cells was counted using a phase-contrast microscope at 200X magnification. The cell images were analyzed using ImageJ software version 1.34s (by Wayne Rasband, National Institute of Health, USA). The length of the primary neurite was defined as the distance from the soma to the tip of the longest branch. Processes longer than 1.5 times of the cell body diameters were counted as neurites. For every datum point, the mean value was calculated from five random field observations of three replicate experiments, and at least 150 cells were counted per field.

2.9 Flow cytometry

Cells were plated at a density of 10^5 - 10^6 on 6-well plate (Corning, USA). Each wells were transfected with the null plasmid, pcDNA3.1(-)_fl nm23-M2_GFP individually. Cells in one well were differentiated using *n*-butyric acid as mentioned. The cell culture medium was discarded and the cells were washed twice with 1X PBS. The cells were trypsinized and harvested with fresh DMEM culture medium by pipetting into 15ml Falcon tubes, followed by centrifugation at $1,500 \times g$ for 10 min at 4°C . The supernatant was discarded and the pellet was washed with 5ml of 1X PBS. The cell pellet was re-suspended with 1X PBS and spun down for another 10 min at 4°C . The supernatant was decanted and the pellet was fixed with 0.5% paraformaldehyde for 5 min on ice to prevent GFP leakage.

The samples in the tubes were centrifuged again and the paraformaldehyde was discarded. The cell pellets were re-suspended with 0.5ml of PBS and added drop by drop with 4.5ml of ice-cold (pre-chilled at -20°C) 70% ethanol. After which, the cells in the tubes can be stored up to 1 month at -20°C until proceeding to flow cytometry.

The distribution of the cells in G_0 , G_1 , S, and G_2/M cell cycle phases was determined by DNA flow cytometry or Fluorescence Activated Cell Sorting (FACS). Before proceeding to flow cytometry, the stored cells were centrifuged at $2,700 \times g$ for 10 min at 4°C and the ethanol was then discarded. The cell pellets were re-suspended with PI staining solution {Stock solution of 1g glucose and 1 litre PBS (filtered and sterilized) with propidium iodide ($50\mu\text{g/ml}$) (Sigma, USA) in presence of RNase A (50mg/ml) (Sigma, USA)} and incubated in dark at room temperature for 30 min. The cell samples were filtered through the $41\mu\text{m}$ nylon filter and then subjected to flow cytometry. Flow cytometric analysis was carried out on 20,000 cells using EPICS Elite ESP cytometer (Beckman Coulter, USA). The FACS data were then analyzed and the histogram plotted using WinMDI (Windows Multiple Document Interface for Flow Cytometry Application version 2.8 by Dr. Joseph Trotter, La Jolla, CA).

2.10 siRNA interference

MN9D cells in 6-wells plate (Corning, USA) were transfected as followed. The siRNA (*nm23-M2_RN*: r(GAA CAC CUG AGC AGC AUU)d(TT) (Qiagen, USA) recognized the target sequence in *nm23-M2* sequence: 5'-AAG AAC ACC TGA AGC AGC ATT-3') were transfected into cells. For each well, $1.2\mu\text{g}$ of siRNA was used. The ratio of amount of siRNA used to RNAiFect transfection

reagent is 1 : 6. First, 4.8µl of siRNA stock was diluted with 95.2µl of Buffer EC-R and mixed by vortexing. Next, 7.2µl of RNAiFect transfection reagent was added and mixed by pipetting up and down five times. The mix was then incubated for 10 to 15 min at room temperature to allow for complex formation before adding to the cells. The culture medium from the plate was first aspirated and 3ml of fresh culture medium containing serum and antibiotics was added to the cells. The complexes were added drop-wise onto the cells and the plate was swirled gently to ensure uniform distribution of the transfection complexes. The cells were then incubated with the transfection complexes under normal growth conditions. After 24 hr incubation, the cells were harvested and the total RNA was extracted by using RNeasy Mini Kit (Qiagen, USA) as mentioned in section 2.2.1. The gene silencing of *nm23-M2* at the mRNA level was monitored after 24 hr by RT-PCR using the specific primers (*nm23-M2* mRNA: NdpkB(28)-Forward: 5'-CCT CGAGCG TAC CTT CAT TGC-3' and NdpkB(154)-Reverse: 5'-TTC AGA GGC CCG AAG GAA C-3'). After siRNA interference, the protein levels of SNAP-25 and cyclin D1 in sodium butyric acid-treated MN9D cells were investigated by SDS PAGE and western immunoblot analysis as mentioned in section 2.6.

C. pGEM®-T Easy Vector Map and Sequence Reference Points

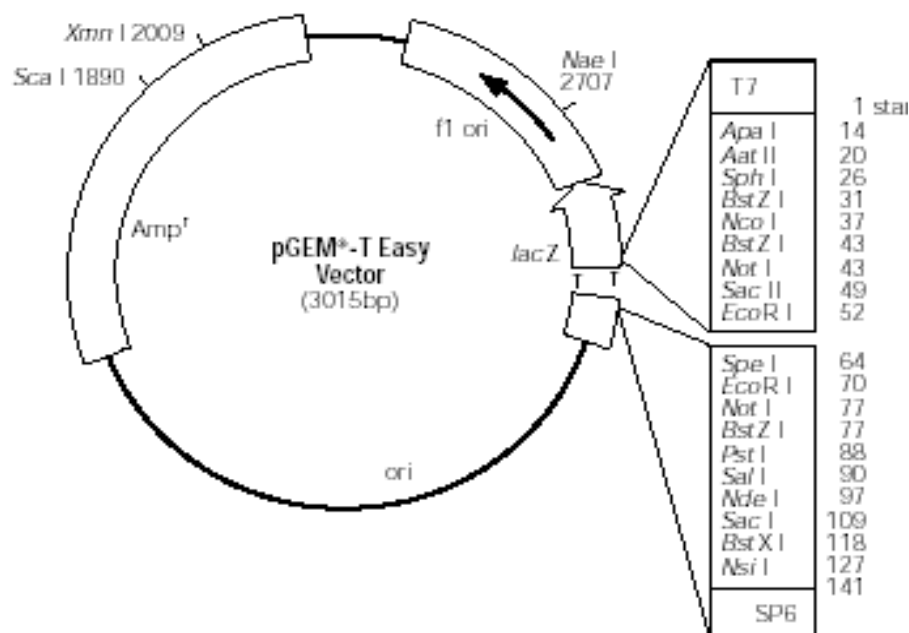


Figure 3. pGEM®-T Easy Vector circle map and sequence reference points.

pGEM®-T Easy Vector sequence reference points:

T7 RNA polymerase transcription initiation site	1
multiple cloning region	10–128
SP6 RNA polymerase promoter (–17 to +3)	139–158
SP6 RNA polymerase transcription initiation site	141
pUC/M13 Reverse Sequencing Primer binding site	176–197
<i>lacZ</i> start codon	180
<i>lac</i> operator	200–216
β -lactamase coding region	1337–2197
phage f1 region	2380–2835
<i>lac</i> operon sequences	2836–2996, 166–395
pUC/M13 Forward Sequencing Primer binding site	2949–2972
T7 RNA polymerase promoter (–17 to +3)	2999–3

Figure 2.1 Plasmid map and sequence reference points of pGEM-T Easy cloning vector. (The figure is reproduced from Promega, pGEM-T Easy vector systems protocol)

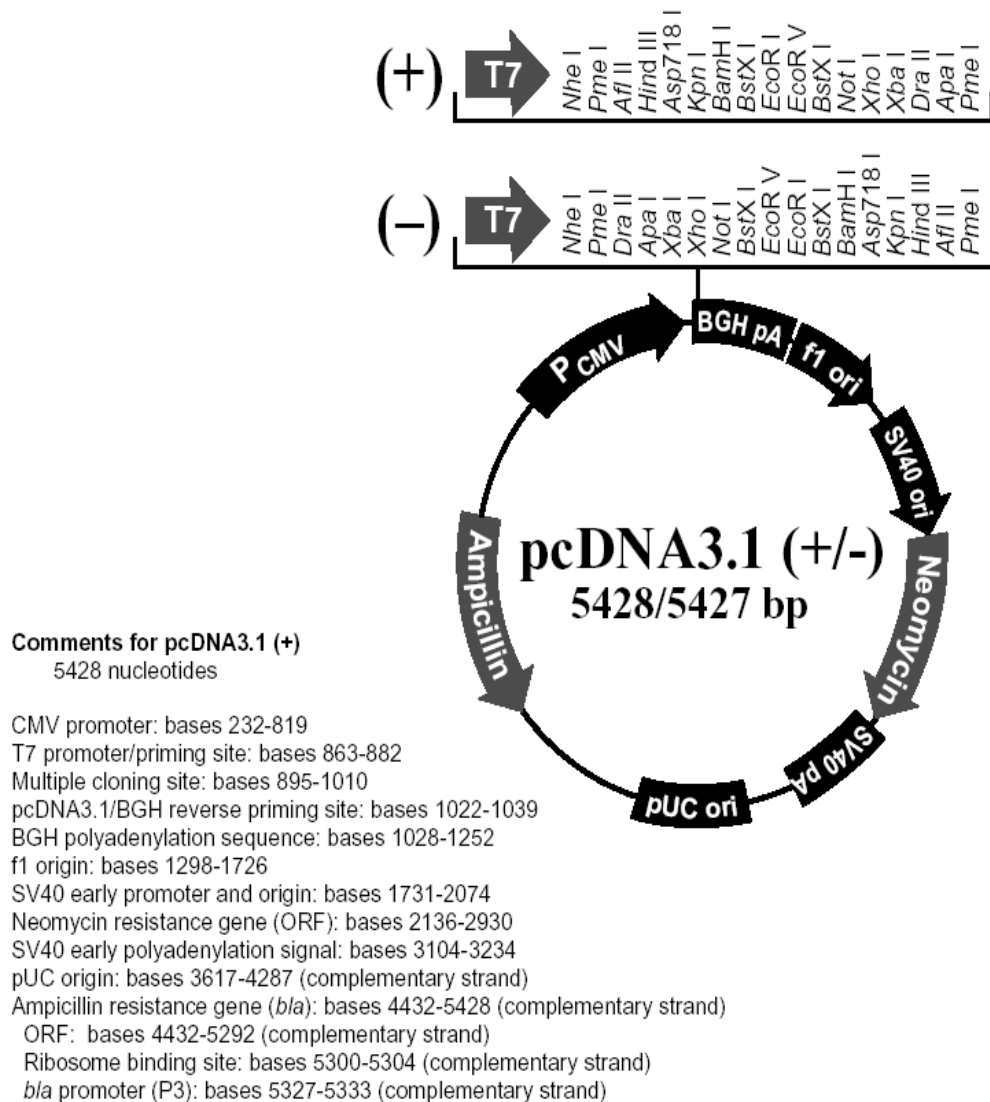


Figure 2.2 Plasmid map and sequence reference points of pcDNA3.1(+/-) cloning vector. (The figure is reproduced from website of Invitrogen, life technologies, USA)

Preparation of SDS-PAGE gel	
12% Resolving gel component	Volume (ml)
30% Bis-acrylamide	4
Tris-HCl pH 8.8	2.5
MilliQ water	3.39
10% Ammonium persulphate	0.1
TEMED	0.01
4% Stacking gel component	Volume
30% Bis-acrylamide	0.455
Tris-HCl pH 6.8	0.875
MilliQ water	2.1315
10% Ammonium persulphate	0.035
TEMED	0.0035

Table 2.1 Preparation of SDS-PAGE gel with the listed required components.

Primary antibody	Manufacturer	Dilution factor	Blocking condition	Incubation condition
Cyclin D1 (DCS6)	Cell Signaling (USA)	1:2000, 2% non-fat milk	5% non-fat milk, 30min at RT	Overnight at 4°C
β-Tubulin	Sigma (USA)	1:1000, 2% non-fat milk	5% non-fat milk, 30min at RT	Overnight at 4°C
C-Myc (C-8): sc-41	Santa Cruz Biotech. (USA)	1:1000, 2% non-fat milk	5% non-fat milk, 30min at RT	Overnight at 4°C
GFP: sc-8334 HRP	Santa Cruz Biotech. (USA)	1:1000, 2% non-fat milk	5% non-fat milk, 30min at RT	Overnight at 4°C
Oct-1 (C-21): sc-232	Santa Cruz Biotech. (USA)	1:1000, 2% non-fat milk	5% non-fat milk, 30min at RT	Overnight at 4°C
SNAP-25 (SP12): sc-20038	Santa Cruz Biotech. (USA)	1:1000, 2% non-fat milk	5% non-fat milk, 30min at RT	Overnight at 4°C
Secondary antibody	Manufacturer	Dilution factor	Blocking condition	Incubation condition
goat anti-rabbit IgG HRP: sc-2004	Santa Cruz Biotech. (USA)	1:1000, 2% non-fat milk	-	2hr at RT
goat anti-mouse IgG HRP: sc-2005	Santa Cruz Biotech. (USA)	1:1000, 2% non-fat milk	-	2hr at RT

Table 2.2 Primary and secondary antibodies application for western blotting in this thesis.

Chapter 3:

Results

Chapter 3: Results

3.1 Cloning and characterization of full-length *nm23-M2* cDNA

3.1.1 Cloning of full-length pcDNA3.1(-)_fl *nm23-M2*_GFP and pcDNA3.1(-)_fl *nm23-M2*_MYC

Figure 3.1 shows an agarose gel electrophoresis photograph on the total RNA isolated from undifferentiated MN9D cell lines. The photograph image shows the presence of two band fragments, where 28S rRNA fragment band was higher than 18S rRNA fragment band. The integrity of the total RNA was also determined by the intensity of the 28S rRNA band relative to the intensity of 18S rRNA band. The intensity of the upper 28S rRNA band was 1.5 – 2 times higher than the intensity of lower 18S rRNA band which indicated that the total RNA was not degraded during the experimental procedure of total RNA isolation.

In order to clone the full-length *nm23-M2* cDNA, the nucleotide coding sequence of *nm23-M2* should be known and specific primers were designed to prime out the specific *nm23-M2* cDNA product. The PCR amplification to generate full-length *nm23-M2* cDNA insert was carried out using Access RT-PCR System (Promega, USA) with 1 sets of specific primers (NdpkB-Forward: 5'-ATG GCC AAC CTC GAG CGT-3' and NdpkB-Reverse: 5'-CTA CTC GTA CAC CCA GTC-3') and the template used was the total RNA isolated from undifferentiated MN9D cells. The full-length nucleotide sequence of *nm23-M2* (NM_008705) and the annealing site of the specific primers are shown in figure 3.2. The PCR product was analyzed by DNA agarose electrophoresis and shown in figure 3.3. The PCR product was also sent for capillary sequencing to confirm its identity as full-length *nm23-M2* cDNA.

The full-length *nm23-m2* PCR product was TA cloned into pGEMT-Easy vector. Colony PCR screening as mentioned in section 2.2.6 was carried out using T7 and SP6 primers to prime out the cloned insert into pGEMT-Easy vector. In order to double check for the positive clones which contained the full-length *nm23-m2* insert, restriction enzymes, *XbaI* and *EcoRI* were added to cut out the insert from pGEMT-Easy vector. The samples were then analyzed by DNA agarose electrophoresis and shown in figure 3.4.

PCR amplification of the full-length *nm23-M2* gene using pGEMT-Easy_ *mNm23-M2* plasmid as a template with the following set of specific primers (NdpkB(*XbaI*+KS)-Forward: 5'-GGG CCC TCT AGA ACC ATG GCC AAC CTC GAG CGT A-3' and NdpkB(Stop+*EcoRI*)-Reverse: 5'-GTG GTG GAA TTC CTC GTA CAC CCA GTC ATG-3'. The amplified DNA product was then digested with the restriction enzymes *XbaI* and *EcoRI* and ligated into the pcDNA3.1(-)_GFP and pcDNA3.1(-)_MYC vector. In order to choose for positive clones that contained the full-length *nm23-M2* insert, restriction enzymes, *XbaI* and *EcoRI* were added to cut out the insert from individual pcDNA3.1(-) vector. The samples were then analyzed by DNA agarose electrophoresis and shown in figure 3.5.



Figure 3.1 **Total RNA isolation.** A photograph image of an agarose gel under UV light excitation showing the presence of total RNA isolated from undifferentiated MN9D cell line (Lane A to D), differentiated MN9D cell line (Lane E to L).

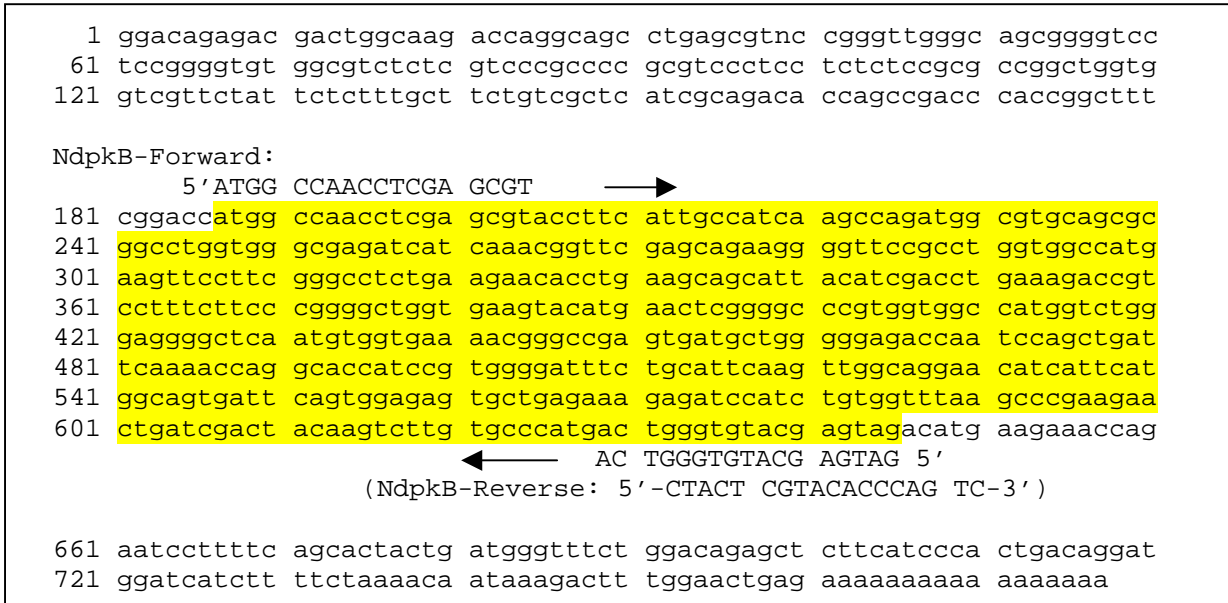


Figure 3.2 **NM_008705 *nm23*-M2 mRNA.** The coding sequence of *nm23*-M2 is highlighted in yellow and specific primer annealing sites are indicated for cloning of the full-length cDNA.

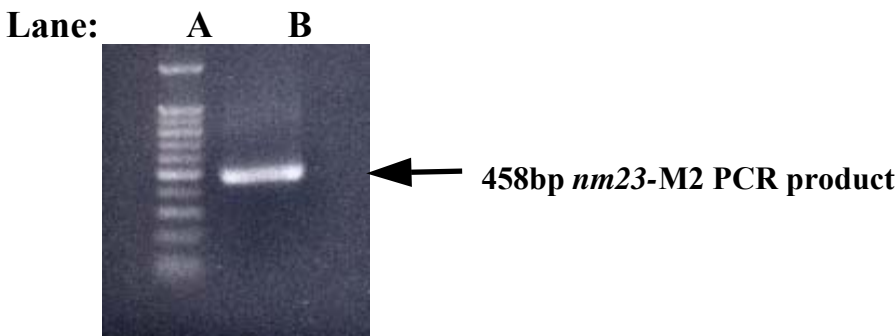


Figure 3.3 **RT-PCR amplification of full-length *nm23*-M2 cDNA.** A photograph image of an agarose gel under UV light excitation showing 100bp DNA ladder (Lane A) and *nm23*-M2 PCR product ~458bp (Lane B).

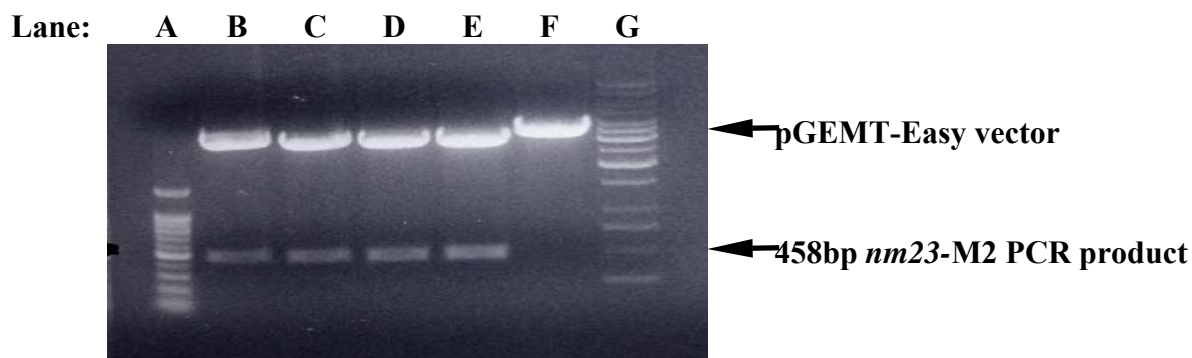


Figure 3.4 Restriction enzyme digestion of pGEM-T Easy_ *mNm23-M2* recombinant plasmid. A photograph image of an agarose gel under UV light excitation showing 100bp DNA ladder (Lane A), positive pGEMT-Easy vector clones containing *nm23-M2* insert (Lane B-E), negative clones without the insert (Lane F) and 1kbp DNA ladder (Lane G).

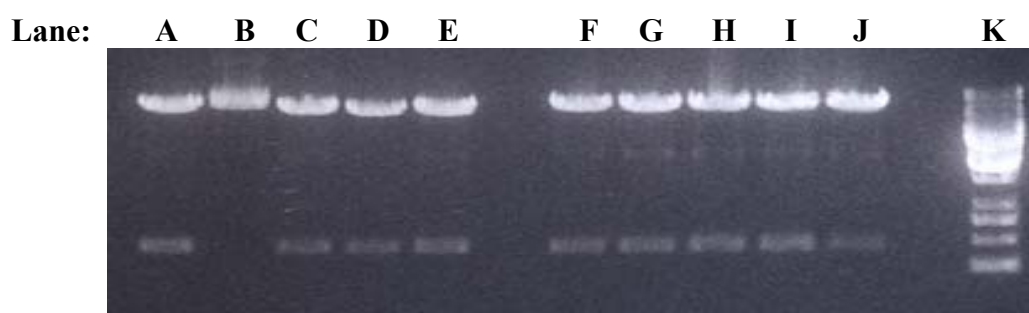
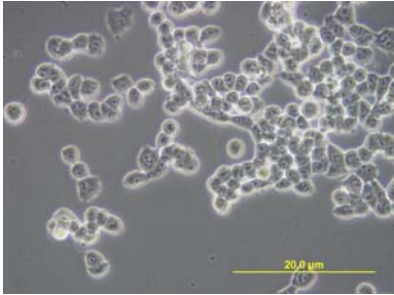
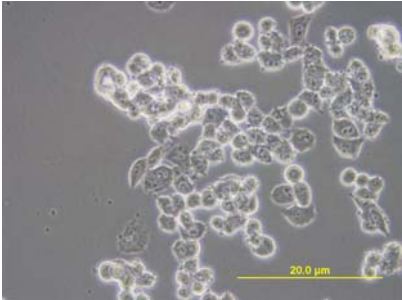

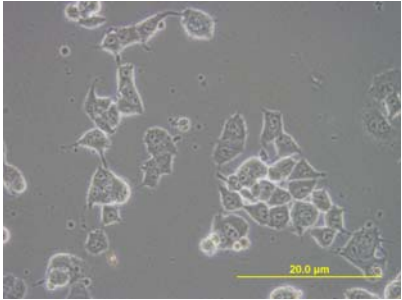
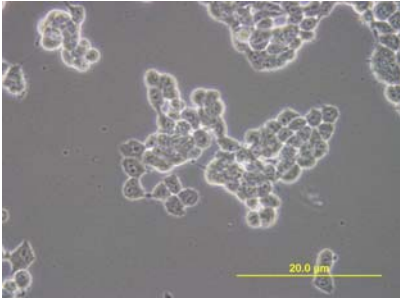
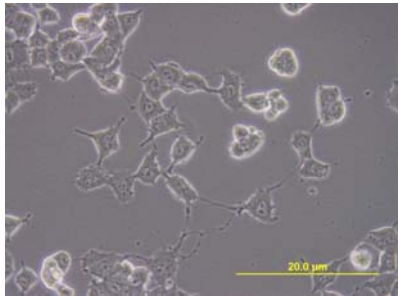
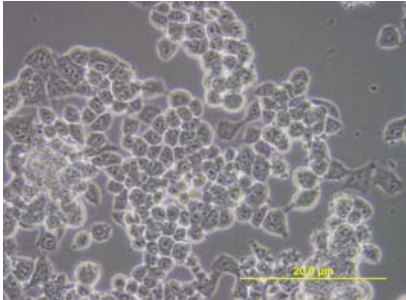



Figure 3.5 Restriction enzyme digestion of pcDNA3.1(-)_ *mNm23-M2* recombinant plasmid. A photograph image of an agarose gel under UV light excitation showing positive pcDNA3.1(-)_GFP vector clones containing *nm23-M2* insert (Lane A, C-E), negative pcDNA3.1(-)_GFP vector clones without the insert (Lane B), positive pcDNA3.1(-)_MYC vector clones containing *nm23-M2* insert (Lane F-I) and 1kb DNA ladder (Lane K).

3.1.2 Routine tissue culture

Both undifferentiated and differentiated MN9D cell lines were routinely cultured for the extraction of total RNA from both phenotypes and for transfection of recombinant plasmids for overexpression and siRNA interference studies. In order to differentiate MN9D hybrid cell line into mesencephalic dopaminergic neurons, the supplement of DMEM culture medium with the addition of 1mM of *n*-butyric acid was essential. Morphological characteristics of both undifferentiated and differentiated MN9D cell lines at day 0-7 are shown in figure 3.6. Differentiated MN9D cells have different morphological characteristics with undifferentiated MN9D cells as they can be recognized by the presence of interconnecting neurite outgrowth and flattened appearance while undifferentiated MN9D cells are relatively more rounded in shape as compared to those differentiated MN9D cells. From day 1 onwards, MN9D cells which were treated with 1mM *n*-butyric acid started to change its morphological appearance as most of the cells were exhibiting a flattened appearance. Neurite outgrowth began from day 2 onwards as more cells showed extension of neurites and longer neurite extension were observed during the 6th and 7th day of 1mM *n*-butyric acid treatment.

Day	DMEM	DMEM with 1mM <i>n</i> -butyric acid
0		
1		
2		
3		

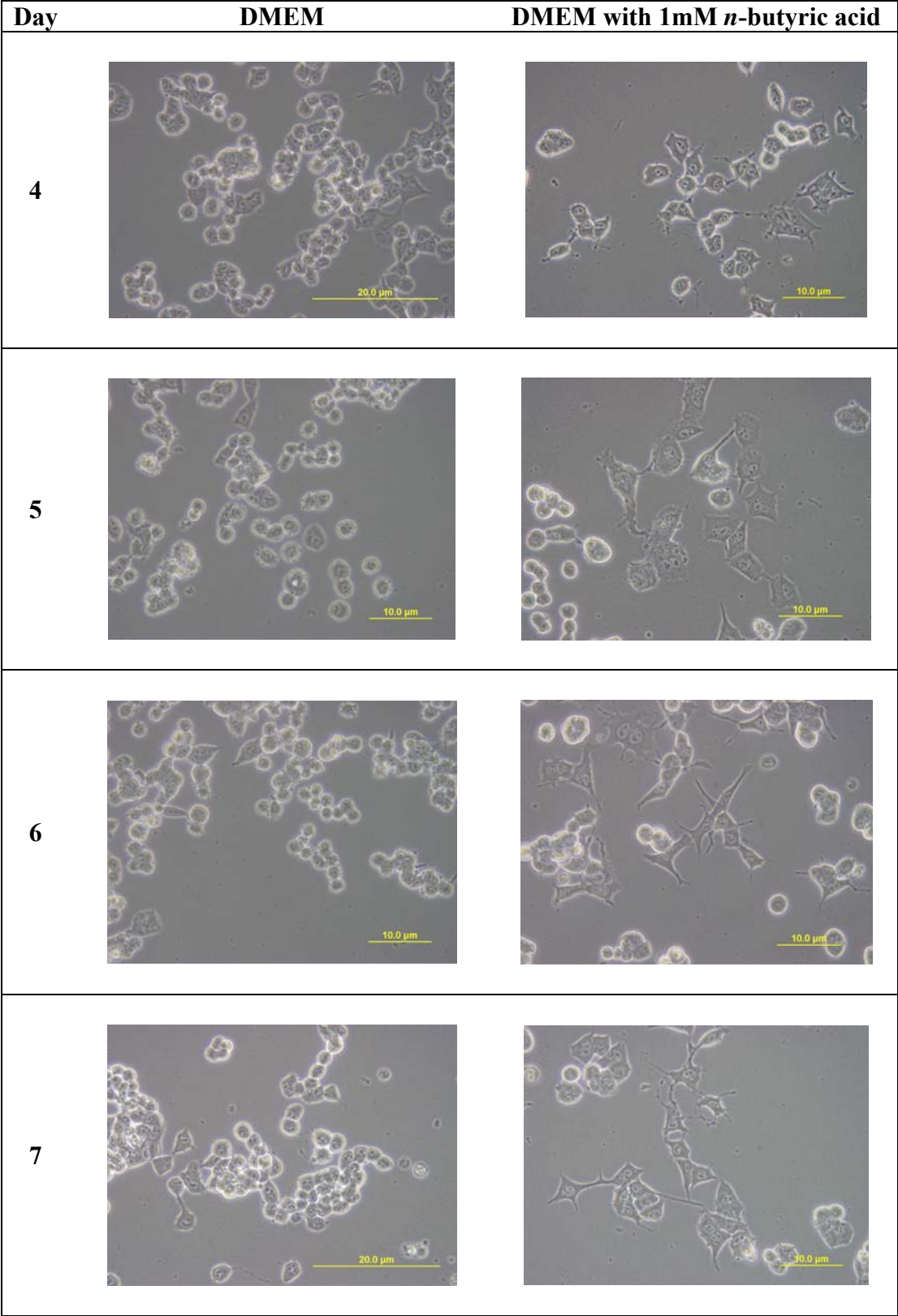


Figure 3.6 MN9D time-course differentiation. A panel of photographs showing the morphological appearance of MN9D cells with and without treatment of 1mM *n*-butyric acid for differentiation induction in a time course of 7 days.

3.1.3 Temporal expression of *nm23-M2* in MN9D cells

The endogenous levels of *nm23-M2* in differentiating MN9D cells from day 1 to day 7 upon addition of 1mM *n*-butyric acid were investigated using quantitative real-time PCR. It is the most sensitive and reliable method for the detection and quantification of nucleic acids levels. The cDNAs of differentiating MN9D cells from day 1 to day 7 were reverse-transcribed from total RNA isolated from MN9D cells harvested at day 1 to day 7 respectively. Specific real-time PCR primers were designed to amplify a small fragment of the full-length *nm23-M2* gene. The SYBR green dye allows detection of any double-stranded DNA generated during PCR. Reactions were characterized by the point in time during cycling when amplification of a PCR product is first detected rather than the amount of PCR product accumulated after a fixed number of cycles. The higher the starting copy number of the nucleic acid target, the sooner a significant increase in fluorescence is observed. Model of a single amplification plot showing terms commonly used in real-time quantitative PCR are shown in figure 3.7 and the multiple amplification plots during the real-time PCR run were captured in figure 3.8. The real-time analysis of *nm23-M2* PCR product was carried out using the ABI Prism SDS software and the graphical representation of the results are shown in figure 3.9.

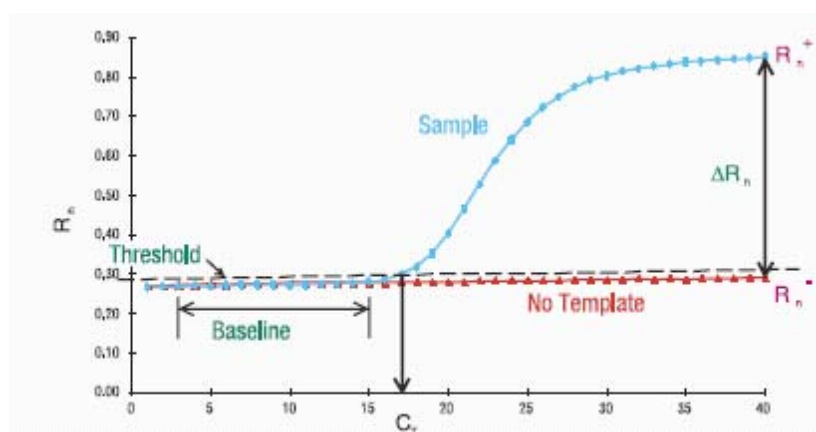


Figure 3.7 Model of a single amplification plot used in real-time PCR

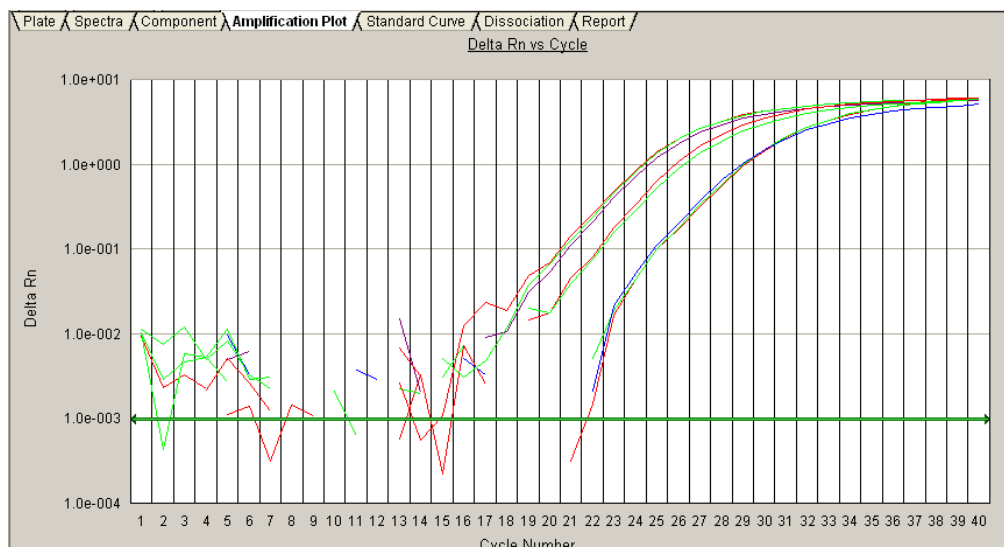


Figure 3.8 A graph showing multiple amplification plots during the real-time PCR run.

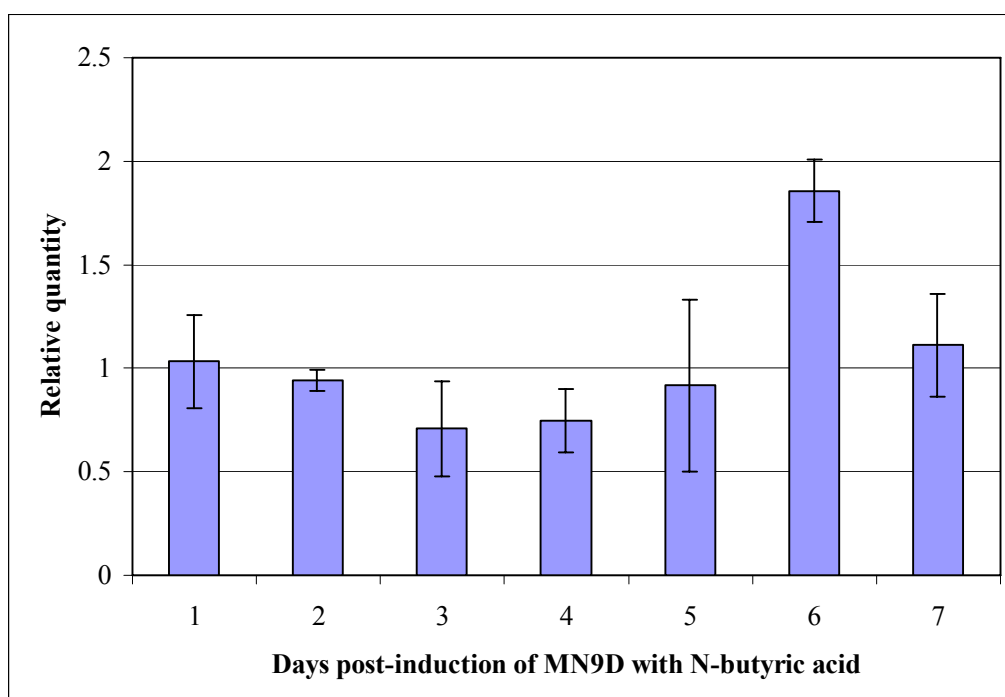


Figure 3.9 A graphical representation showing changes in endogenous mRNA level of *nm23-M2* post-induction of MN9D cells with 1mM *n*-butyric acid. The results were derived from 3 sets of experimental replication.

The bar chart in figure 3.9 showed that the relative quantity of endogenous *nm23-M2* in MN9D cells was the highest at the 6th day upon addition of 1mM *n*-butyric acid. This further confirmed that *nm23-M2* endogenous mRNA level was up-regulated during differentiation of MN9D cells which coincide with the previous micro-array studies.

3.1.4 Spatial expression of *nm23-M2* in MN9D and SH-SY5Y cells

MN9D and SH-SY5Y cells were transfected with the control null plasmid and pcDNA3.1(-)_fl *nm23-M2*_GFP plasmid. The gene expression was examined under a fluorescent microscope after 48hr incubation, while photographs of the both transfected cell lines were captured and are shown in figure 3.10. The fluorescence detected in the photographs indicated that exogenous GFP proteins were expressed in these cells. For cells that were transfected with the control null plasmid, they exhibited general GFP expression in the whole cell bodies including the nucleus and cytoplasm. For cells that were transfected with pcDNA3.1(-)_fl *nm23-M2*_GFP plasmid, GFP expression was only exclusive to the cytoplasm but not the nucleus. This observation led to the conclusion that pcDNA3.1(-)_fl *nm23-M2*_GFP plasmid only localized in the cytoplasm but not in the nucleus in both MN9D and SH-SY5Y cell line. This indicated that the localization of the *nm23-M2* does not differ in different cell types as illustrated in both the mouse MN9D cell line and the human SH-SY5Y cell line.

Western immunoblot analysis using anti-GFP antibody were also carried out on extracted MN9D cell protein lysate to indicate that the transfections of individual recombinant vectors were performed successfully and the western blot results are shown in figure 3.11.

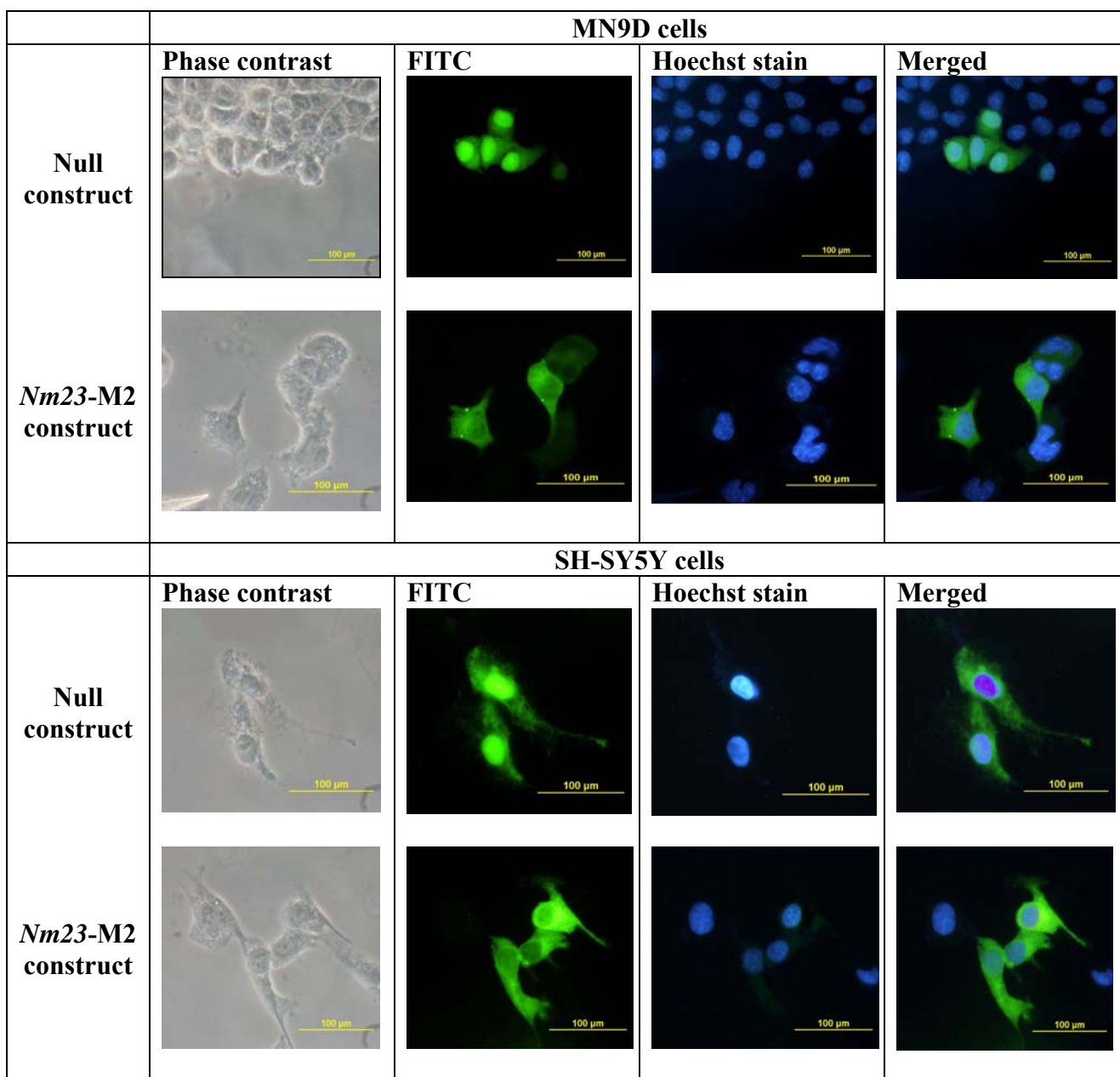


Figure 3.10 Spatial expression of *nm23-M2* in MN9D and SH-SY5Y cells. A panel of photographs indicating MN9D and SH-SY5Y cells transfected with individual null pcDNA3.1(-) plasmid vector and pcDNA3.1(-)_fl *nm23-M2*_GFP plasmid vector. Fluorescein isothiocyanate (FITC) filter were used to detect GFP fluorescence. Hoechst stain to indicate nucleus staining.

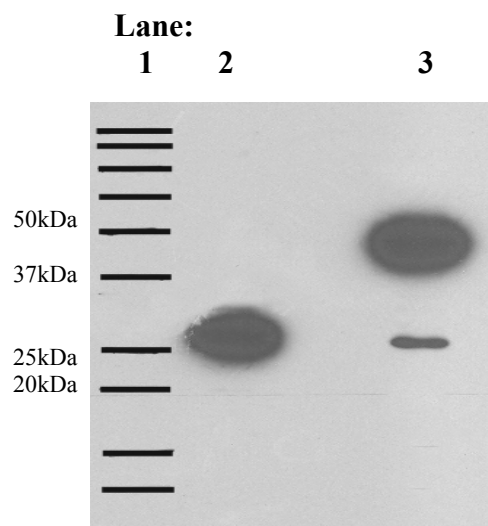


Figure 3.11 Western immunoblot analysis of GFP in MN9D cells transfected with pcDNA3.1(-)_GFP plasmid (Lane 2) and pcDNA3.1(-)_fl *nm23-M2*_GFP plasmid (Lane 3). Lane 1 denotes Precision Plus Protein Standards.

In the western blot as shown in figure 3.11, we can confirm that the transfections of the two plasmids, 1) control null GFP plasmid (pcDNA3.1(-)_GFP) and 2) pcDNA3.1(-)_fl *nm23-M2*_GFP plasmid, were performed successfully as we can detect the GFP protein bands by using anti-GFP antibody. The protein size of control null GFP plasmid is around 30kDa. The full-length *nm23-M2* gene insert was added to form pcDNA3.1(-)_fl *nm23-M2*_GFP plasmid and the GFP protein band was detected at around 47kDa (shown in Lane 3) as the protein size of *nm23-M2* is around 17kDa.

3.1.5 Subcellular localization of *nm23-M2*

The purpose of cloning *nm23-M2* into pcDNA3.1(-)_MYC plasmid and transfecting it into MN9D and SH-SY5Y cells was to investigate the subcellular localization of *nm23-M2* in both different cell types. This was achieved by carrying out subcellular fractionation of MN9D and SH-SY5Y cells to obtain the nuclear and

cytoplasm fractions separately. The individual protein fraction was resolved by protein SDS-PAGE and probed with C-Myc and Oct-1 antibodies as shown in figure 3.12.

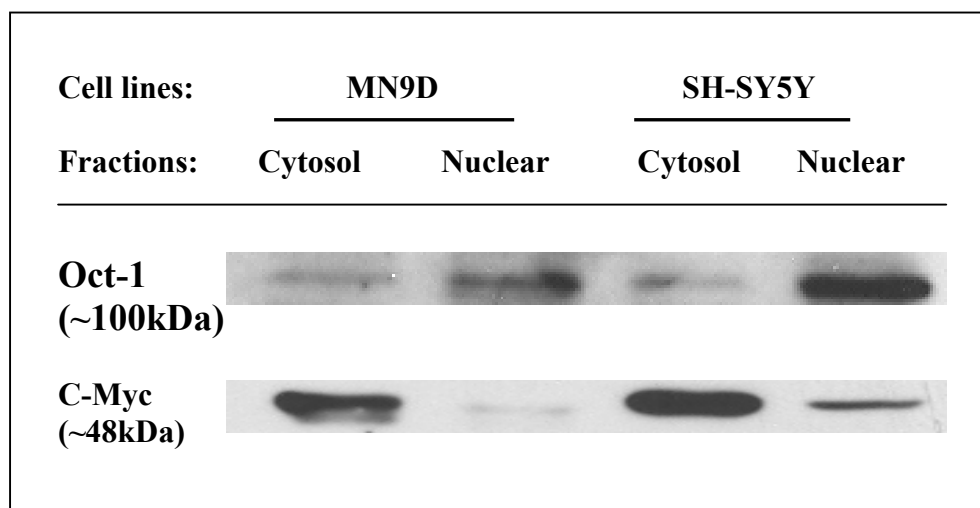


Figure 3.12 Western immunoblot analysis of Oct-1 and C-Myc antibodies in subcellular fractions of MN9D and SH-SY5Y cell lines.

Oct-1, a transcription factor which is a member of the POU homeodomain family plays an important role in activating the transcription of various genes that contain an Oct-1 binding motif, ATGCAAAT (Sturm et al. 1988). Oct-1 transcription factors are known to localize mainly in the nucleus of the cells. The results shown in figure 3.12 also confirmed that the fractionation was carried out properly as Oct-1 protein bands were prominent in the nuclear fractions of both cell lines. As the full-length *nm23-M2* was tagged with the C-Myc protein fragment, we can conclude that *nm23-M2* localized mainly in the cytosolic fractions in both mouse and human cell types. This observation also corresponds to the fluorescence photographs in figure 3.10 that *nm23-M2* localized mostly in the cytoplasm but lesser in the nucleus of the cells. There is a possibility that *nm23-M2* localized in the nucleus as there are reports

suggesting that *nm23* gene, particularly, *nm23-H2* acts as transactivating factor to activate transcription (Postel et al. 1993).

3.2 Overexpression studies of *nm23*-M2 in MN9D cells

3.2.1 Morphological appearance of MN9D overexpressing pcDNA3.1(-)_fl *nm23*-M2_GFP

The morphology of MN9D cells overexpressing the full-length *nm23*-M2 gene were investigated by transfecting the cells with pcDNA3.1(-)_fl *nm23*-M2_GFP plasmid. The experimental control used was MN9D cells transfected with a null GFP plasmid (pcDNA3.1(-)_GFP). After 48hr post-transfection, the cells were taken out from the CO₂ incubator and placed under fluorescent microscope for phototaking. The photographs taken are shown in figure 3.13. From the pictures shown in figure 3.13, cells that were transfected with the null GFP plasmid did not show any changes in the cell morphology, which corresponded to the typical morphology of undifferentiated MN9D cells. The cells still remained relatively rounded in shape and tend to aggregate together in small clumps of cells. Whereas for cells that were transfected with pcDNA3.1(-)_fl *nm23*-M2_GFP plasmid, morphological appearance was obviously different from the undifferentiated MN9D cells as more cells were exhibiting a flattened appearance and neurite outgrowth was observed. The cells were much similar to those differentiated cells after being treated with 1mM of *n*-butyric acid as shown in figure 3.6.

The number of transfected MN9D cells bearing neurites were also counted and the data were then analyzed and plotted into a bar chart as shown in figure 3.14. The bar chart showed that MN9D cells that were transfected with pcDNA3.1(-)_fl

nm23-M2_GFP had significantly more cells with neurites than MN9D/null GFP plasmid.

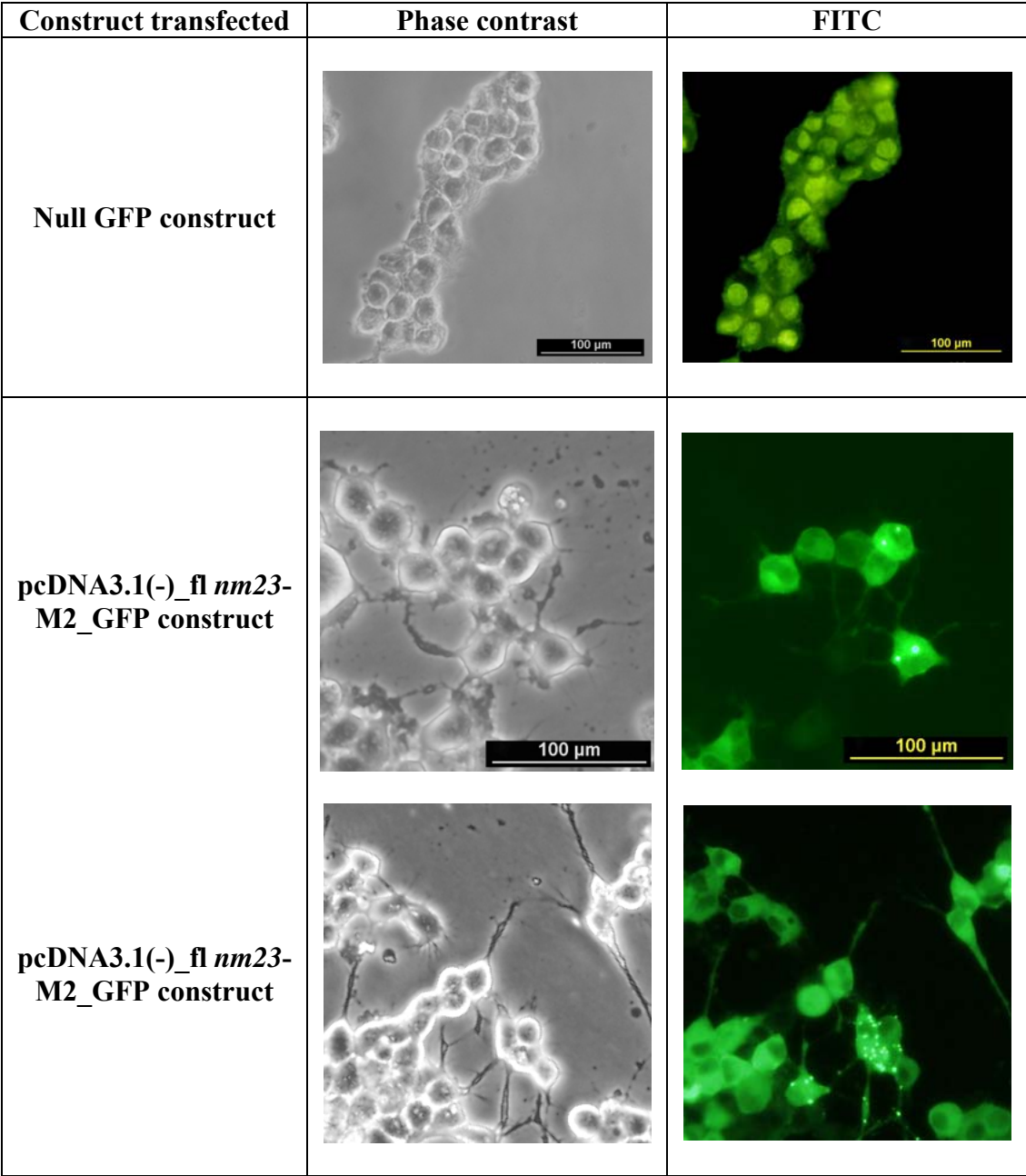


Figure 3.13 Morphology of transfected MN9D cells. A panel of fluorescent microscopy photographs showing the morphological appearance of MN9D cells overexpressing null GFP plasmid (upper panel) and full-length *nm23-M2* tagged with GFP plasmid (lower panel). Cells overexpressed with *nm23-M2* displayed a flattened appearance with neurite outgrowth.

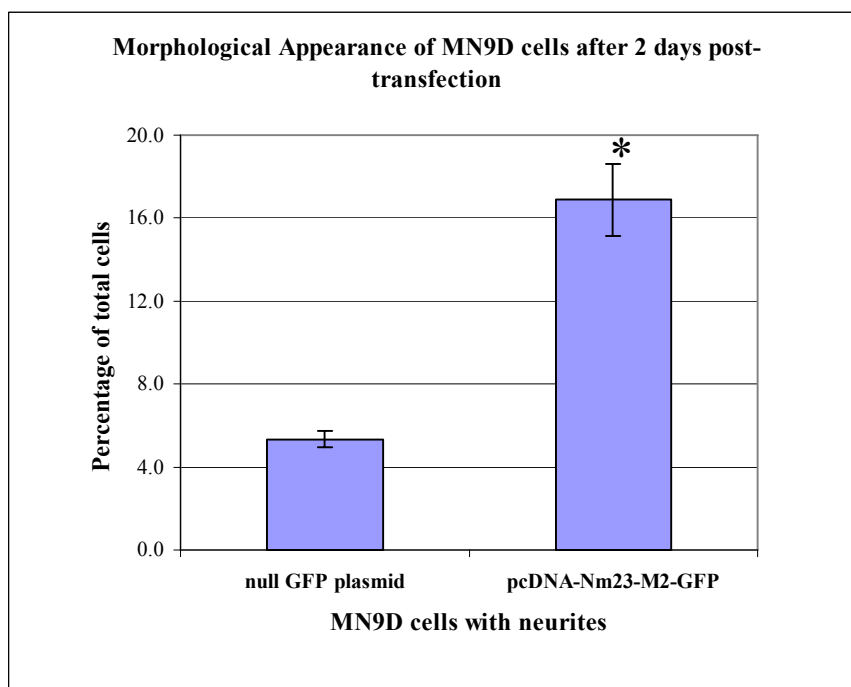


Figure 3.14 A graph showing the morphological changes of MN9D cells after 2 days post-transfection of *nm23-M2*. MN9D cells transfected with *nm23-M2* had significantly more cells with neurites than MN9D/null GFP plasmid as determined by Student's T-test using SPSS statistical software. * $P < 0.05$.

3.2.2 MN9D cells showed cell growth arrest when treated with *n*-butyric acid and transfected with *nm23-M2*

Flow cytometry analysis of EGFP-positive cells by FACS was carried out to examine the cell cycle stages of MN9D cells in both cases when 1) they were treated with 1mM of *n*-butyric acid and 2) they were transfected with the full-length *nm23-M2*. Upon treatment with 1mM *n*-butyric acid, MN9D cells exhibited a mature neuronal morphology, characterized by a flattened cell body and the extension of neurites. There was a decrease in the doubling time of the treated cells (data not shown), indicating they were exiting the cell cycle, as a result of differentiation. This was accompanied by an increase in G1-phase stage cells when the cells were treated with *n*-butyric acid as shown in figure 3.15 and 3.16. MN9D cells that were

transfected with *nm23-M2* plasmid construct also exhibited an increase in G₁-phase stage cells. This was confirmed by an arrest of differentiated cells in the G₁ phase as shown in the figure 3.15 and 3.16.

	G0	G1	S	G2/M
MN9D Control	1.84	44.94	24.21	28.98
MN9D treated with <i>n</i>- butyric acid (1mM)	12.45	63.66	5.53	17.8
MN9D transfected with <i>pcDNA3.1</i>-GFP null plasmid	3.23	47.13	22.59	25.97
MN9D transfected with <i>Nm23-M2</i>- GFP plasmid	4.34	56.57	20.89	17.23

Figure 3.15 A table showing the percentage of MN9D cells at different stages of the cell cycle in different conditions.

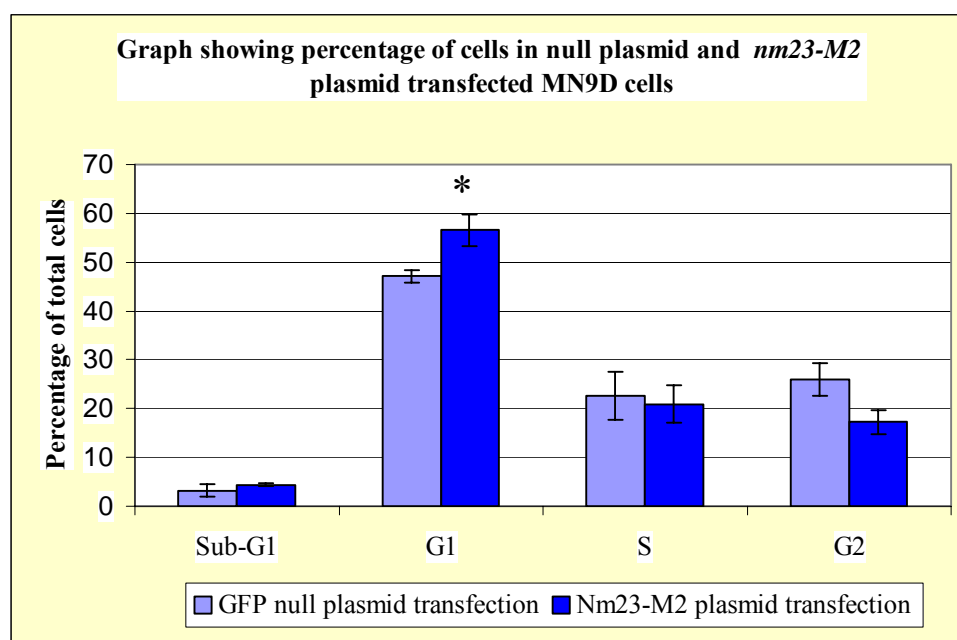


Figure 3.16 A graph showing the percentage of MN9D cells after 2 days post-transfection of GFP null plasmid and *nm23-M2* plasmid. MN9D cells transfected with *nm23-M2* had significantly more cells at G₁ phase than MN9D/null plasmid as determined by Student's T-test using SPSS software. * $P < 0.05$.

3.2.3 SNAP-25 protein expression was up-regulated in MN9D cells overexpressing pcDNA3.1(-)_fl nm23-M2_GFP

Proteins associated with the presynaptic terminal play critical roles during neurite outgrowth and synaptogenesis. SNAP-25 (Synaptosomal-associated protein of 25 kDa) is an essential component of the core complex that mediates presynaptic vesicle trafficking and is directly involved in the release of neurotransmitters. It also interacts with syntaxin and synaptobrevin through its N-terminal and C-terminal α -helical domains. In previous studies by other investigators, it was shown that expression of the protein, SNAP-25, is sufficient to induce neuronal differentiation. Both the expression of SNAP-25 and its subcellular distribution are linked closely with the transformation of growth cones to synaptic terminals (Catsicas et al. 1991). Antisense oligonucleotides of SNAP-25 block neuritic elongation in rat cortical neurons and PC-12 cells *in vitro*, and in amacrine cells of the developing chick retina *in vivo* (Osen-Sand et al. 1993). Furthermore, overexpression of SNAP-25 itself enhanced neurite elongation in PC-12 cells (Zhou et al. 2000). Hence, the protein expression level of the phenotypic marker of maturation, SNAP-25 was chosen to be examined in MN9D cells overexpressing pcDNA3.1(-)_fl nm23-M2_GFP, to test the hypothesis that nm23-M2 indeed regulates differentiation.

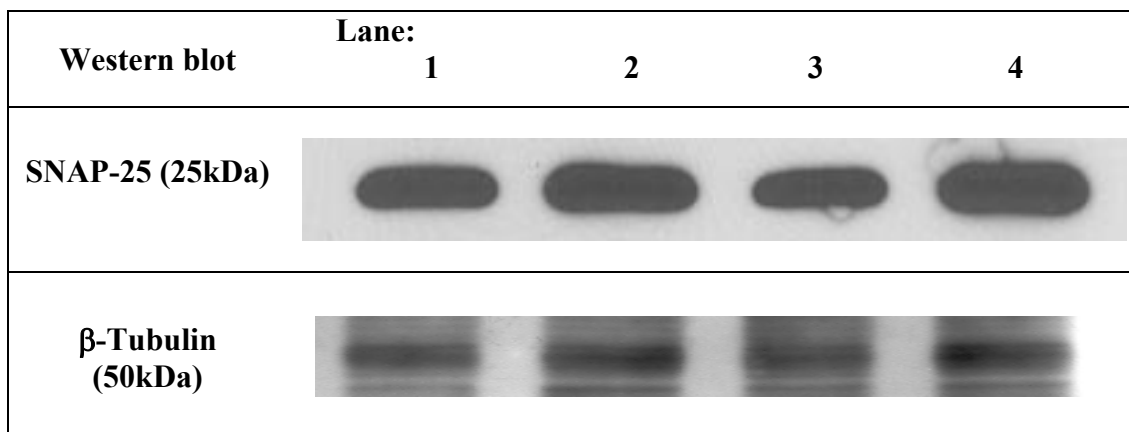


Figure 3.17 Western immunoblots showing overexpression results after 48hr of transfection using mouse anti-SNAP-25 monoclonal antibody and mouse anti- β -tubulin monoclonal antibody as loading control. Lane: 1) MN9D with mock transfection, 2) MN9D treated with 1mM *n*-butyric acid, 3) MN9D transfected with null GFP plasmid as control, 4) MN9D transfected with pcDNA3.1(-)_fl *nm23*-M2_GFP. The blot was from one experiment representative of three similar repeats.

The western immunoblot in figure 3.17 showed that the level of SNAP-25 protein was higher in both cases where a) MN9D cells treated with *n*-butyric acid (Lane 2) as compared to the MN9D with mock transfection (Lane 1) as control, b) MN9D cells transfected with MN9D transfected with pcDNA3.1(-)_fl *nm23*-M2_GFP (Lane 4) as compared to MN9D transfected with null GFP plasmid (Lane 3) as control. Analysis of this immunoblot confirmed that the morphological differentiation of MN9D cells was accompanied by an increase in protein expression in such marker of maturation as the synaptosomal protein SNAP-25.

3.2.4 Cyclin D1 mRNA and protein expression was down-regulated in MN9D cells overexpressing pcDNA3.1(-)_fl *nm23*-M2_GFP

A hallmark of terminal differentiation is an irreversible arrest in the G₀/G₁ phase of the cell cycle. This arrest involves the coordinate regulation of signals that negatively control the cell cycle machinery and inhibit the G₁/S transition. The G₁/S transition is known to be sequentially controlled by D-type cyclins, which activate cyclin-dependent kinases, CDK4 and CDK6, and subsequently by cyclin E, which associates with CDK2 (Grana and Reddy, 1995). CDK activity is dependent on association with cyclins and subsequent phosphorylation-dephosphorylation events, and may be inhibited by 2 different groups of CDK inhibitors (CKIs), namely the Ink4 family and the Cip/Kip family (Vidal and Koff, 2000). Thus, growth arrest associated with differentiation could be achieved by several mechanisms including the down-regulation of cyclins or up-regulation of CKIs or both. In the previous section 3.2.2, MN9D cells when overexpressing pcDNA3.1(-)_fl *nm23*-M2_GFP showed cell growth arrest where there was a significant increase in the percentage of G₁ phase staged cells. Therefore, the mRNA and protein level of the G₁ phase cell cycle key regulatory gene, cyclin D1 will be studied in this section.

The mRNA and protein levels of cyclin D1 were examined by RT-PCR and western immunoblot using anti-cyclin D1 antibody, respectively as shown in figure 3.18. Both the mRNA and protein levels of cyclin D1 were down-regulated in MN9D cells treated with 1mM *n*-butyric acid (Lane 2) and MN9D cells transfected with pcDNA3.1(-)_fl *nm23*-M2_GFP (Lane 4). RT-PCR of *nm23*-M2 presented in panel (A) (i) showed the increased expression of *nm23*-M2 mRNA in MN9D cells transfected with pcDNA3.1(-)_fl *nm23*-M2_GFP (Lane 4).


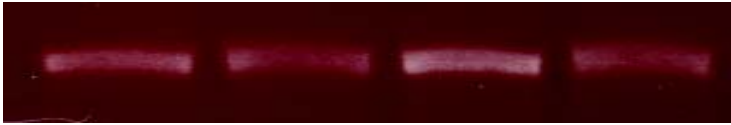

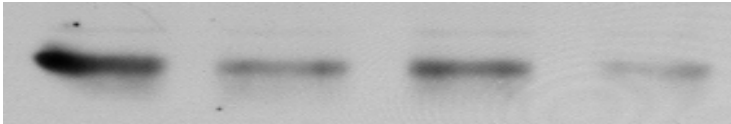
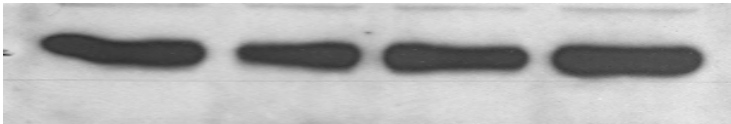
(A) RT-PCR	Lane:			
	1	2	3	4
(i) <i>Nm23-M2</i>				
(ii) Cyclin D1				
(iii) β -actin				
(B) Western blot	Lane:			
	1	2	3	4
(i) Cyclin D1 (36kDa)				
(ii) β -Tubulin (50kDa)				

Figure 3.18 **A) RT-PCR.** Gel photos showing reverse transcription of individual genes for (i) *nm23-M2*, (ii) cyclin D1 and (iii) β -actin by RT-PCR.
B) Western immunoblot analysis. Protein levels of cyclin D1 and β -tubulin (loading control) to investigate its relative expression in transfected MN9D cells.
Lane: 1) MN9D with mock transfection, 2) MN9D treated with *n*-butyric acid (1mM), 3) MN9D transfected with null GFP plasmid as control, 4) MN9D transfected with pcDNA3.1(-)_{fl} *nm23-M2*_GFP.

3.3 SiRNA interference studies of *nm23-M2* in MN9D cells

3.3.1 Knockdown expression of *nm23-M2* mRNA upon siRNA interference

The knockdown effect of *nm23-M2* was investigated by using RT-PCR. After MN9D cells were transfected with mock siRNA as control and *nm23-M2* siRNA individually for 24hr, the cells were subjected to total RNA isolation. The total RNA isolated were then used for templates for RT-PCR. Specific sets of primers were used to generate the inserts of *nm23-M2* and β -actin. The PCR products were analyzed using DNA agarose gel electrophoresis and the gel photographs taken are shown in figure 3.19. From the figure, the RT-PCR of *nm23-M2* showed that there was a knockdown expression of *nm23-M2* mRNA in the sample where *nm23-M2* siRNA was added to the cells (Lane 2) as compared to the sample where the mock siRNA was added (Lane 1). This confirmed that the *nm23-M2* siRNA worked well and indeed had a transient knockdown effect on the *nm23-M2* mRNA level. However, further experiment such as real-time PCR can be perform as RT-PCR may not be sensitive to show the quantitative differences.

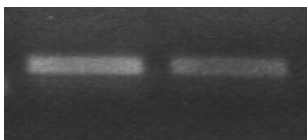
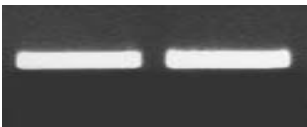
RT-PCR	Lane:	1	2
(i) <i>nm23-M2</i>			
(ii) β -actin			

Figure 3.19 RT-PCR of *nm23-M2* after siRNA interference. Gel photos showing reverse transcription of individual genes for (i) *nm23-M2* and (ii) β -actin by RT-PCR. Lane 1) MN9D transfected with a mock control siRNA for 24hr, 2) MN9D transfected with *nm23-m2* siRNA for 24hr.

3.3.2 Morphological appearance of MN9D cells after transient siRNA knockdown of *nm23-M2*

All MN9D cells plated in 6-well plates were first treated with 1mM of *n*-butyric acid except the control cells, to allow the cells to undergo cell differentiation. After adding control siRNA and *nm23-M2* siRNA in separate wells for 24hr incubation, the morphological appearance of these MN9D cells were examined by counting the number of cells bearing neurites using photographs taken from a phase contrast inverted microscope. The consolidated data collected were analyzed and plotted into a bar chart as shown in figure 3.20.

Majority of the MN9D cells that were treated with 1mM *n*-butyric acid generally exhibited neurite extension as shown in figure 3.6 as mentioned previously in the time-course MN9D differentiation experiment. No significant changes were observed for cells that were added with control siRNA as majority of the cells still displayed neurite outgrowth. This implied that the control siRNA did not have any considerable effect on the differentiated MN9D cells. For MN9D cells that were added with siRNA specific to *nm23-M2*, there was a significant decrease in the number of cells bearing neurites even though there was 1mM *n*-butyric acid present in the cell medium.

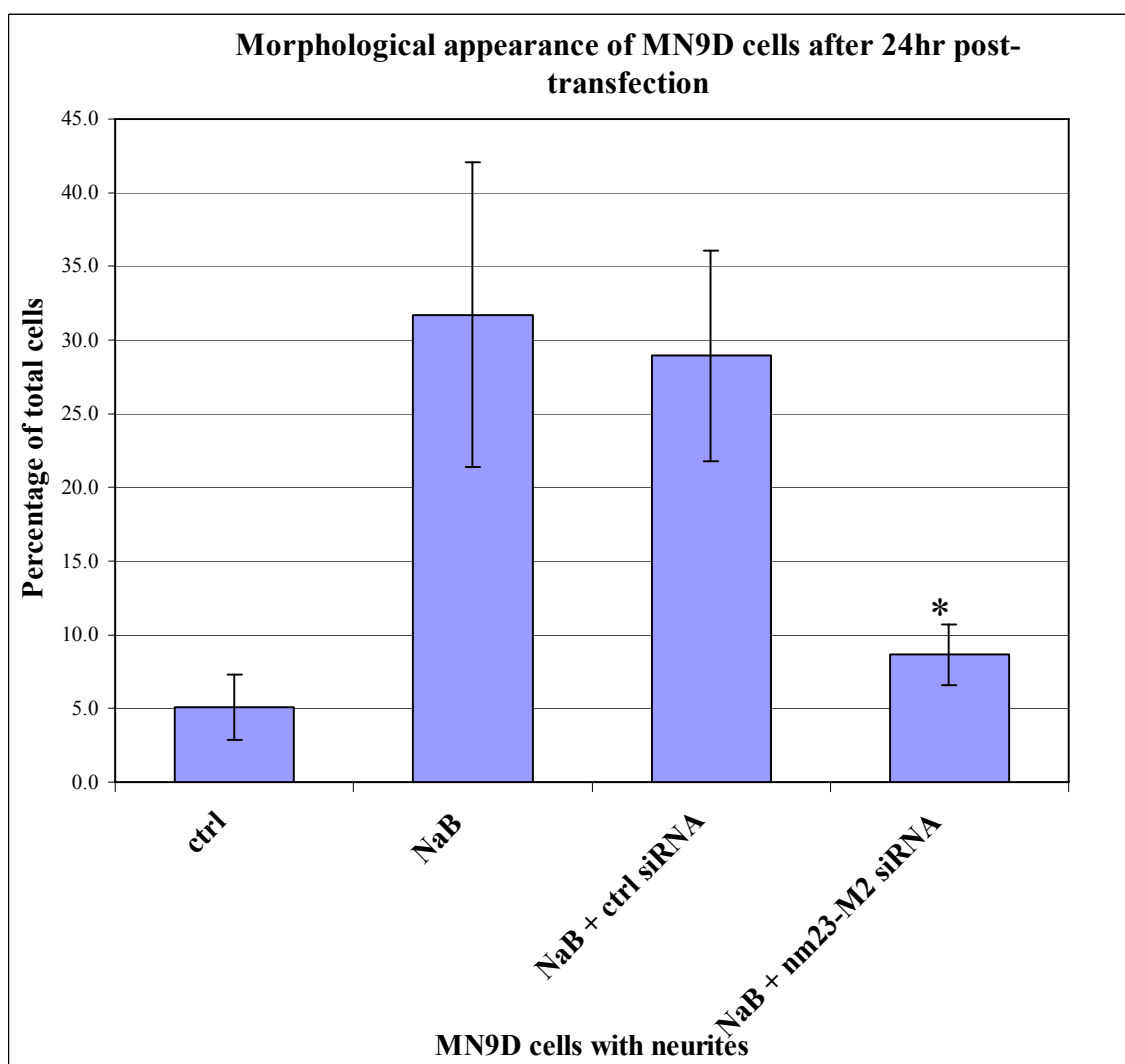


Figure 3.20 A graph showing the morphological changes of MN9D cells after 24hr post-transfection of control siRNA and *nm23-M2* siRNA. MN9D cells transfected with *nm23-M2* siRNA had significantly lesser cells with neurites than cells that were transfected with the control siRNA as determined by one-way ANOVA test using SPSS statistical software. * $P < 0.05$.

3.3.3 Cell cycle analysis of *n*-butyric acid-treated MN9D cells when *nm23*-M2 siRNA was added

Flow cytometry analysis by FACS were also performed to examine the cell cycle stages of *n*-butyric acid treated MN9D cells when added with control siRNA and *nm23*-M2 specific siRNA after 48hr of incubation. There were no significant changes in the cell cycle stages of the cells after 24hr, therefore 48hr of incubation was chosen. The FACS data were analyzed and plotted as a graph shown below in figure 3.21. Interestingly, MN9D cells that were transfected with *nm23*-M2 siRNA did not have any significant change in cell cycle stages as compared to those transfected with control siRNA.

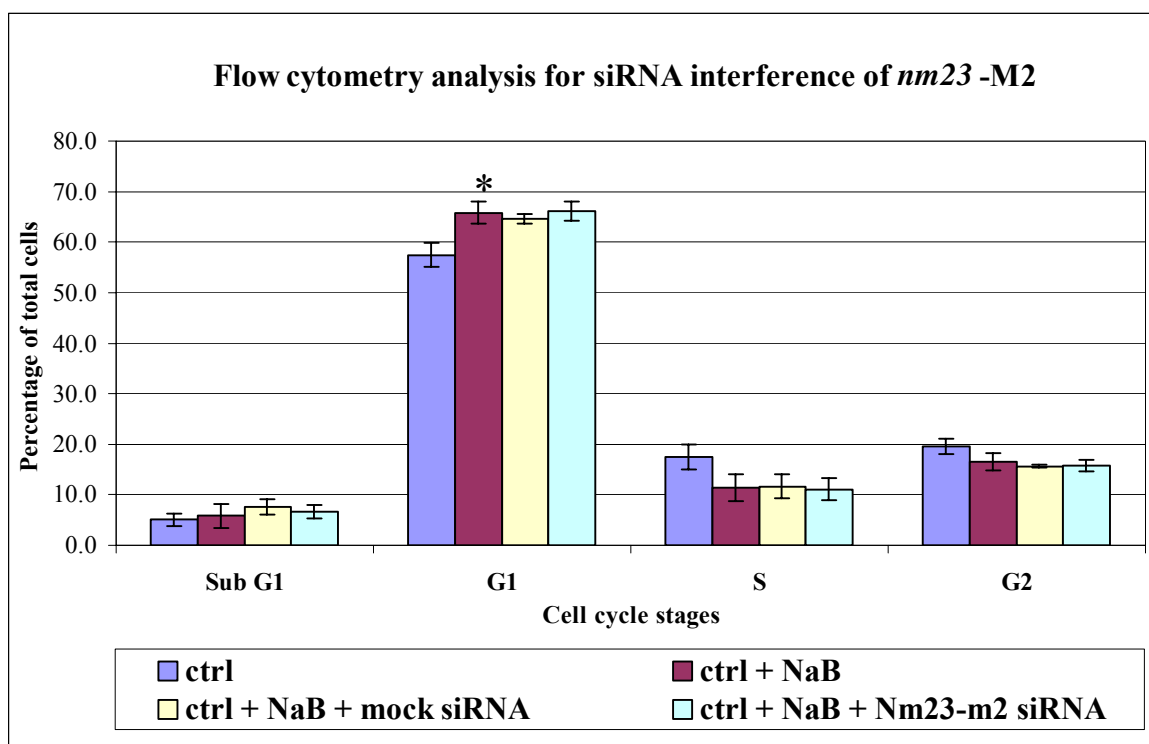


Figure 3.21 A graph showing the percentage of MN9D cells after 48hr post-transfection of control and *nm23*-M2 siRNA. MN9D cells treated with 1mM *n*-butyric acid had significantly more cells at G₁ phase than MN9D control cells as determined by one-way ANOVA using SPSS software. **P*<0.05. NaB: 1mM *n*-butyric acid, CS: control siRNA, S1: *nm23*-M2 siRNA

3.3.4 SNAP-25 protein level of *n*-butyric acid-treated MN9D cells did not increase when *nm23-M2* siRNA was added

The phenotypic marker of maturation, SNAP-25 were also examined in MN9D cells treated with *n*-butyric acid and *nm23-M2* siRNA. The western immunoblot analysis of SNAP-25 is shown in figure 3.22. Both samples of MN9D cells treated with *n*-butyric acid (Lane 2) and with the addition of control siRNA (Lane 3) showed up-regulation of protein levels of SNAP-25. MN9D cells treated with *n*-butyric acid plus *nm23-M2*-specific siRNA (Lane 4) displayed the same protein level as the control MN9D cells (Lane 1) as the level of SNAP-25 did not increase even though 1mM of *n*-butyric acid was present in the culture medium.

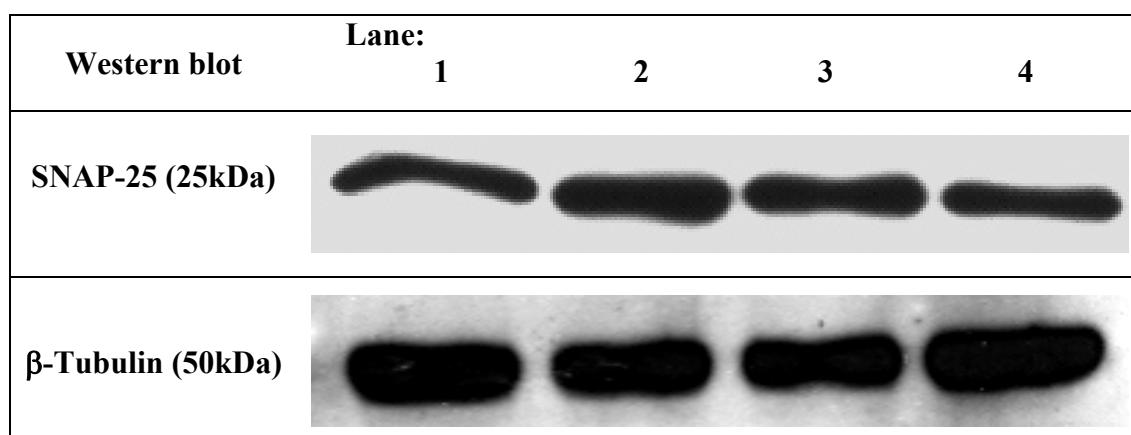


Figure 3.22 Western immunoblots showing siRNA interference results after 24hr of transfection using mouse anti-SNAP-25 monoclonal antibody and mouse anti- β -tubulin monoclonal antibody as loading control. Lane 1) MN9D control, 2) MN9D treated with *n*-butyric acid, 3) MN9D treated with *n*-butyric acid and mock siRNA, 4) MN9D treated with *n*-butyric acid and *Nm23-m2* siRNA. The blot was from one experiment representative of three similar repeats.

3.3.5 Cyclin D1 protein level of *n*-butyric acid-treated MN9D cells did not decrease when *nm23*-M2 siRNA was added

The protein expression of the key cell cycle regulatory gene, cyclin D1, was also investigated after transient siRNA knockdown of *nm23*-M2. The western immunoblot analysis of cyclin D1 is shown in figure 3.23. As mentioned in the overexpression studies in section 3.2.4, the protein levels of cyclin D1 were down-regulated in differentiated cells. Both samples of MN9D cells treated with *n*-butyric acid (Lane 2) and with the addition of control siRNA (Lane 3) showed down-regulation of protein levels of cyclin D1. Whereas in those MN9D cells treated with *n*-butyric acid and with the addition of *nm23*-M2-specific siRNA, displayed the same protein level as the control MN9D cells as the level of cyclin D1 did not decrease even though 1mM of *n*-butyric acid was present in the culture medium.

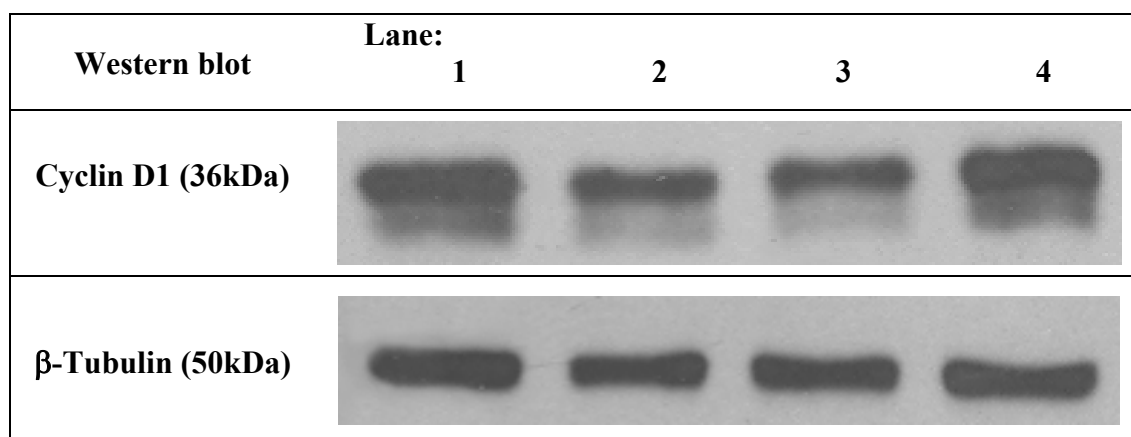


Figure 3.23 Western immunoblots showing siRNA interference results after 24hr of transfection using mouse anti-Cyclin D1 monoclonal antibody and mouse anti- β -tubulin monoclonal antibody as loading control. Lane 1) MN9D control, 2) MN9D treated with *n*-butyric acid, 3) MN9D treated with *n*-butyric acid and mock siRNA, 4) MN9D treated with *n*-butyric acid and *Nm23-m2* siRNA. The blot was from one experiment representative of three similar repeats.

Chapter 4:

Discussion

Chapter 4: Discussion

4.1 Choice of cell line model

The use of a mouse cell line model to elucidate the role of *nm23*-M2 represents a powerful means to analyze individual gene expression changes affected by various manipulations in a closely controlled environment. The choice of a mouse mesencephalic MN9D cell line was most appropriate since both the mouse and human species have a high sequence homology in their genetic makeup and gene organization, in addition to the possibility of performing *in vivo* experiments on mouse animal model in future investigation. This mesencephalic derived cell line has the advantage of representing homogeneous cell population and can be readily manipulated, therefore it is used in this study as a valuable tool to address the role of *nm23*-M2 in dopaminergic neuronal differentiation.

4.2 Temporal and spatial expression of *nm23*-M2 gene

Since it is known that *nm23*/NDPK has several different functions in the cell, knowing the expression patterns of *nm23*-M2 could reveal some clues on its function and imply the specific role in cells of different characteristics and origin, hence the temporal and spatial expressions of *nm23*-M2 gene in dopaminergic cell lines were investigated in the present study.

The temporal expression was studied during *n*-butyric acid induced MN9D differentiation by measuring the endogenous level of *nm23*-M2 mRNA by semi-quantitative real-time PCR. It was shown that the endogenous level of *nm23*-M2 mRNA in MN9D cells was the highest at the 6th day upon addition of 1mM *n*-butyric acid. From the morphological changes that took place during the 1st to 7th days of

differentiation, the first indication of differentiation in MN9D cells was the change of its morphology by the flattened cell body appearance, followed by the outgrowth of neurites, which eventually leads to the neurite extension which usually takes place on the 6th to 7th day. This indicated that *nm23*-M2 might be involved in the later stages of the differentiation pathway where most of the downstream maturation genes involving neuritogenesis, synaptogenesis, etc, will be activated. Several previously published papers implied a possible connection between *nm23* proteins and cytoskeleton structures such as intermediate filaments and microtubular network (Lombardi et al. 1995; Biggs et al. 1990; Pinon et al. 1999; Roymans et al. 2000), and such neuritogenesis events bring about dynamic changes in the cytoskeleton structures. These findings might indicate a direct involvement of *nm23* in pathways regulating cell shape and/or motility.

The decision to analyze the localization of *nm23*-M2 using green fluorescent protein techniques was based on the fact that several problems were met during the pursuit of this work, such as lack of good commercially available *nm23*-M2 antibodies and weak immunoreactivity of the commercially available *nm23*-M2 antibodies in MN9D cells. Additionally, GFP-based methods are very sensitive and enable us to track fusion proteins in living cells. The spatial expression of the GFP-tagged *nm23*-M2 proteins and the subcellular localization experiment using c-MYC-tagged *nm23*-M2 proteins revealed that *nm23*-M2 principally localized in the cytoplasm of both MN9D and SH-SY5Y cell lines, despite the difference in the cell lineage. GFP-*nm23*-M2 staining was observed in the form of granum-like structures together with the abundantly present diffuse cytosolic staining as shown in figure 3.13. This observation bears much similarity with a recent report (Bosnar et al. 2004) on human *nm23*-GFP staining in the form of granum-like structure in the cytoplasm

of HEp-2 (squamous cell carcinoma of the larynx). Confocal microscopy observations by the authors confirmed that the granum-like particles are full structure (not hollow) bearing a roughly spherical, but not necessarily symmetrical, shape. Considering that a) the granum-like structures never appear in cells transfected with the “empty” pcDNA3.1-GFP construct, b) in the cells where they appear, the number of the granum-like structures varies from one to several (rarely they can be seen in abundance); they are of different size and distribution but often seen adjacent to the nucleus, the authors have speculated that the granum-like structures could possibly be a consequence of the hetero-multimerization of subunits, leading to a catalytically active heterohexamer.

4.3 The role of *nm23*-M2 in dopaminergic MN9D differentiation

The up-regulation of *nm23*-M2 during dopaminergic MN9D differentiation in our previous suppressive subtractive hybridization and micro-array studies (manuscript in preparation) led us to speculate that *nm23*-M2 may play some specific roles in dopaminergic neuronal cells and to investigate the role of *nm23*-M2/NDPK β in neuronal differentiation of MN9D cells. To our surprise, when *nm23*-M2 was overexpressed in MN9D cells, the cells became capable of extending neurites without any differentiation inducers. Furthermore, overexpression of *nm23*-M2 leads to the increased protein expression in a maturation marker, SNAP-25. SNAP-25 is a presynaptic nerve terminal protein, which is essential for the process of neurite outgrowth *in vivo* and *in vitro* (Oyler et al. 1989; De Camilli, 1993; Osen-Sand et al. 1993). Because its expression and subcellular distribution is highly correlated with the transformation of growth cones to synaptic terminals, SNAP-25 has been used as a marker for synaptogenesis (Catsicas et al. 1991). Previous studies also reported that

morphological differentiation was usually accompanied by the increased in SNAP-25 expression (Oh et al. 1996; Choi et al. 2001; Greenlee et al. 2001). In nerve terminals, SNAP-25 participates in docking and/or fusion of synaptic vesicles with the plasmalemma, a process essential for synaptic vesicle exocytosis (Hodel, 1998; Sorensen, 2005). Decreased SNAP-25 protein levels in the brain of Down syndrome and Alzheimer's disease patients may reflect impaired synaptogenesis or represent neuronal loss (Greber et al. 1999).

Lakin et al. (1995) reported that the increased expression of Brn-3a POU (Pit-Oct-Unc) family transcription factor occurs upon differentiation of ND7 cells (rat dorsal root ganglion neurons fused with C1300 mouse neuroblastoma cell line) by serum removal. The authors have also showed that Brn-3a can activate the SNAP-25 gene promoter, and the up-regulation of this factor in ND7 cell differentiation may therefore be responsible for the corresponding increase in SNAP-25 expression during this process. Similarly, the inhibition of Brn-3a expression using an antisense approach results in the observed decrease in SNAP-25 expression and hence the failure of neurite outgrowth. These results therefore implicate that Brn-3a regulates neurite outgrowth acting via the modulation of SNAP-25 gene expression. This present study bears certain similarities in the experimental approach to what Lakin et al. (1995) has reported. Indeed, overexpression of *nm23-M2* induced an increased expression of SNAP-25 without any differentiation inducer.

SiRNA interference approach instead of antisense approach was used to reduce the exogenous expression of *nm23-M2* in MN9D cells and SNAP-25 expression was not increased even though the cells were treated with the differentiation inducer, *n*-butyric acid, hence the low number of cells exhibiting neurite outgrowth. Therefore, it is plausible that *nm23-M2* gene regulates neurite

outgrowth in dopaminergic MN9D cells acting via the modulation of SNAP-25 gene expression. However, whether up-regulation of SNAP-25 protein in MN9D/*nm23*-M2 directly results in neurite extension or is secondary to other signal transduction pathways triggered by *nm23*-M2 is not known at present.

4.4 The role of *nm23*-M2 in inducing cell cycle arrest

Cell cycle withdrawal or growth arrest is mandatory for differentiation in many cell types, and genes that regulate the transition from the G₁ to the S-phase of the cell cycle are involved in such a phenomenon. Cyclin D1 encodes the regulatory subunit of a holoenzyme that accelerates cell transit through the G₁ phase by forming complexes with Cdk4 and Cdk6 (Figure 4.1), which phosphorylate the retinoblastoma (Rb) protein (Sherr, 1995), blocking the function of Rb as a repressor of genes required for cell proliferation (Chen et al. 1995; Beijersbergen and Bernards, 1996). The factors that determine whether cells continue to proliferate or arrest growth and differentiate operate during the G₁ phase of the cell cycle (Sherr, 1994; Weinberg, 1995; Bartek et al. 1996).

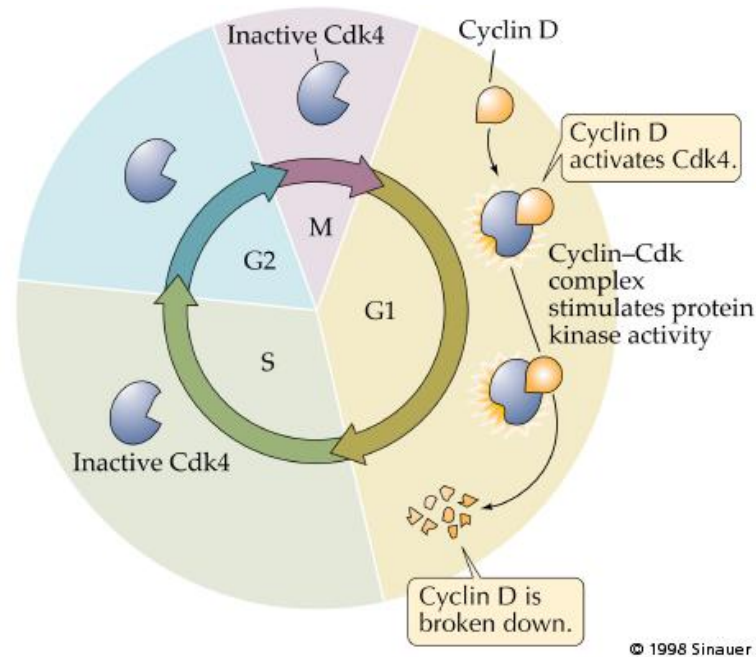


Figure 4.1 A schematic representation of cell cycle progression showing cyclins function as regulators of CDK kinases. This cyclin forms a complex with and functions as a regulatory subunit of CDK4 or CDK6, whose activity is required for cell cycle G₁/S transition.

Source: <http://www.mie.utoronto.ca/labs/lcdlab/biopics/biofigures.htm>

Previous studies by other investigators have shown that overexpression of *nm23* genes could lead to cell cycle arrest in some cell types, such as PC12 cells (Lombardi et al. 2001), colon carcinoma cells (Hsu et al. 1994) and human breast carcinoma cells (Howlett et al. 1994). In this study, the FACS results indicated that MN9D cells which were overexpressed with *nm23*-M2 underwent cell cycle arrest and have a significant increase in the number of cells in G₁ stage, which is also reflected by their slow doubling time. The cell cycle marker, cyclin D1 expression was also investigated upon overexpression of *nm23*-M2 in MN9D cells and the results showed that cyclin D1 expression both in transcriptional and translational levels was significantly decreased. The observation of the increase in number of cells in G₁ stage and decreased expression of cyclin D1 were also consistent as reflected in

MN9D cells treated with the differentiating agent, *n*-butyric acid. Therefore, it is possible that *nm23*-M2 activates transcription of negative regulators (such as Rb) of cell cycle and represses transcription of positive regulators (such as cyclin D1, Cdk4/Cdk6, etc) of cell cycle, to initiate cell cycle arrest (Figure 4.2).

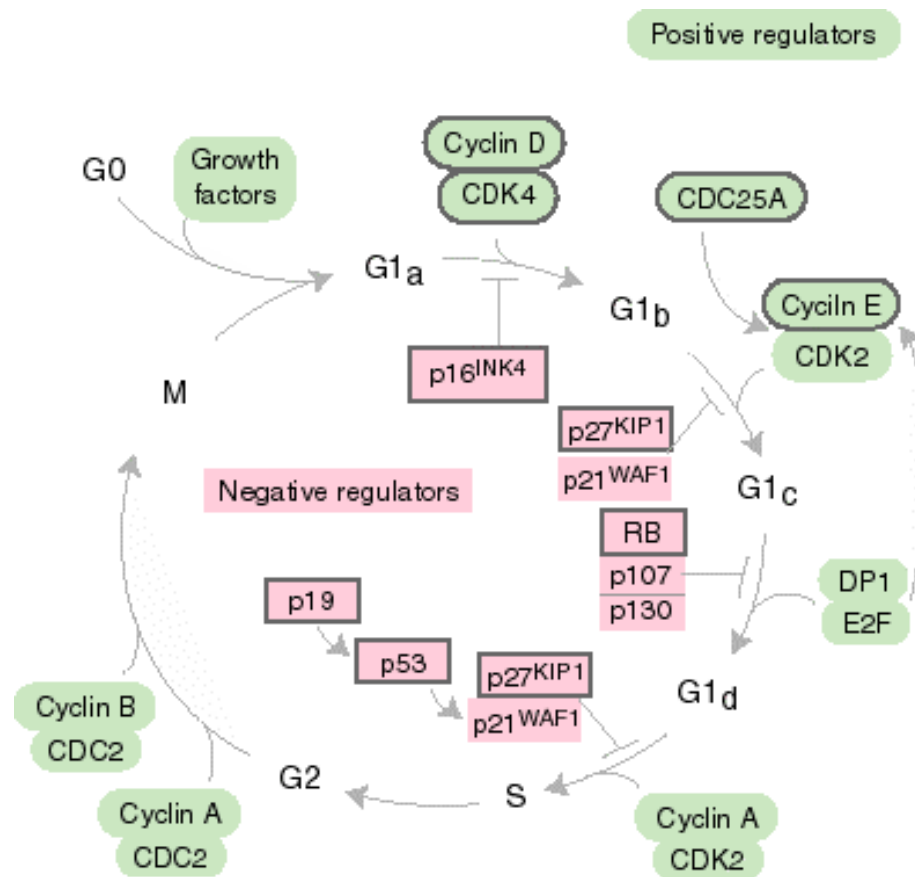


Figure 4.2 A schematic representation showing positive and negative regulators in the cell cycle progression.

Source:

http://www.fhcr.org/science/education/courses/cancer_course/basic/approaches/fundamentals/cellcycle.html

SiRNA interference of *nm23-M2* also has an effect on the expression of cyclin D1 in MN9D cells under differentiation condition (addition of 1mM *n*-butyric acid). Upon addition of *nm23-M2* siRNA, the protein level of cyclin D1 was not decreased in MN9D cells even though they were subjected to the differentiating effect of *n*-butyric acid. However, the FACS results showed otherwise, as the G₁ phase cell cycle arrest in *nm23-M2* siRNA-treated MN9D cells under differentiation condition was not reversed. This unexpected result led us to speculate that perhaps the knockdown effect of *nm23-M2* siRNA was transient and short-lived hence the cells were able to recover the endogenous level of *nm23-M2* after 48 hours. Another possible reason that *nm23-M2* siRNA approach was not able to overcome *n*-butyric acid-mediated block at G₁ phase of cell cycle arrest may be due to the fact that many regulatory genes such as Rb, Cdk4/Cdk6, etc (Figure 4.2), that are involved in controlling the machinery of G₁ to S phase cell cycle transition, thus by reducing the endogenous expression of *nm23-M2* may not be sufficient enough to prevent cell cycle arrest induced by *n*-butyric acid in MN9D cells. Nonetheless, more experiments are needed to be devised in order to elucidate the role of *nm23-M2* in modulating the regulatory genes controlling the cell cycle progression. It is worth exploring the link between *nm23-M2* and the cell cycle machinery.

4.5 Further studies to elucidate the differentiation pathway

Many studies in the past have tried to gain insight of the differentiation pathway underlying the role of the *nm23* protein but until now, it is still not known which signaling pathway(s) is involved in *nm23*-mediated neurite extension. Recent studies have indicated that activation of stress-activated protein kinases such as c-Jun N-terminal kinase (JNK) and p38 mitogen-activated protein kinase (MAPK) has been

implicated in a broad range of biological activities including neuronal differentiation (Yao et al. 1997; Iwasaki et al. 1999; Coffey et al. 2000; Takeda et al. 2000; Waetzig and Herdegen, 2003). In a previous study by Choi et al. (2001), it was demonstrated that phosphorylation of p38 is directly involved in neurite extension of MN9D dopaminergic neuronal cells overexpressing calbindin-D28K. Results from Eom et al. (2004) indicate that the JNK signal activated by Bcl-2 may play an important role in the morphological and in certain aspects of biochemical differentiation of MN9D dopaminergic neuronal cells. Hence, it is possible to devise experiments (such as treating MN9D/*nm23*-M2 with a specific JNK inhibitor, SP600125, or a p38 inhibitor, PD169316), to investigate whether *nm23*-M2 gene activate the JNK and MAPK pathway in the differentiation of dopaminergic neuronal cells.

Further studies are also needed to elucidate certain critical questions. These questions include (i) whether *nm23*-M2 induces neurite outgrowth in a specific population of neuronal cells considering its ubiquitous distribution in many of the cell types *in vivo*; (ii) whether neurite outgrowth in MN9D cells mediated by *nm23*-M2 is dependent on its known phosphotransferase activity; (iii) which specific neuronal differentiation pathway is activated by *nm23*-M2; (iv) what target protein(s) downstream in the neuronal pathway act as final effector(s) of neurite elongation. Answers to these and other critical questions may enlighten our understanding of the potential role of *nm23*-M2/NDPK β in neuronal differentiation.

4.6 Future experiments

Since proteins that are found in the same complex or in the same location are likely to be involved in the same or related cellular process, a useful approach to unravel the function of a protein is to identify other interacting proteins, possibly of known functions. Likewise, protein chemistry or genetic methods can reveal protein-protein interaction of *nm23*-M2/NDPK β . Due to the hexameric structures of eukaryotic NDPKs, they can form homo- or hetero-hexamers with different ratios of the subunits (Gilles et al. 1991; Urano et al. 1992). It may be postulated that the affinity of the interaction between subunits is higher than any other interaction with other different proteins. On the other side, the interactions of *nm23* with other proteins might require the assembly of the hexameric structure, hence the studies of protein-protein interaction of *nm23*/NDPK were much hindered. Many attempts have been made by other investigators to discover novel *nm23* protein-protein interactions using yeast two-hybrid system, the members of the ROR/RZR nuclear orphan receptor subfamily interact with *nm23* protein (Paravicini et al. 1996). More precisely, rat RZR β and human ROR α were found to strongly interact with *nm23*-M2 and they suggested putative synergistic effects of ROR/RZR and *nm23*-H2 on the N-myc gene transcription. N-myc gene is essential for normal neurogenesis, regulating neural progenitor cell proliferation, differentiation, and nuclear size. Its effects on proliferation and differentiation appear due, at least in part, to down-regulation of a specific subset of cyclin-dependent kinase inhibitors (Knoepfler et al. 2002). The heterogeneity of the interactions so far identified further indicates that *nm23* proteins cannot be merely regarded as NDPKs, but are multifunctional, hence it will be noteworthy to investigate whether the interactions require the hexameric structure,

known to be essential for the catalytic activity (Lascu et al. 1992), or are otherwise mediated by monomeric or dimeric forms of the *nm23* proteins.

This present study has made use of an *in vitro* MN9D cell model to give a better understanding to the role of *nm23*-M2 in dopaminergic neuronal differentiation. The current findings will provide a stepping-stone to transfer the experimental procedures into primary culture of mouse midbrain mesencephalic progenitor neurons to see whether overexpression of *nm23*-M2 have any effect on neuronal differentiation of the primary cell culture into dopaminergic neurons. The dopaminergic neurons could then be subsequently transplanted into animal models for further *in vivo* studies such as behavioural rescue of MPP⁺ or 6-OHDA lesion animal model (O'Malley et al. 2003). If this is promising, these dopaminergic neurons could be put into good use in cell replacement therapy for future treatment of neurodegenerative brain disorders.

4.7 Conclusion

Several biochemical functions have been proposed for the *nm23* genes in many studies, among which the NDPK activity is the most documented. However, it appears that such unspecific enzymatic activity does not solely account for the biological effects observed in differentiation process. In this regard, this present study is novel in two ways. Firstly, it was demonstrated for the first time that overexpression of *nm23*-M2 itself in MN9D dopaminergic neuronal cells leads to robust neuritic outgrowth as typified by the increase in the number of cells bearing neurites, increased expression in synaptogenesis marker, SNAP-25 and inducing cell cycle arrest as illustrated in the increase in proportion of cells in G₁ stage of the cell cycle and the decreased expression in a G₁-phase cell cycle key regulatory gene,

cyclin D1. Secondly, treatment with *nm23-M2* siRNA largely abolishes neurite outgrowth mediated by differentiation inducing agent, *n*-butyric acid in MN9D cells, implying that *nm23-M2* is one of the major contributors to the neurite outgrowth in MN9D cells induced by *n*-butyric acid. Whatever the case, it is clear that up-regulation of *nm23-M2* gene in dopaminergic MN9D cell model promotes neuronal differentiation through initiating neurite outgrowth and inducing growth arrest.

In conclusion, the present study and the proposed future work aim to elucidate the multifunctional role of *nm23-M2*, particularly in dopaminergic neuronal differentiation. These findings may eventually contribute to the understanding of pathways or mechanisms on the induction of dopaminergic neuron differentiation that could facilitate the development of gene delivery or cell replacement therapeutics for brain neurodegenerative disorders.

References

References

Agid, Y., Graybiel, M., Ruberg, M., Hirsch, E., Blin, J., Dubois, B., Javoy-Agid, F. (1990). The efficacy of levodopa treatment declines in the course of Parkinson's disease: do non-dopaminergic lesions play a role? *Adv. Neurol.* 53: 83-100.

Agou, F., Raveh, S., Mesnildrey, S., Veron, M. (1999). Single strand DNA specificity analysis of human nucleoside diphosphate kinase B. *J. Biol. Chem.* 274(28): 19630-19638.

Alex Mohit, A., Samii, A., Slimp, J.C., Grady, M.S., Goodkin, R. (2004). Mechanical failure of the electrode wire in deep brain stimulation. *Parkinsonism Relat. Disord.* 10(3): 153-156.

Allam, M.F., Del Castillo, A.S., Navajas, R.S. (2005). Parkinson's disease risk factors: genetic, environmental, or both? *Neurol. Res.* 27(2): 206-208.

Amendola, R., Martinez, R., Negroni, A., Venturelli, D., Tanno, B., Calabretta, B., Raschella, G. (1997). DR-nm23 gene expression in neuroblastoma cells: relationship to integrin expression, adhesion characteristics, and differentiation. *J. Natl. Cancer Inst.* 89(17): 1300-1310.

Amendola, R., Martinez, R., Negroni, A., Venturelli, D., Tanno, B., Calabretta, B., Raschella, G. (2001). DR-nm23 expression affects neuroblastoma cell differentiation, integrin expression, and adhesion characteristics. *Med. Pediatr. Oncol.* 36(1): 93-96.

- Amrein, L., Barraud, P., Daniel, J.-Y., Pérel, Y., Landry, M. (2005). Expression patterns of nm23 genes during mouse organogenesis. *Cell Tissue Res.* 5: 1-14.
- Arenas, E. (2002). Stem cells in the treatment of Parkinson's disease, *Brain Res. Bulletin* 57(6): 795-808.
- Arnaud-Dabernat, S., Masse, K., Smani, M., Peuchant, E., Landry, M., Bourbon, P.M., Le Floch, R., Daniel, J.Y., Larou, M. (2004). Nm23-M2/NDP kinase B induces endogenous c-myc and nm23-M1/NDP kinase A overexpression in BAF3 cells. Both NDP kinases protect the cells from oxidative stress-induced death. *Exp Cell Res.* 301(2): 293-304.
- Baba, H., Urano, T., Okada, K., Furukawa, K., Nakayama, E., Tanaka, H., Iwasaki, K., Shiku, H. (1995). Two isotypes of murine nm23/nucleoside diphosphate kinase, nm23-M1 and nm23-M2, are involved in metastatic suppression of a murine melanoma line. *Cancer Res.* 55(9): 1977-1981.
- Backer, M.V., Kamel, N., Sandoval, C., Jayabose, S., Mendola, C.E., Backer, J.M. (2000). Overexpression of NM23-1 enhances responsiveness of IMR-32 human neuroblastoma cells to differentiation stimuli. *Anticancer Res.* 20(3A): 1743-1749.
- Barker, R.A., Dunnett, S.B., Faissner, A., Fawcett, J.W. (1996). The time course of loss of dopaminergic neurons and the gliotic reaction surrounding grafts of embryonic mesencephalon to the striatum, *Exp. Neurol.* 141: 79-93.

- Bartek, J., Bartkova, J., Lukas, J. (1996). The retinoblastoma protein pathway and the restriction point. *Curr. Opin. Cell Biol.* 8: 805-814.
- Barraud, P., Amrein, L., Dobremez, E., Dabernat, S., Masse, K., Larou, M., Daniel JY, Landry M. (2002). Differential expression of nm23 genes in adult mouse dorsal root ganglia. *J. Comp. Neurol.* 444(4): 306-323.
- Beijersbergen, R.L., Bernards, R. (1996). Cell cycle regulation by the retinoblastoma family of growth inhibitory proteins. *Biochim. Biophys. Acta.* 1287: 103-120.
- Bennett, J.P. Jr. and Piercey, M.F. (1999). Pramipexole--a new dopamine agonist for the treatment of Parkinson's disease. *J. Neurol. Sci.* 163(1): 25-31.
- Bergman, H., Deuschl, G. (2002). Pathophysiology of Parkinson's disease: from clinical neurology to basic neuroscience and back. *Mov. Disord.* 17 Suppl 3: S28-40.
- Bevilacqua, G., Sobel, M.E., Liotta, L.A., Steeg, P.S. (1989). Association of low nm23 RNA levels in human primary infiltrating ductal breast carcinomas with lymph node involvement and other histopathological indicators of high metastatic potential. *Cancer Res.* 49: 5185-5190.
- Biggs, J., Hersperger, E., Steeg, P.S., Liotta, L.A., Shearn, A. (1990). A *Drosophila* gene that is homologous to a mammalian gene associated with tumor metastasis codes for a nucleoside diphosphate kinase. *Cell* 63: 933-940.

Biggs, J., Tripoulas, N., Hersperger, E., Dearolf, C., Shearn, A. (1988). Analysis of the lethal interaction between the prune and Killer of prune mutations of *Drosophila*. *Genes Dev.* 2(10):1333-43.

Björklund, A., & Lindvall, O. (1984). Dopamine-containing systems in the CNS. In *Handbook of Chemical Neuroanatomy: Vol. 2. Classical Transmitters in the CNS* (Eds: Björklund A. and Hökfelt, T.), Part I: 55-122. Elsevier Science Publishers, Amsterdam.

Björklund, L., Herlihy, D., Isacson, O. (2000). Cell and synaptic replacement therapy for Parkinson's disease: Current status and future directions, *Neurosci. News* 3: 6-12.

Bosnar, M.H., De Gunzburg, J., Bago, R., Brecevic, L., Weber, I., Pavelic, J. (2004). Subcellular localization of A and B Nm23/NDPK subunits. *Exp. Cell Res.* 298(1): 275-284.

Bowers, W., Howard, D., Federoff, H. (1997). Gene therapeutic strategies for neuroprotection: Implications for Parkinson's disease, *Exp. Neurol.* 144: 58-68.

Breit, S., Schulz, J.B., Benabid, A.L. (2004). Deep brain stimulation. *Cell Tissue Res.* 318(1): 275-88.

Brundin, P., Karlsson, J., Emgård, M., Schierle, G.S., Hansson, O., Petersen, A., Castilho, R.F. (2000). Improving the survival of grafted dopaminergic neurons: A review over current approaches, *Cell Transplant.* 9: 179-195.

Castro, D.S., Hermanson, E., Joseph, B., Wallen, A., Aarnisalo, P., Heller, A., Perlmann, T. (2001). Induction of cell cycle arrest and morphological differentiation by Nurr1 and retinoids in dopamine MN9D cells, *J. Biol. Chemistry* 276: 43277-43284.

Catsicas, S., Larhammar, D., Blomqvist, A., Sanna, P. P., Milner, R. J., Wilson, M. C. (1991). Expression of a conserved cell-type-specific protein in nerve terminals coincides with synaptogenesis. *Proc. Natl. Acad. Sci. USA.* 88: 785-789.

Carvey, P.M., Ling, Z.D., Sortwell, C.W., Pitzer, M.R., Collier, T.J. (2000). Hematopoietic cytokines convert mesencephalic progenitor cells into dopamine neurons which survive grafting into rats, *Abs. Soc. Neurosci.* 26: 2056.

Cassidy, R., Frisen, J. (2001). Stem cells on the brain, *Nature* 412: 690-691.

Charles, P.D., Padaliya, B.B., Newman, W.J., Gill, C.E., Covington, C.D., Fang, J.Y., So, S.A., Tramontana, M.G., Konrad, P.E., Davis, T.L. (2004). Deep brain stimulation of the subthalamic nucleus reduces antiparkinsonian medication costs. *Parkinsonism Relat Disord.* 10(8): 475-479.

Chen, P.L., Riley, D.J., Lee, W.H. (1995) The retinoblastoma protein as a fundamental mediator of growth and differentiation signals. *Crit. Rev. Eukaryot. Gene Expr.* 5: 79-95.

- Chiadmi, M., Morera, S., Lascu, I., Dumas, C., LeBras, G., Veron, M., Janin, J. (1993). Crystal structure of the Awd nucleotide diphosphate kinase from *Drosophila*. *Structure*. *1*(4): 283-93.
- Choi, H. K., Won, L. A., Kontur, P. J., Hammond, D. N., Fox, A. P., Wainer, B. H. (1991). Immortalization of embryonic mesencephalic dopaminergic neurons by somatic cell fusion. *Brain Res.* *552*: 67–76.
- Choi, H.K., Won, L., Roback, J.D., Wainer, B.H., Heller, A. (1992). Specific modulation of dopamine expression in neuronal hybrid cells by primary cells from different brain regions, *Proc. Natl. Acad. Sci.* *89*: 8943-8947.
- Choi-Lundberg, D.L., Lin, Q., Chang, Y.N., Chiang, Y.L., Hay, C.M., Mohajeri, H., Davidson, B.L., Bohn, M.C. (1997). Dopaminergic neurons protected from degeneration by GDNF gene therapy, *Science* *275*: 838-841.
- Choi, W.K., Chun, S.Y., Markelonis, G.J., Oh, T.H., Oh, Y.J. (2001). Overexpression of calbindin-D28K induces neurite outgrowth in dopaminergic neuronal cells via activation of p38 MAPK. *Biochem. Biophys. Res. Commun.* *287*(3): 656-661.
- Coffey, E.T., Hongisto, V., Dickens, M., Davis, R.J., Courtney, M.J. (2000). Dual roles for c-Jun N-terminal kinase in developmental and stress responses in cerebellar granule neurons. *J. Neurosci.* *20*: 7602-7613.

Curtis, L., Lees, A.J., Stern, G.M., Marmot, M.G. (1984). Effect of L-dopa on course of Parkinson's disease, *Lancet* 2: 211-212.

Dabernat, S., Larou, M., Masse, K., Hokfelt, T., Mayer, G., Daniel, J.Y., Landry, M. (1999). Cloning of a second nm23-M1 cDNA: expression in the central nervous system of adult mouse and comparison with nm23-M2 mRNA distribution. *Mol. Brain Res.* 63: 351-365.

Deacon, T., Dinsmore, J., Costantini, L. C., Ratliff, J., Isacson, O. (1998). Blastula-derived stem cells can differentiate into dopaminergic and serotonergic neurons after transplantation, *Exp. Neurol.* 149: 28-41.

Deacon, T., Schumacher, J., Dinsmore, J., Thomas, C., Palmer, P., Kott, S., Edge, A., Penney, D., Kassissieh, S., Dempsey, P., Isacson, O. (1997). Histological evidence of fetal pig neural cell survival after transplantation into a patient with Parkinson's disease, *Nat. Med.* 3: 350-353.

Dearolf, C.R., Hersperger, E., Shearn, A. (1988). Developmental consequences of awdb3, a cell-autonomous lethal mutation of *Drosophila* induced by hybrid dysgenesis. *Dev Biol.* 129(1): 159-68.

De Camilli, P. (1993). Exocytosis goes with a SNAP. *Nature.* 364(6436): 387-388.

Diamond, A., Jankovic, J. (2005). The effect of deep brain stimulation on quality of life in movement disorders. *J. Neurol. Neurosurg. Psychiatry.* 76(9):1188-1193.

Dumas, C., Lascu, I., Morera, S., Glaser, P., Fourme, R., Wallet, V., Lacombe, M.-L., Veron, M., Janin, J. (1992). X-ray structure of nucleoside diphosphate kinase. *EMBO J. 11*: 3203-3208.

Dunnett, S.B., Bjorklund, A. (1999). Prospect for new restorative and neuroprotective treatments in Parkinson's disease, *Nature 399*: A32-A39.

During, M., Naegele, J., O'Malley, K.L., Gellar, A. (1994). Long-term behavioral recovery in parkinsonian rats by an HSV vector expressing tyrosine hydroxylase, *Science 266*: 1399-1403.

Eom, D.S., Choi, W.S., Oh, Y.J. (2004). Bcl-2 enhances neurite extension via activation of c-Jun N-terminal kinase. *Biochem. Biophys. Res. Commun. 314*(2): 377-381.

Eom, D.S., Choi, W.S., Oh, Y.J. (2005). Activation of c-Jun N-terminal kinase is required for neurite outgrowth of dopaminergic neuronal cells. *Neuroreport 16*(8): 823-828.

Fahn, S. (2003). Description of Parkinson's disease as a clinical syndrome. *Ann. N. Y. Acad. Sci. 991*: 1-14.

Favor, J., Sandulache, R., Neuhauser-Klaus, A., Pretsch, W., Chat-terjee, B., Senft, E., Wurst, W., Blanquet, V., Grimes, P., Sporle, R., Schughart, K. (1996). The mouse

Pax2(1Neu) mutation is identical to a human PAX2 mutation in a family with renal-coloboma syndrome and results in developmental defects of the brain, ear, eye, and Kidney, *Proc. Natl. Acad. Sci. USA* 93: 13870-13875.

Fawcett, J. W., Barker, R.A., Dunnett, S.B. (1995). Dopaminergic neuronal survival and the effects of bFGF in explant, three dimensional and monolayer cultures of embryonic rat ventral mesencephalon, *Exp. Brain Res.* 106: 275–282.

Fjord-Larsen, L., Johansen, J.L., Kusk, P., Tornøe, J., Gronborg, M., Rosenblad, C., Wahlberg, L.U. (2005). Efficient in vivo protection of nigral dopaminergic neurons by lentiviral gene transfer of a modified Neurturin construct. *Exp Neurol.* 195(1): 49-60.

Forno, L.S. (1996). Neuropathology of Parkinson's disease. *J. Neuropathol. Exp. Neurol.* 55(3): 259-272.

Fraefel, C., Song, S., Lim, F., Lang, P., Yu, L., Wang, Y., Wild, P., Geller, A. (1996). Helper virus-free transfer of herpes simplex virus type 1 plasmid vectors into neural cells, *J. Virol.* 70: 7190-7197.

Freije, J.M., Blay, P., MacDonald, N.J., Manrow, R.E., Steeg, P.S. (1997). Site-directed mutation of Nm23-H1. Mutations lacking motility suppressive capacity upon transfection are deficient in histidine-dependent protein phosphotransferase pathways in vitro. *J. Biol. Chem.* 272(9): 5525-5532.

Fujimoto, Y., Ohtake, T., Nishimor, H., Ikuta K., Ohhira, M., Ono, M., Kohgo, Y. (1998). Reduced expression and rare genomic alteration of nm23-H1 in human hepatocellular carcinoma and hepatoma cell lines. *J. Gastroenterol.* 33: 368-375.

Galpern, W.R., Burns, L.H., Deacon, T.W., Dinsmore, J., Isacson, O. (1996). Xenotransplantation of porcine fetal ventral mesencephalon in a rat model of Parkinson's disease: functional recovery and graft morphology, *Exp. Neurol.* 140: 1-13.

Gervasi, F., D'Agnano, I., Vossio, S., Zupi, G., Sacchi, A., Lombardi, D. (1996). nm23 influences proliferation and differentiation of PC12 cells in response to nerve growth factor. *7(12)*: 1689-1695.

Gervasi, F., Capozza, F., Bruno, T., Fanciulli, M., Lombardi, D. (1998). Identification of novel mRNA transcripts of the nm23-M1 gene that are modulated during mouse embryo development and are differently expressed in adult murine tissues. *DNA and Cell Biol.* 17: 1047-1055.

Gilles, A.M., Presecan, E., Vonica, A., Lascu, I. (1991). Nucleoside diphosphate kinase from human erythrocytes. Structural characterization of the two polypeptide chains responsible for heterogeneity of the hexameric enzyme. *J. Biol. Chem.* 266: 8784-8789.

Ghika, J., Villemure, J.G., Fankhauser, H., Favre, J., Assal, G., Ghika-Schmid, F. (1998). Efficiency and safety of bilateral contemporaneous pallidal stimulation (deep brain stimulation) in levodopa-responsive patients with Parkinson's disease with severe motor fluctuations: a 2-year follow-up review. *J. Neurosurg.* 89(5): 713-718.

Grana, X., Reddy, E.P. (1995). Cell cycle control in mammalian cells: role of cyclins, cyclin dependent kinases (CDKs), growth suppressor genes and cyclin-dependent kinase inhibitors (CKIs). *Oncogene.* 11: 211-219.

Greber, S., Lubec, G., Cairns, N., Fountoulakis, M. (1999). Decreased levels of synaptosomal associated protein 25 in the brain of patients with Down syndrome and Alzheimer's disease. *Electrophoresis.* 20(4-5): 928-934.

Greenlee, M.H., Roosevelt, C.B., Sakaguchi, D.S. (2001). Differential localization of SNARE complex proteins SNAP-25, syntaxin, and VAMP during development of the mammalian retina. *J.Comp.Neurol.* 430(3): 306-320.

Grondin, R. and Gash D.M. (1998). Glial cell line-derived neurotrophic factor (GDNF): a drug candidate for the treatment of Parkinson's disease. *J. Neurol.* 245(11 Suppl 3): 35-42.

Hanks, M., Wurst, W., Anson-Cartwright, L., Auerbach, A.B., Joyner, A.L. (1995). Rescue of the En-1 mutant phenotype by replacement of En-1 with En-2. *Science* 269(5224): 679 –682.

Hantraye, P., Riche, D.M.M., Isacson, O. (1992). Intrastratial grafting of cross-species fetal striatal cells reduces abnormal movements in a primate model of Huntington's disease. *Proc. Natl. Acad. Sci. USA* 89: 4187-4191.

Hartsough, M.T., Steeg, P.S. (2000). *Nm23*/nucleoside diphosphate kinase in human cancers. *J. Bioenerg. Biomembr.* 32: 301-308.

Heller, A., Freeney, A., Hessefort, S., Villereal, M., Won, L. (2000). Cellular dopamine is increased following exposure to a factor derived from immortalized striatal neurons in humans, *Neurosci. Letters* 295: 1-4.

Heller, A., Price, S., Won, L. (1996). Glial-derived neurotrophic factor (GDNF) induced morphological differentiation of an immortalized monoclonal hybrid dopaminergic cell line of mesencephalic neuronal origin, *Brain Res.* 725: 132-136.

Hildebrandt, M., Lacombe, M.L., Mesnildrey, S., Veron, M. (1995). A human NDP-kinase B specifically binds single-stranded poly-pyrimidine sequences. *Nucleic Acids Res.* 23(19): 3858-3864.

Hodel, A. (1998). SNAP-25. *Int. J. Biochem. Cell Biol.* 30(10):1069-1073.

Hou, J.G., Lin, L.H., Mytilineou, C. (1996). Glial cell-line derived neurotrophic factor exerts neurotrophic effects on dopaminergic neurons in vitro and promotes their survival and regrowth after damage by 1-methyl-4-phenylpyridinium, *J. Neurochem.* 66: 74-82.

Howlett, A.R., Petersen, O.W., Steeg, P.S., Bissell, M.J. (1994). A novel function for the nm23-H1 gene: overexpression in human breast carcinoma cells leads to the formation of basement membrane and growth arrest. *J. Natl. Cancer Inst.* 86(24): 1838-1844.

Hsu, S., Huang, F., Wang, L., Banerjee, S., Winawer, S., Friedman, E. (1994). The role of nm23 in transforming growth factor beta 1-mediated adherence and growth arrest. *Cell Growth Differ.* 5(9): 909-917.

Huitorel, P., Simon, C., Pantaloni, D. (1984). Nucleoside diphosphate kinase from brain. Purification and effect on microtubule assembly in vitro. *Eur. J. Biochem.* 144: 233-241.

Hyman, C., Goffer, M., Barde, Y., Juhasz, M., Yancopoulos, G., Squinto, S., Lindsay, R. (1991). BDNF is a neurotrophic factor for dopaminergic neurons of the substantia nigra, *Nature* 350: 230-232.

Hyman, C., Juhasz, M., Jackson, C., Wright, P., Ip, N. Y., Lindsay, R. M. (1994). Overlapping and distinct actions of the neurotrophins BDNF, NT-3, and NT-4/5 on cultured dopaminergic and GABAergic neurons of the ventral mesencephalon, *Neuroscience* 14: 335-347.

Hynes, M., Porter, J.A., Chiang, C., Chang, D., Tessier-Lavigne, M., Beachy, P.A., Rosenthal, A. (1995). Induction of midbrain dopaminergic neurons by Sonic hedgehog. *Neuron* 15(1): 35-44.

Hynes, M. A., Poulsen, K., Armanini, M., Berkemeier, L., Phillips, H., Rosenthal, A. (1994). Neurotrophin-4/5 is a survival factor for embryonic midbrain dopaminergic neurons in enriched cultures, *J. Neurosci. Res.* 37: 144-154.

Isacson, O., Costantini, L., Schumacher, J.M., Cicchetti, F., Chung, S., Kim, K. (2001). Cell implantation therapies for Parkinson's disease using neural stem, transgenic or xenogeneic donor cells, *Parkinsonism & Related Disorder* 7(3): 205-212.

Isacson, O., Deacon, T.W., Pakzaban, P., Galpern, W.R., Dinsmore, J., Burns, L.H. (1995). Transplanted xenogeneic neural cells in neurodegenerative disease models exhibit remarkable axonal target specificity and distinct growth patterns of glial and axonal fibres, *Nat. Med.* 1: 1189-1194.

Isacson, O., Riche, D., Hantraye, P., Sofroniew, M.V., Maziere, M. (1989). A primate model of Huntington's disease: cross-species implantation of striatal precursor cells to the excitotoxically lesioned baboon caudate-putamen, *Exp. Brain Res.* 75: 213-220.

Ishijima, Y., Shimada, N., Fukuda, M., Miyazaki, H., Orlov, N.Y., Orlova, T.G., Yamada, T., Kimura, N. (1999). Overexpression of nucleoside diphosphate kinases induces neurite outgrowth and their substitution to inactive forms leads to suppression of nerve growth factor- and dibutyryl cyclic AMP-induced effects in PC12D cells. *FEBS Lett.* 445(1): 155-159.

Israel, Z., Hassin-Baer, S. (2005). Subthalamic stimulation for Parkinson's disease. *Isr. Med. Assoc. J.* 7(7): 458-63.

Iwasaki, S., Iguchi, M., Watanabe, K., Hoshino, R., Tsujimoto, M., Kohno, M. (1999). Specific activation of the p38 mitogen-activated protein kinase signaling pathway and induction of neurite outgrowth in PC12 cells by bone morphogenetic protein-2. *J. Biol. Chem.* 274: 26503-26510.

Kantor, J.D., McCormick, B., Steeg, P.S., Zetter, B.R. (1993). Inhibition of cell motility after nm23 transfection of human and murine tumor cells. *Cancer Res.* 53(9): 1971-1973.

Kastner, P., Mark, M., Chambon, P. (1995). Nonsteroid Nuclear Receptors: What Are Genetic Studies Telling Us about Their Role In Real Life?, *Cell* 83: 859-869.

Keim, D., Hailat, N., Melhem, R., Zhu, X.X., Lascu, I., Veron, M., Strahler, J., Hanash, S.M. (1992). Proliferation-related expression of p19/nm23 nucleoside diphosphate kinase. *J. Clin. Invest.* 89(3): 919-924.

Klein, R.L., Meyer, E.M., Peel, A.L., Zolotukhin, S., Meyers, C., Muzyczka, N., King, M.A. (1998). Neuron-specific transduction in the rat septohippocampal or nigrostriatal pathway by recombinant adeno-associated virus vectors, *Exp. Neurol.* 150: 183-194.

Kimura, N., Shimada, N., Nomura, K., Watanabe, K. (1990). Isolation and characterization of a cDNA clone encoding rat nucleoside diphosphate kinase. *J. Biol. Chem.* 265: 15744-15749.

Kim, S.H., Fountoulakis, M., Cairns, N.J., Lubec, G. (2002). Human brain nucleoside diphosphate kinase activity is decreased in Alzheimer's disease and Down syndrome. *Biochem. Biophys. Res. Commun.* 296(4): 970-5.

Kimura, N., Shimada, N., Fukuda, M., Ishijima, Y., Miyazaki, H., Ishii, A., Takagi, Y., Ishikawa, N. (2000). Regulation of cellular functions by nucleoside diphosphate kinases in mammals. *J. Bioenerg. Biomembr.* 32: 309-315.

Kitamura, Y., Kohno, Y., Nakazawa, M., Nomura, Y. (1997). Inhibitory effects of talipexole and pramipexole on MPTP-induced dopamine reduction in the striatum of C57BL/6N mice. *Jpn. J. Pharmacol.* 74: 51-57.

Knoepfler, P.S., Cheng, P.F., Eisenman, R.N. (2002). N-myc is essential during neurogenesis for the rapid expansion of progenitor cell populations and the inhibition of neuronal differentiation. *Genes Dev.* 16(20): 2699-2712.

Knusel, B., Michel, P. P., Schwaber, J. S., Hefti, F. (1990). Selective and non-selective stimulation of central cholinergic and dopaminergic development in vitro by nerve growth factor, basic fibroblast growth factor, epidermal growth factor, insulin and the insulin-like growth factors I and II, *J. Neurosci.* 10: 558-570.

Kordower, J.H., Emborg, M.E., Bloch, J., Ma, S.Y., Chu, Y., Leventhal, L., McBride, J., Chen, E.Y., Palfi, S., Roitberg, B.Z., Brown, W.D., Holden, J.E., Pyzalski, R., Taylor, M.D., Carvey, P., Ling, Z., Trono, D., Hantraye, P., Deglon, N., Aebischer, P. (2000). Neurodegeneration prevented by lentiviral vector delivery of GDNF in primate models of Parkinson's disease, *Science* 290: 767-773.

Kriegstein, K., Unsicker, K. (1994). Transforming growth factor-B promotes survival of midbrain dopaminergic neurons and protects them against N-methyl-4-phenylpyridinium ion toxicity, *Neuroscience* 63: 1189-1196.

Lacombe, M.L., Milon, L., Munier, A., Mehus, J.G., Lambeth, D.O. (2000). The human Nm23/nucleoside diphosphate kinases. *J. Bioenerg. Biomembr.* 32: 247-258.

Lakin, N.D., Morris, P.J., Theil, T., Sato, T.N., Moroy, T., Wilson, M.C., Latchman, D.S. (1995). Regulation of neurite outgrowth and SNAP-25 gene expression by the Brn-3a transcription factor. *J. Biol. Chem.* 270(26): 15858-15863.

Lakso, M., Steeg, P.S., Westphal, H. (1992). Embryonic expression of nm23 during mouse organogenesis. *Cell Growth Differ.* 3: 873-879.

Lascu, I., and Gonin, P. (2000). The catalytic mechanism of nucleoside diphosphate kinases. *J. Bioenerg. Biomembr.* 32(3): 237-246.

Lee, I.H., Chang, S.I., Okada, K., Baba, H., Shiku, H. (1997). Transcription effect of nm23-M2/NDP kinase on c-myc oncogene. *7(5):* 589-593.

Lestienne, P., Nelson, J., Riederer, P., Jellinger, K., Reichmann, H. (1990). Normal mitochondrial genome in brain from patients with Parkinson's disease and complex I defect. *J. Neurochem.* 55: 1810–1812.

Leone, A., Flatow, U., King, C.R., Sandeen, M.A., Margulies, I.M., Liotta, L.A., Steeg, P.S. (1991). Reduced tumor incidence, metastatic potential, and cytokine responsiveness of nm23-transfected melanoma cells. *Cell.* 65(1): 25-35.

Leone, A., Flatow, U., VanHoutte, K., Steeg, P.S. (1993). Transfection of human nm23-H1 into the human MDA-MB-435 breast carcinoma cell line: effects on tumor metastatic potential, colonization and enzymatic activity. *Oncogene.* 8(9): 2325-2333.

Lin, L., Doherty, D., Lile, J., Bektesh, S., Collins, F. (1993). GDNF: A glial cell line-derived neurotrophic factor for midbrain dopaminergic neurons, *Science* 260: 1130-1132.

Ling, Z.D., Potter, E.D., Lipton, J.W., Carvey, P.M. (1998). Differentiation of mesencephalic progenitor cells into dopaminergic neurons by cytokines, *Exp. Neurol.* 149: 411-423.

Lombardi, D., Lacombe, M.L., Paggi, M.G. (2000). nm23: unraveling its biological function in cell differentiation. *J. Cell. Physiol.* 182: 144-149.

Lombardi, D., Palescandolo, E., Giordano, A., Paggi, M.G. (2001). Interplay between the antimetastatic nm23 and the retinoblastoma-related Rb2/p130 genes in promoting neuronal differentiation of PC12 cells. *Cell Death Differ.* 8(5): 470-476.

Lombardi, D., Sacchi, A., D'Agostino, G., Tibursi, G. (1995). The association of the Nm23-M1 protein and β -tubulin correlates with cell differentiation. *Exp Cell Res.* 217: 267-271.

MacDonald, N.J., Freije, J.M., Stracke, M.L., Manrow, R.E., Steeg, P.S. (1996). Site-directed mutagenesis of nm23-H1. Mutation of proline 96 or serine 120 abrogates its motility inhibitory activity upon transfection into human breast carcinoma cells. *J Biol Chem.* 271(41): 25107-25116.

Mandel, R., Rendahl, K., Spratt, S., Snyder, R., Cohen, L., Leff, S. (1998). Characterization of intrastriatal recombinant adeno-associated virus-mediated gene transfer of human tyrosine hydroxylase and human GTP-cyclohydrolase I in a rat model of Parkinson's disease, *J. Neurosci.* 18: 4271-4284.

Martinez, R., Venturelli, D., Perrotti, D., Veronese, M.L., Kastury, K., Druck, T., Huebner, K., Calabretta, B. (1997). Gene structure, promoter activity, and chromosomal location of the DR-nm23 gene, a related member of the nm23 gene family. *Cancer Res.* 57(6): 1180-1187.

Masse, K., Dabernat, S., Bourbon, P.M., Larou, M., Amrein, L., Barraud, P., Perel, Y., Camara, M., Landry, M., Lacombe, M.L., Daniel, J.Y. (2002). Characterization of

the nm23-M2, nm23-M3 and nm23-M4 mouse genes: comparison with their human orthologs. *Gene*. 296(1-2): 87-97.

Mayer, E., Dunnett, S. B., Pellitteri, R., Fawcett, J. W. (1993). Basic fibroblast growth factor promotes the survival of embryonic ventral mesencephalic dopaminergic neurons-I. Effects in vitro, *Neuroscience* 56: 379-388.

Meyers, E.N., Lewandoski, M., Martin, G.R. (1998). An Fgf8 mutant allelic series generated by Cre- and Flp-mediated recombination, *Nat. Genet.* 18: 136 –141.

McMahon, A. P., Bradley, A. (1990). The Wnt-1 (int-1) proto-oncogene is required for development of a large region of the mouse brain, *Cell* 62: 1073–1085.

Milon, L., Rousseau-Merck, M.F., Munier, A., Erent, M., Lascau, I., Capeau, J., Lacombe, M.L. (1997). nm23-H4, a new member of the family of human nm23/nucleoside diphosphate kinase genes localised on chromosome 16p13. *Hum Genet.* 99(4): 550-7.

Moller, J.C and Oertel, W.H. (2005). Pramipexole in the treatment of Parkinson's disease: new developments. *Expert Rev Neurother.* 5(5): 581-586.

Montgomery, R., Warner, M., Lum, B., Spear, P. (1996). Herpes simplex virus-1 entry into cells mediated by a novel member of the TNF/NGF receptor family, *Cell* 87: 427-436.

- Moon, H., Lee, B., Choi, G., Shin, D., Prasad, D.T., Lee, O., Kwak, S.S., Kim, D.H., Nam, J., Bahk, J., Hong, J.C., Lee, S.Y., Cho, M.J., Lim, C.O., Yun, D.J. (2003). NDP kinase 2 interacts with two oxidative stress-activated MAPKs to regulate cellular redox state and enhances multiple stress tolerance in transgenic plants. *Proc. Natl. Acad. Sci. USA*. *100*(1): 358-363.
- Mourad, N., Parks, Jr. R.E. (1966). Erythrocytic nucleoside diphosphate kinases. *J. Biol. Chem.* *241*: 271-278.
- Munier, A., Feral, C., Milon, L., Pinon, V.P., Gyapay, G., Capeau, J., Guellaen, G., Lacombe, M.L. (1998). A new human nm23 homologue (nm23-H5) specifically expressed in testis germinal cells. *FEBS Lett.* *434*(3): 289-94.
- Munoz-Dorado, J., Inouye, M., Inouye, S. (1990). Nucleoside diphosphate kinase from *Myxococcus xanthus*. I. Cloning and sequencing of the gene. *J Biol. Chem.* *265*: 2702–2706.
- Negroni, A., Venturelli, D., Tanno, B., Amendola, R., Ransac, S., Cesi, V., Calabretta, B., Raschella, G. (2000). Neuroblastoma specific effects of DR-nm23 and its mutant forms on differentiation and apoptosis. *Cell Death Differ.* *7*(9): 843-850.
- Nickerson, J.A., Wells, W.W. (1984). The microtubule-associated nucleoside diphosphate kinase. *J Biol Chem* *259*: 11297-11304.

- Oh, Y.J., Swarzenski, B.C., O'Malley, K.L. (1996). Overexpression of Bcl-2 in a murine dopaminergic neuronal cell line leads to neurite outgrowth. *Neurosci. Lett.* 202(3):161-164.
- Okabe-Kado, J., Kasukabe, T., Baba, H., Urano, T., Shiku, H., Honma, Y. (1995). Inhibitory action of nm23 proteins on induction of erythroid differentiation of human leukemia cells. *Biochim. Biophys. Acta.* 1267(2-3): 101-106.
- Okabe-Kado, J., Kasukabe, T., Honma, Y. (2002). Expression of cell surface NM23 proteins of human leukemia cell lines of various cellular lineage and differentiation stages. *Leuk Res.* 26(6): 569-576.
- Okabe-Kado, J., Kasukabe, T., Hozumi, M., Honma, Y., Kimura, N., Baba, H., Urano, T., Shiku, H. (1995). A new function of Nm23/NDP kinase as a differentiation inhibitory factor, which does not require it's kinase activity. *FEBS Lett.* 363(3): 311-315.
- Olanow, C.W., Brin, M.F., Obeso, J.A. (2000). The role of deep brain stimulation as a surgical treatment for Parkinson's disease. *Neurology.* 55 (12 Suppl 6): S60-6. Review.
- Olanow, C.W., Kordower, J.H., Freeman, T.B. (1996). Fetal nigral transplantation as a therapy for Parkinson's disease, *Trends Neurosci.* 19: 102-109.

O'Malley, K.L., Liu, J., Lotharius, J., Holtz, W. (2003). Targeted expression of BCL-2 attenuates MPP⁺ but not 6-OHDA induced cell death in dopaminergic neurons. *Neurobiol. Dis.* 14(1): 43-51.

Osen-Sand, A., Catsicas, M., Staple, J. K., Jones, K. A., Ayala, G., Knowles, J., Grenningloh, G., Catsicas, S. (1993). Inhibition of axonal growth by SNAP-25 oligonucleotides *in vitro* and *in vivo*. *Nature* 364: 445-448.

Otero, A.S. (2000) NM23/nucleoside diphosphate kinase and signal transduction. *J. Bioenerg. Biomembr.* 32: 269-275.

Ouatas, T., Selo, M., Sadjji, Z., Hourdry, J., Denis, H., Mazabraud, A. (1998). Differential expression of nucleoside diphosphate kinases (NDPK/NM23) during *Xenopus* early development. *Int. J. Dev. Biol.* 42: 43-52.

Oyler, G.A., Higgins, G.A., Hart, R.A., Battenberg, E., Billingsley, M., Bloom, F.E., Wilson, M.C. (1989). The identification of a novel synaptosomal-associated protein, SNAP-25, differentially expressed by neuronal subpopulations. *J. Cell Biol.* 109(6 Pt 1): 3039-3052.

Paravicini, G., Steinmayr, M., Andre, E., Becker-Andre, M. (1996). The metastasis suppressor candidate nucleotide diphosphate kinase NM23 specifically interacts with

members of the ROR/RZR nuclear orphan receptor subfamily. *Biochem. Biophys. Res. Commun.* 227(1): 82-87.

Parks, R.E. Jr., Agarwal, R.P. (1973). Nucleoside diphosphokinases. In: Boyer PD (ed) *The enzymes*, vol 8, 3rd edn. Academic, New York, 307-334.

Park, T.H., Mytilineou, C. (1992). Protection from 1-methyl-4-phenylpyridinium (MPP⁺) toxicity and stimulation of regrowth of MPP⁺-damaged dopaminergic fibers by treatment of mesencephalic cultures with EGF and basic FGF, *Brain Res.* 599: 83-97.

Pedersen, E., Poulsen, F., Zimmer, J., Finsen, B. (1995). Prevention of mouse-rat brain xenograft rejection by a combination therapy of cyclosporin A, prednisolone and azathioprine, *Exp. Brain Res.* 106: 181-186.

Pinon, V.P., Millot, G., Munier, A., Vassy, J., Linares-Cruz, G., Capeau, J., Calvo, F., Lacombe, M.L. (1999). Cytoskeletal association of the A and B nucleoside diphosphate kinases of interphasic but not mitotic human carcinoma cell lines: specific nuclear localization of the B subunit. *Exp. Cell Res.* 246(2): 355-367.

Postel, E.H. (1998). NM23-NDP kinase. *Int. J. Biochem. Cell. Biol.* 30(12): 1291-1295.

Postel, E.H., Berberich, S.J., Flint, S.J., Ferrone, C.A. (1993). Human c-myc transcription factor PuF identified as nm23-H2 nucleoside diphosphate kinase, a candidate suppressor of tumor metastasis. *Science*. 261: 478-480.

Postel, E.H., Berberich, S.J., Rooney, J.W., Kaetzel, D.M. (2000). Human NM23/nucleoside diphosphate kinase regulates gene expression through DNA binding to nuclease-hypersensitive transcriptional elements. *J. Bioenerg. Biomembr.* 32: 277-284.

Postel, E.H., Ferrone, C.A. (1994). Nucleoside diphosphate kinase enzyme activity of NM23-H2/PuF is not required for its DNA binding and in vitro transcriptional functions. *J. Biol. Chem.* 269(12): 8627-8630.

Potter, E.D., Ling, Z.D., Carvey, P.M. (1999). Cytokine-induced conversion of mesencephalic-derived progenitor cells into dopaminergic neurons, *Cell Tissue Res.* 296: 235-246.

Poulson, K. T., Armanini, M. P., Klein, R. D., Hynes, M. A., Phillips, H. S., Rosenthal, A. (1994). TGF β 2 and TGF β 3 are potent survival factors for midbrain dopaminergic neurons, *Neuron* 13: 1245-1252.

Prasad, K.N., Cole, W.C., Kumar, B. (1999). Multiple antioxidants in the prevention and treatment of Parkinson's disease. *J. Am. Coll. Nutr.* 18(5):413-423.

Rolletschek, A., Chang, H., Guan, K., Czyz, J., Meyer, M., Wobus, A.M. (2001). Differentiation of embryonic stem cell-derived dopaminergic neurons is enhanced by survival-promoting factors, *Mech. Dev.* *105*: 93-104.

Rosengard, A.M., Krutzsch, H.C., Shearn, A. (1989). Reduced nm23/awd protein in tumor metastasis and aberrant *Drosophila* development. *Nature* *342*: 177-180.

Roymans, D., Willems, R., Vissenberg, K., De Jonghe, C., Grobben, B., Claes, P., Lascu, I., Van Bockstaele, D., Verbelen, J.P., Van Broeckhoven, C., Slegers, H. (2000). Nucleoside diphosphate kinase beta (Nm23-R1/NDPKbeta) is associated with intermediate filaments and becomes upregulated upon cAMP-induced differentiation of rat C6 glioma. *Exp. Cell Res.* *261(1)*: 127-138.

Russell, R.L., Pedersen, A.N., Kantor, J., Geisinger, K., Long, R., Zbieranski, N., Townsend, A., Shelton, B., Brunner, N., Kute, T.E. (1998). Relationship of nm23 to proteolytic factors, proliferation and motility in breast cancer tissues and cell lines. *Br. J. Cancer.* *78(6)*: 710-717.

Schapira, A.H., Mann, V.M., Cooper, J.M., Dexter, D., Daniel, S.E., Jenner, P., Clark, J.B., Marsden, C.D. (1990). Anatomic and disease specificity of NADH CoQ1 reductase (complex I) deficiency in Parkinson's disease. *J. Neurochem.* *55*: 2142-2145.

Saucedo-Cardenas, O., Quintana-Hau, J.D., Le, W.-D., Smidt, M.P., Cox, J.J., Mayo, F.D., Burbach, J.P.H., Conneely, O.M. (1998). Nurr1 is essential for the induction of the dopaminergic phenotype and the survival of ventral mesencephalic late dopaminergic precursor neurons, *Proc. Natl. Acad. Sci. USA* 95, 4013-4018.

Schwarz, M., Alvarez-Bolado, G., Urbanek, P., Busslinger, M., Gruss, P. (1997) Conserved biological function between Pax-2 and Pax-5 in midbrain and cerebellum development: Evidence from targeted mutations, *Proc. Natl. Acad. Sci. USA* 94: 14518–14523.

Seifert, M., Welter, C., Mehraein, Y., Seitz, G. (2005). Expression of the nm23 homologues nm23-H4, nm23-H6, and nm23-H7 in human gastric and colon cancer. *J Pathol.* 205(5): 623-32.

Seo, B.B., Nakamaru-Ogiso, E., Flotte, T.R., Yagi, T., Matsuno-Yagi, A. (2002). A single-subunit NADH-quinone oxidoreductase renders resistance to mammalian nerve cells against complex I inhibition. *Mol. Ther.* 6(3): 336-341. Erratum in: *Mol. Ther.* 2003, 7(6): 859.

Sherr, C.J. (1994). G₁ phase progression: cycling on cue. *Cell.* 79: 551-555.

Sherr, C.J. (1995). D-type cyclins. *Trends Biochem. Sci.* 20(5):187-190.

Shimada, N., Ishikawa, N., Munakata, Y., Toda, T., Watanabe, K., Kimura, N. (1993). A second form (beta isoform) of nucleoside diphosphate kinase from rat.

Isolation and characterization of complementary and genomic DNA and expression. J. Biol. Chem. 268: 2583-2589.

Shults, C.W. (2005). Antioxidants as therapy for Parkinson's disease. Antioxid. Redox. Signal. 7(5-6): 694-700.

Smidt, M.P., Criel, H.J.A., Cox, J.J., Chen, H., Johnson, R.L., Burbach, J.P.H. (2000). A second independent pathway for development of mesencephalic dopaminergic neurons requires *Lmx1b*, Nature Neuroscience 3, no. 4: 337-341.

Smidt, M.P., Van Schaick, H.S.A., Lanctot, C., Tremblay, J.J., Cox, J.J., Van der Kleij, A.A.M., Wolterink, G., Drouin, J., Burbach, J.P.H. (1997). A homeodomain gene *Ptx3* has highly restricted brain expression in mesencephalic dopaminergic neurons, Proc. Natl. Acad. Sci. USA 94: 13305-13310.

Song, S., Wang, Y., Bak, S.-Y., Lang, P., Ullrey, D., Neve, R.L., O'Malley, K.L., Geller, A.J. (1997). An HSV-1 vector containing the rat tyrosine hydroxylase promoter enhances both long-term and cell type-specific expression in the midbrain, J. Neurochem. 68: 1792-1803.

Sorensen, J.B. (2005). SNARE complexes prepare for membrane fusion. Trends Neurosci. 28(9): 453-455.

- Spina, M.B., Squinto, S.P., Miller, J., Lindsay, R.M., Hyman, C. (1992). Brain-derived neurotrophic factor protects dopamine neurons against 6-hydroxydopamine and N-methyl-4-phenylpyridinium ion toxicity: Involvement of the glutathione system, *J. Neurochem.* 59: 99-106.
- Stahl, J.A., Leone, A., Rosengard, A.M., Porter, L., King, C.R., Steeg, P.S. (1991). Identification of a second human nm23 gene, nm23-H2. *Cancer Res.* 51(1): 445-9.
- Steeg, P.S., Bevilacqua, G., Kopper, L., Thorgeirsson, U.P., Talmadge, J.E., Liotta, L.A., Sobel, M.E. (1988). Evidence for a novel gene associated with low tumor metastasis potential. *J. Natl. Cancer Inst.* 80: 200-204.
- Stein, G.S., Lian, J.B. (1993). Molecular mechanisms mediating proliferation / differentiation interrelationships during progressive development of the osteoblast phenotype. *Endocr Rev.* 14(4): 424-442.
- Sturm, R.A., Das, G., Herr, W. (1988). The ubiquitous octamer-binding protein Oct-1 contains a POU domain with a homeobox subdomain. *Genes Dev.* 2: 1582-1599.
- Swarzenski, B.C., O'Malley, K.L., Todd, R.D. (1996). PTX-sensitive regulation of neurite outgrowth by the dopamine D3 receptor. *Neuroreport* 7(2): 573-576.
- Swarzenski, B.C., Tang, L., Oh, Y.J., O'Malley, K.L., Todd, R.D. (1994). Morphogenic potentials of D2, D3, and D4 dopamine receptors revealed in transfected neuronal cell lines. *Proc. Natl. Acad. Sci. U.S.A.* 91(2):649-653.

Swerdlow, R.H., Parks, J.K., Miller, S.W., Tuttle, J.B., Trimmer, P.A., Sheehan, J.P., Bennett, J.P. Jr., Davis, R.E., Parker, W.D. Jr. (1996). Origin and functional consequences of the complex I defect in Parkinson's disease. *Ann. Neurol.* 40: 663–671.

Takayama, H., Ray, J., Raymon, H.K., Baird, A., Hogg, J., Fisher, L.J., Gage, F.H. (1995). Basic fibroblast growth factor increases dopaminergic graft survival and function in a rat model of Parkinson's disease, *Nat. Med.* 1: 53-58.

Takeda, K., Hatai, T., Hamazaki, T.S., Nishitoh, H., Saitoh, M., Ichijo, H. (2000). Apoptosis signal-regulating kinase 1 (ASK1) induces neuronal differentiation and survival of PC12 cells. *J. Biol. Chem.* 275: 9805-9813.

Tan, E.K., Khajavi, M., Thornby, J.I., Nagamitsu, S., Jankovic, J., Ashizawa, T. (2000). Variability and validity of polymorphism association studies in Parkinson's disease. *Neurology* 55: 533–538.

Tan, A.K. (2001). Current and emerging treatments in Parkinson's disease, *Ann. Acad. Med. Singapore* 30: 128-133.

Tan, L.C, Venketasubramanian, N., Hong, C.Y., Sahadevan, S., Chin, J.J., Krishnamoorthy, E.S., Tan, A.K., Saw, S.M. (2004). Prevalence of Parkinson disease in Singapore: Chinese vs Malays vs Indians. *Neurology.* 62(11):1999-2004.

- Timmons, L., Hersperger, E., Woodhouse, E., Xu, J., Liu, L.Z., Shearn, A. (1993). The expression of the *Drosophila* *awd* gene during normal development and in neoplastic brain tumors caused by *lgl* mutations. *Dev Biol.* 158(2): 364-79.
- Tsuiki, H., Nitta, M., Furuya, A., Hanai, N., Fujiwara, T., Inagaki, M., Kochi, M., Ushio, Y., Saya, H., Nakamura, H. (1999). A novel human nucleoside diphosphate (NDP) kinase, Nm23-H6, localizes in mitochondria and affects cytokinesis. *J Cell Biochem.* 76(2): 254-69.
- Urano, T., Takamiya, K., Furukawa, K., Shiku, H. (1992). Molecular cloning and functional expression of the second mouse *nm23*/NDP kinase gene, *nm23*-M2. *FEBS*, 309(3): 358-362.
- Urbanek, P., Wang, Z.Q., Fetka, I., Wagner, E.F., Busslinger, M. (1994). Complete block of early B cell differentiation and altered patterning of the posterior midbrain in mice lacking Pax5/BSAP, *Cell* 79: 901–912.
- Venturelli, D., Martinez, R., Melotti, P., Casella, I., Peschle, C., Cucco, C., Spampinato, G., Darzynkiewicz, Z., Calabretta, B. (1995). Overexpression of DR-nm23, a protein encoded by a member of the nm23 gene family, inhibits granulocyte differentiation and induces apoptosis in 32Dc13 myeloid cells. *Proc. Natl. Acad. Sci. U.S.A.* 92(16): 7435-9.
- Verma, I., Somia, N. (1997). Gene therapy: Promises, problems, and prospects, *Nature* 389: 239-242.

- Vidal, A., Koff, A. (2000). Cell-cycle inhibitors: three families united by a common cause. *Gene*. 247: 1-15.
- Wagner, P.D., Steeg, P.S., Vu, N.D. (1997). Two-component kinase-like activity of nm23 correlates with its motility-suppressing activity. *Proc. Natl. Acad. Sci. USA*. 94(17): 9000-9005.
- Waetzig, V., Herdegen, T. (2003). A single c-Jun N-terminal kinase isoform (JNK3-p54) is an effector in both neuronal differentiation and cell death. *J. Biol. Chem*. 278: 567-572.
- Wagner, P.D., Vu, N.D. (1995). Phosphorylation of ATP-citrate lyase by nucleoside diphosphate kinase. *J. Biol. Chem*. 270(37): 21758-21764.
- Wainwright, M.S., Perry, B.D., Won, L.A., O'Malley, K.L., Wang, W.-Y., Ehrlich, M.E., Heller, A. (1995). Immortalized murine striatal neuronal cell lines expressing dopamine receptors and cholinergic properties, *J. Neurosci*. 15: 676-688.
- Wallace, D.C., Shoffner, J.M., Watts, R.L., Juncos, J.L., Torroni, A. (1992). Mitochondrial oxidative phosphorylation defects in parkinson's disease. *Ann. Neurol*. 32: 113–114.
- Weinberg, R.A. (1995). The retinoblastoma protein and cell cycle control. *Cell*. 81: 323-330.

Weiner, M. (1982). Update on antiparkinsonian agents, *Geriatrics* 37, 81-84, see also pp. 89-91.

Willems, R., Van Bockstaele, D.R., Lardon, F., Lenjou, M., Nijs, G., Snoeck, H.W., Berneman, Z.N., Slegers, H. (1998). Decrease in nucleoside diphosphate kinase (NDPK/nm23) expression during hematopoietic maturation. *J. Biol. Chem.* 273(22): 13663-13668.

Williams, R.L., Oren, D.A., Munoz-Dorado, J., Inouye, S., Inouye, M., Arnold, E. (1993). Crystal structure of *Myxococcus xanthus* nucleoside diphosphate kinase and its interaction with a nucleotide substrate at 2.0 Å resolution. *J Mol Biol.* 234(4): 1230-1247.

Witjas, T., Baunez, C., Henry, J.M., Delfini, M., Regis, J., Cherif, A.A., Peragut, J.C., Azulay, J.P. (2005). Addiction in Parkinson's disease: impact of subthalamic nucleus deep brain stimulation. *Mov. Disord.* 20(8):1052-1055.

Wurst, W., Auerbach, A. B., Joyner, A. L. (1994). Multiple developmental defects in *Engrailed-1* mutant mice: An early mid-hindbrain deletion and patterning defects in forelimbs and sternum, *Development* 120: 2065–2075.

Yamashiro, S., Urano, T., Shiku, H., Furukawa, K. (1994). Alteration of nm23 gene expression during the induced differentiation of human leukemia cell lines. *Oncogene*. 9(9): 2461-2468.

Yao, R., Yoshihara, M., Osada, H. (1997). Specific activation of a c-Jun NH2-terminal kinase isoform and induction of neurite outgrowth in PC-12 cells by staurosporine. *J. Biol. Chem.* 272: 18261-18266.

Ye, W., Shimamura, K., Rubenstein, J.L., Hynes, M.A., Rosenthal, A. (1998). FGF and Shh signals control dopaminergic and serotonergic cell fate in the anterior neural plate. *Cell.* 93(5): 755-66.

Zetterström, R.H., Williams, R., Perlmann, T., Olson, L. (1996). Cellular expression of the immediate early transcription factors Nurr1 and NGFI-B suggests a gene regulatory role in several brain regions including the nigrostriatal dopamine system, *Mol. Brain Res.* 41: 111-120.

Zhang, Z.X., Roman, G.C. (1993). Worldwide occurrence of Parkinson's disease: an updated review. *Neuroepidemiology* 12: 195–208.

Zhou, Q., Xiao, J., Liu, Y. (2000). Participation of syntaxin 1A in membrane trafficking involving neurite elongation and membrane expansion. *J. Neurosci. Res.* 61: 321-328.

Zhu, N., Lu, Q., Zhou, Y. (2001). Cell differentiation and down regulation of nm23 gene expression in HL-60 cells induced by 1,25 dihydroxyvitamin D3. *Zhonghua Xue Ye Xue Za Zhi.* 22(12): 639-641.

Zigova, T., Sanberg, P.R., (1998). The rising star of neural stem cell research, Nat. Biotech. 16: 1007-1008.

Zinyk, D.L., McGonnigal, B.G., Dearolf, C.R. (1993). *Drosophila* *awd*^{K-pn}, a homologue of the metastasis suppressor gene nm23, suppresses the Tum-1 haematopoietic oncogene. Nat Genet. 4(2): 195-201.